Pacific Northwest
NATIONAL LABORATORY

Proudly Operated by **Battelle** *Since 1965*

Assessing the Characterization Potential of Flowing Fluid Electrical Conductivity (FFEC) Surveys within Deep Boreholes for Crystalline Basement Disposal

September 2017

FA Spane
PD Thorne

U.S. DEPARTMENT OF
ENERGY

DISCLAIMER

This report was prepared as an account of work sponsored by an agency of the United States Government. Neither the United States Government nor any agency thereof, nor Battelle Memorial Institute, nor any of their employees, makes **any warranty, express or implied, or assumes any legal liability or responsibility for the accuracy, completeness, or usefulness of any information, apparatus, product, or process disclosed, or represents that its use would not infringe privately owned rights**. Reference herein to any specific commercial product, process, or service by trade name, trademark, manufacturer, or otherwise does not necessarily constitute or imply its endorsement, recommendation, or favoring by the United States Government or any agency thereof, or Battelle Memorial Institute. The views and opinions of authors expressed herein do not necessarily state or reflect those of the United States Government or any agency thereof.

Assessing the Characterization Potential of Flowing Fluid Electrical Conductivity (FFEC) Surveys within Deep Boreholes for Crystalline Basement Disposal

September 2017

FA Spane
PD Thorne

Pacific Northwest National Laboratory
Richland, Washington 99352

Abstract

This report discusses the design, performance, and analysis of Flowing Fluid Electrical Conductivity (FFEC) logging surveys within deep boreholes, with special emphasis on possible application for characterizing permeable features within the open borehole crystalline basement section (i.e., 2 to 5 km depth) of the proposed Deep Borehole Field Test (DBFT) Characterization Borehole (CB). This work supports the DOE Office of Nuclear Energy (DOE-NE), Spent Fuel and Waste Science and Technology Campaign. The primary objective of performing the FFEC surveys is to provide a rapid means of determining the permeability profile distribution over large open borehole basement sections, particularly where the crystalline basement section's permeability is localized by relatively widely spaced, fluid-conducting, discrete fracture systems that collectively possess a composite borehole transmissivity of 10^{-5} m^2/sec, or less. For these environmental conditions, standard dynamic flowmeter surveys that are commonly used for reconnaissance-level, open borehole permeability profile characterization are not feasible because of either the associated low-flow, borehole velocity conditions (i.e., velocity resolution limitations for conventional spinner, full-bore velocity flowmeters) or anticipated testing conditions that exceed instrument operational capabilities (e.g., heat-pulse flowmeters).

The rapidity and sensitivity of the FFEC method within low-permeability test sections, as well as the availability of standard, commercially obtainable standard test equipment to perform the tests makes FFEC testing particularly attractive for deep borehole characterizations. The use of FFEC testing as a primary characterization tool for fracture zone hydraulic property determination within deep boreholes may be limited, however, based on the issues and conditions identified. The test method can be best applied for quantitative characterization applications within boreholes that exhibit minimal well-skin damage, and for fracture zones that have well-established, equilibrated pressure conditions. For more restrictive borehole conditions, FFEC tests can still be used effectively as a reconnaissance-level characterization tool to identify the location of higher permeability/fluid-conducting fracture zones within large open borehole intervals. In this capacity, FFEC survey results would *complement* and focus test characterizations performed by more exacting (and more costly) hydrologic test methods (e.g., packer tests) that can accommodate more complex borehole test conditions.

Summary

This report fulfils milestone M4SF-17PN010306093 under work package SF-17PN01030609 as part of the Deep Borehole Field Test (DBFT) control account within the U.S. Department of Energy (DOE) Office of Nuclear Energy's Spent Fuel and Waste Science and Technology Campaign.

The research documented in this report was performed as part of the Deep Borehole Field Test (DBFT) project that was developed to assess the potential for disposing of some types of nuclear waste in deep boreholes drilled in low permeability crystalline rock. This effort was part of the DOE Office of Nuclear Energy, Spent Fuel and Waste Science and Technology Campaign. Based on revised U.S. Department of Energy (DOE) priorities in mid-2017, the DBFT and other research related to a deep borehole disposal (DBD) option for high-level nuclear wastes has been discontinued; current work is being closed out and associated documentation will be completed by the end of fiscal year 2017. Further DBFT work, for example implementation of an engineering demonstration (SNL 2016a), would require resumption of DBD research and development at some future time. Although the report discussion specifically refers to the applicability and performance of FFEC surveys conducted within the proposed DBFT program Characterization Borehole (CB), the information and considerations presented are also applicable for conducting these tests in other deep borehole environments (e.g., for crystalline borehole depths ≥ 2 km).

Briefly stated, the FFEC logging characterization method is most commonly implemented by first establishing a uniform and contrasting fluid salinity baseline profile (i.e., in comparison to fracture fluid salinity) within the open borehole interval. In most deep borehole applications where the crystalline basement rocks contain elevated formation fluid salinities, a low-salinity borehole emplacement water (e.g., 60 to 300 μS/cm) is routinely used. Following emplacement of the contrasting borehole fluid, the ambient, pre-test fluid electrical conductivity (FEC) and fluid temperature vs. depth profile characteristics within the borehole are determined using commercially available FEC and fluid temperature wireline probe/recording systems. After completion of the ambient, pre-test logging surveys, the FFEC test is initiated by removing fluid from the borehole at a low and constant rate (e.g., 2 to 20 L/min). Borehole fluid removal during FFEC testing is usually accomplished by using a submersible pump installed at a depth commonly ≤ 250 m below static fluid-level conditions. To minimize interpretation and testing uncertainties, multiple constant-rate pumping steps (e.g., 2 to 3) are used during performance of the FFEC test, and the combined pumping test period duration ranges from 1 to 7 days. FFEC wireline logging is accomplished using an access tube (e.g., oil-field "Y-tool") to bypass the set submersible pump within the well.

During the pumping or dynamic "flowing" period, multiple FFEC profile surveys are logged (2 to 5 up/down FEC logging passes per each individual constant-rate pumping step) across the selected open borehole characterization section. The comparison of repeated logging results obtained progressively during the pumping period establishes changes in the FFEC depth profile within the borehole over time. The inflow of fluid from hydraulically conductive fractures (which must have significantly different salinities from the initially emplaced, pre-test borehole fluid to be observed) generate discernable FFEC peak patterns that evolve and expand over time within the borehole depth interval during the FFEC test period. Analysis of the evolving FFEC patterns provides a wide spectrum of information for hydraulically conductive fractures intersected by the borehole, including the following:

- precise inflow/outflow location depths
- inflow rates (q_i) and fracture fluid salinity (C_i)
- fracture zone hydraulic head conditions (h_i).

Fracture inflow location depths are delineated by the FFEC peak locations and relative skewness of the profile pattern. Fracture inflow rates and fluid salinities are determined analytically or numerically (e.g., using BORE II; Doughty and Tsang 2002) through analysis of repetitive FFEC profile runs. Fracture hydraulic head relationships are discerned by comparing the analysis results for repetitive FFEC profile runs with similar comparisons derived during multiple pumping steps. FFEC-derived analysis results obtained for q_i and h_i are then used with standard transient and steady-state analytical equation relationships to determine discrete fracture transmissivity (T_i) and hydraulic conductivity (K_i).

The assessment results presented in this report support the application of FFEC testing within deep crystalline boreholes that exhibit fracture zone transmissivity values of $\leq 10^{-5}$ m^2/sec. The results are consistent with previous reports of successful characterization applications at a number of deep borehole locations. The rapidity and sensitivity of the method within low-permeability test sections, as well as the availability of standard, commercially obtainable standard test equipment to perform the tests, make FFEC testing particularly attractive for deep borehole characterizations. The use of FFEC testing as a primary characterization tool for fracture zone hydraulic property determination within deep boreholes may be limited, however, based on the issues identified and discussed herein. These issues may limit the quantitative characterization applications of FFEC testing within boreholes that exhibit minimal well-skin damage, and in fracture zones that have well-established, equilibrated pressure conditions. For more restrictive borehole conditions, FFEC testing can still be used effectively as a reconnaissance-level characterization tool to identify the location of higher permeability/fluid-conducting fracture zones within large open borehole intervals. In this capacity, FFEC survey results would *complement* and focus test characterizations performed by more exacting (and more costly) packer tests that can accommodate more complex borehole test conditions. FFEC logging can be conducted in boreholes with severe breakouts (e.g., under high differential stress conditions), where packers may not make a seal good enough to allow meaningful hydrologic tests, and core recovery may be low due to discing. And if a hydraulic property correspondence between limited fracture zone packer testing and FFEC analysis can be established, then hydraulic property characterization for the entire borehole can be extended through the use of FFEC survey profile analysis. This particular complementary characterization aspect of FFEC testing was also originally recognized by Tsang et al. (1990), and more descriptively articulated by Doughty et al. (2005).

Similar combined characterization approaches for extending and calibrating open borehole wireline logging surveys (e.g., combined magnetic resonance and dynamic flowmeter logging) with more precise (but more limited) straddle-packer hydrologic field tests and core laboratory analysis results have been reported by Spane et al. (2006, 2013). These successful applications of extending wireline survey results for continuous permeability borehole profile determinations, however, were conducted at shallower borehole depths (e.g., 1.2 to 2.8 km) and within sedimentary rock formation environments.

Of the two alternative tracer test methods considered, the tracer-dilution circulation (TDC) test appears to provide the most practical application for deep borehole characterization settings. BORE II simulations indicate that for similar test conditions, TDC tests can be conducted more rapidly than FFEC tests, but they also exhibit an inherent lack of sensitivity for characterizing discrete fracture zones exhibiting T_i values lower than $\sim 10^{-7}$ m^2/sec. The limitations identified in this assessment for FFEC testing would be applicable for the TDC method as well. Because of these limitations and rapid performance times, TDC testing may also find its best application as an initial reconnaissance tool prior to conducting FFEC and hydrologic packer tests.

Acknowledgments

Acronyms and Abbreviations

CB	Characterization Borehole
DBD	Deep Borehole Disposal
DBFT	Deep Borehole Field Test
DDP – GSF	Deep Drilling Project of the Geological Survey of Finland
DOE	U.S. Department of Energy
DOE-NE	U.S. Department of Energy - Office of Nuclear Energy
EC	electrical conductivity
ESP	electrical submersible pump
FEC	Fluid Electrical Conductivity
FFEC	Flowing Fluid Electrical Conductivity (logging surveys)
IRF	infinite-acting radial flow (conditions)
LBNL	Lawrence Berkeley National Laboratory
NAGRA	Nationale Genossenschaft für die Lagerung radioaktiver Abfälle
PNNL	Pacific Northwest National Laboratory
SNL	Sandia National Laboratories
TDC	tracer-dilution circulation test
TIFL	Tracer-Injection Flow Log

Nomenclature

A	electrical conductivity linear temperature-compensation coefficient; dimensionless
A_i	salinity concentration profile FFEC area for fracture zone, i; L^2
b_i	fracture zone aperture; L
c_r	compressibility of the reservoir layer; ; $(LT^2)/M$
c_w	compressibility of reservoir layer water; $(LT^2)/M$
C	cubic, fracture flow constant; dimensionless
C_{af}	tracer concentration of borehole fluid immediately above the fracture zone; M/L^3
C_b	salinity baseline concentration of fluid within borehole prior to testing; M/L^3
C_{bf}	tracer concentration of borehole fluid immediately below the fracture zone; M/L^3
C_D	dimensionless wellbore storage; dimensionless
C_i	salinity concentration of fluid with fracture zone, i; M/L^3
C_{in}	salinity concentration of tracer fluid injected at the base of the test interval; M/L^3
C_o	initial salinity concentration of fluid within borehole prior to testing; M/L^3
C_{out}	salinity concentration of borehole fluid pumped/removed from well; M/L^3
C_s	salinity concentration of fluid; M/L^3
C_1	bottom fracture zone fluid salinity concentration within a three fracture zone set; M/L^3
C_2	middle fracture zone fluid salinity concentration within a three fracture zone set; M/L^3
C_3	top fracture zone fluid salinity concentration within a three fracture zone set; M/L^3
D_o	vertical borehole dispersion/diffusion parameter used in BORE II; L^2/T
$EC_{25°}$	water electrical conductivity corrected to 25 °C; $(T^3I^2)/L^2M^1)$
EC_t	water electrical conductivity recorded at measurement temperature; $(T^3I^2)/L^2M^1)$
FEC	fluid electrical conductivity; $(T^3I^2)/L^2M^1)$
h	reservoir/test interval hydraulic head; L
h_D	composite head within well; L
h_{Db}	composite head drawdown as measured near bottom of well fluid column; L
h_{Db}	composite head drawdown as measured near top of well fluid column; L
h_{fc}	fluid-column height within well above reference datum; L
h_i	hydraulic head within individual fracture zone, i; L
h_1	hydraulic head within bottom fracture zone; L
h_2	hydraulic head within middle fracture zone; L
h_3	hydraulic head within top fracture zone; L
K_i	hydraulic conductivity of individual fracture zone, i; L/T
L_i	discrete fracture length/extent; L

m	reservoir layer thickness; (L)
m_i	discrete fracture zone thickness, i; (L)
P	pressure measured at a fluid-column location within well/borehole; M/LT^{-2}
P_b	pressure measured near bottom of well/borehole fluid-column; M/LT^{-2}
P_t	pressure measured near top of well/borehole fluid-column; M/LT^{-2}
$\sum q_{fbf}$	sum of inflow rates from fractures located below fracture zone, i
q_i	inflow rate from individual fracture zone, i; L^3/T
q_1	inflow rate from bottom fracture of a three fracture zone set, i; L^3/T
q_2	inflow rate from middle top fracture of a three fracture zone set, i; L^3/T
q_3	inflow rate from top fracture of a three fracture zone set, i; L^3/T
q_{wb}	flow rate from wellbore storage; L^3/T
Q	surface pumping rate; L^3/T
Q_{dif}	difference between Q_{out} and Q_{in}; L^3/T
Q_{in}	tracer solution injection rate at the base of the test interval; L^3/T
Q_{out}	extraction pumping rate of well tracer solution from above the test interval; L^3/T
Q_{tot}	pumping rate from entire test interval; L^3/T
r	radial distance from well; L
r_c	well casing radius; L
r_{out}	radius-of-influence of test, where drawdown = 0; L
r_{wb}	wellbore radius; L
Re	Reynolds number; dimensionless
s_D	dimensionless drawdown; dimensionless
s_K	well skin; dimensionless
S	storativity of entire reservoir/test interval; dimensionless
S_i	storativity of individual fracture zone, i; dimensionless
t	test time; T
t_D	dimensionless time; dimensionless
T	reservoir/fracture zone transmissivity; L^2/T
T_i	transmissivity of individual fracture zone, i; L^2/T
T_{tot}	total transmissivity of the composite open borehole section; L^2/T
T_1	transmissivity of the bottom fracture of a three fracture zone set; L^2/T
T_2	transmissivity of the middle fracture of a three fracture zone set; L^2/T
T_3	transmissivity of the top fracture of a three fracture zone set; L^2/T
u	dimensionless well function; dimensionless
W_i	discrete fracture width; L
γ_w	reservoir/fracture zone fluid specific weight; M/L^3
ρ_{fw}	borehole fluid column density; M/L^3
ρ_i	fracture zone fluid density; M/L^3

ρ_w	reservoir/fracture zone fluid density; M/L^3
μ_w	reservoir/fracture zone fluid dynamic viscosity; M/L^3
ϕ	reservoir/fracture zone porosity; (dimensionless)

Contents

Figures

Tables

1.0 Introduction

The technical assessment contained in this report was performed as part of the U.S. Department of Energy (DOE) Office of Nuclear Energy's Deep Borehole Field Test (DBFT). This effort was part of the DOE Office of Nuclear Energy Spent Fuel and Waste Science and Technology Campaign and was developed to assess the potential for disposing of some types of nuclear waste in deep boreholes drilled in low permeability crystalline rock." Based on revised DOE priorities in mid-2017, the DBFT and other research related to a deep borehole disposal (DBD) option for high-level nuclear wastes has been discontinued; current work is being closed out and documentation will be completed by the end of fiscal year 2017. Further DBFT work, such as implementation of an engineering demonstration (Sandia National Laboratories; SNL 2016a), would require resumption of DBD research and development at some future time. Although the ensuing discussion in this report specifically refers to the applicability and performance of flowing fluid electrical conductivity (FFEC) surveys conducted within the proposed DBFT program Characterization Borehole (CB), the information and technical discussion presented are also applicable for conducting these tests in other deep borehole environments (e.g., for crystalline borehole depths ≥2 km).

This report assesses the applicability of FFEC testing for hydraulic characterization of deep crystalline borehole settings (i.e., between depths of 2 to 5 km). Section 2.0 provides background discussion of previous investigations of permeability within deep crystalline rocks and the use of open borehole test methods. An in-depth discussion concerning FFEC testing, its implementation and analysis, as well as test limitations and test method alternatives is provided in Section 3.0. FFEC and tracer-dilution circulation test simulations performed using the BORE II numerical model (Doughty and Tsang 2000) are presented in Section 4.0, together with observations of the simulation results as they pertain to tracer profile development. Section 5.0 provides a general assessment of the applicability of FFEC testing in deep borehole settings. References cited in the report text are listed in Section 6.0. FFEC test recommendations specific to the DBFT characterization borehole are provided in the Appendix.

2.0   Background

Permeability within deep crystalline basement rocks is primarily controlled by the presence of naturally occurring fracture systems. Numerous detailed characterization studies of deep basement boreholes, however, have identified that only a small percentage of the total number of intersected fractures identified within core or by wireline geophysical methods are open and have sufficient permeability for transmitting fracture fluids within the subsurface. For example, Doughty et al. (2017) reported that less than ~3% of fractures encountered within deep CBs for nuclear repository siting investigations at Laxemar and Forsmark, Sweden, were hydraulically conductive. These general observations about the openness of fractures in the subsurface and their relative fracture permeability in crystalline basement environments are consistent with findings obtained at other deep borehole and mine facility investigation program locations (e.g., DOE 1988; Long et al. 1991). In addition, the permeability of fractured crystalline rock (both gneiss and granite) characteristically exhibits a general decreasing trend with depth, as reported by Stober and Bucher (2007, 2015) from the analysis of hydraulic test results for deep borehole test programs (i.e., for 1 to 5 km borehole depths). A number of borehole comparison studies (e.g., Barton et al. 1995, 1997; Ito and Zoback 2000) have also shown that hydraulically conductive fractures within deep crystalline rocks appear to be positively correlated with fractures that are critically stressed (i.e., a high shear/normal stress ratio: ≥ 0.6 ratio), and are generally significantly higher than crystalline rock fractures not oriented for failure given the currently existing stress-field conditions. As noted by Rogers (2003), critically stressed fractures are subject to failure, and the associated shear dilation displacements can result in significant increases in fracture permeability.

To maximize deep borehole investigative efforts and to reduce costs, open borehole characterization methods (e.g., dynamic flowmeter/fluid logging, FFEC surveys) need to be employed. These open borehole methods need to be capable of rapidly identifying fluid-transmitting fracture zones within the subsurface, so that subsequent detailed hydraulic property test characterization and hydrochemical/ isotopic sampling (e.g., packer tests) can be focused on these transmissive zones. However, for the anticipated lower-permeability test and environmental conditions within deep crystalline boreholes (greater than 2 km in depth), standard dynamic flowmeter surveys commonly used for rapid reconnaissance-level, open borehole permeability profile characterizations within higher permeability formations, may not be feasible. This anticipated lack of applicability is due to either the associated low-flow, borehole velocity conditions (i.e., velocity resolution limitations for conventional spinner, full-bore velocity flowmeters) or the expected deep well test conditions that exceed the operational capabilities of available instruments (e.g., heat-pulse flowmeters). Due to prevailing in-situ stress conditions, borehole breakouts may be significant at greater depths, and it therefore may be difficult to set packers and perform traditional hydraulic tests on discrete borehole intervals. Core recovery may also be low at significant depth in the borehole, which may also make laboratory permeability testing difficult to realize. As a result, FFEC logging surveys may represent a viable option for rapidly characterizing the permeability profile and identifying the presence of hydraulically conductive fractures over extended lower-permeability, open crystalline basement test intervals.

The technical discussion in the ensuing sections pertains to the design, performance, and analysis of FFEC logging surveys within the open crystalline basement section (i.e., 2 to 5 km depth) of the proposed DBFT CB. This discussion represents an expansion of the general information provided regarding production profile logging as originally presented by SNL (2016b). The primary objective of performing the FFEC surveys is to provide a rapid means of determining the permeability profile distribution over large open borehole basement sections within the CB, particularly where the crystalline basement section's permeability is localized by relatively widely spaced, fluid-conducting, discrete fracture systems that collectively possess a composite borehole transmissivity of 10^{-5} m^2/sec, or less. FFEC logging

requires no specialized test equipment and can be performed in the anticipated environmental conditions within the CB with currently available sensor and equipment technology used in the oil industry.

A detailed description of the characterization test program that was planned to be conducted at the proposed DBFT CB is provided by Kuhlman et al. (2015) and SNL (2016b).

3.0   Fluid Electrical Conductivity Testing

Because of the performance limitations of standard, commercially available flowmeter logging for characterizing lower-permeability formations, the FFEC survey method was developed in the late 1980s and early 1990s. Its development was initially a collaborative effort between NAGRA (Nationale Genossenschaft für die Lagerung radioaktiver Abfälle) and the DOE for the purpose of rapidly determining the permeability/depth profile over large open borehole sections (i.e., ~1,000 m) in deep NAGRA boreholes drilled in support of Swiss nuclear repository characterization studies (Long et al. 1990). The collaborative development of the FFEC characterization method is documented in publications by Hale and Tsang (1988), Tsang and Hufschmied (1988), and Tsang et al. (1990). In Europe, deep borehole characterization examples (i.e., for boreholes >700 m depths) generally demonstrate that the FFEC method compares favorably with other detailed hydrologic characterization test results (e.g., packer tests, flowmeter surveys), such as those provided by Tsang et al. (1990), Kelley et al. (1991), Guyonnet et al. (1993), and Adams and Wyss (1994) in Switzerland; Tsang et al. (2016) and Doughty et al. (2017) in Sweden; and Sharma et al. (2016) in Finland. Similar comparative results have also been demonstrated for the FFEC characterization method for more shallow borehole depths (i.e., ≤500 m), as documented by Pedler et al. (1990), Paillet and Pedler (1996), Doughty and Tsang (2005), Beauheim and Pedler (2007), and Doughty et al. (2005, 2013). Pertinent test information concerning FFEC tests conducted in previous, deep borehole test characterization programs (>700 m), i.e., as it may relate to possible FFEC testing in the CB, is summarized in Table 3.1.

3.1   Test Implementation

The FFEC characterization method has undergone some developmental refinements regarding implementation and analysis approaches since it was originally reported by Tsang and Hufschmied (1988) and Tsang et al. (1990). Tsang et al. (2016), Dobson et al. (2016), and Doughty et al. (2017) present the most current and complete summaries about implementing FFEC surveys within deep boreholes, and the discussions contained in Section 3.0 derive much of their background from these publications.

Briefly stated, the FFEC logging characterization method is implemented first by emplacing a uniform and contrasting fluid salinity profile (i.e., in comparison to fracture fluid salinity) within the open borehole interval. To minimize incursion of non-formational emplacement water into surrounding intersecting fracture systems, the emplacement fluid is administered near the base of the test interval at a prescribed low injection rate, while simultaneously removing fluid from the well at the same rate near the top of the fluid column (see Figure 3.1a). The simultaneous injection of emplacement fluid (at the base of the test interval) and removal of well water from near the top of the fluid column using the same rates, minimizes borehole pressure buildup and incursion of non-formation well fluid into permeable fractures. The incursion of non-formational borehole fluid into surrounding hydraulically conductive fractures complicate the analysis of the FFEC profiles that evolve during the dynamic pumping phase of the test. In most deep borehole applications where the crystalline basement rocks contain elevated formation fluid salinities, a low-salinity borehole emplacement water (e.g., 60 to 300 µS/cm) is commonly used.

After emplacement of the contrasting borehole fluid, the ambient, pre-test fluid electrical conductivity (FEC) and fluid temperature vs. depth profile characteristics within the borehole are determined using commercially available FEC and temperature wireline probe/recording systems. The FFEC profile surveys are commonly logged using a stacked, multi-probe assembly system that includes sensors for measuring FEC, temperature, and fluid pressure, as well as formational depth indicators (e.g., gamma ray).

Table 3.1. Summary of General Test Condition Information for FFEC Surveys Conducted in Deep Boreholes for Selected International Programs

	Reference	Borehole	Test/Depth Interval, m	Borehole Diameter, m	Pumping Rate, L/min	Test Drawdown, m	Test Duration, hr	FFEC Surveys, # Up/Down	Fluid-Conductive Fracture Zones Resolved, #	Fracture Zone Transmissivity, m²/sec
NAGREA - DOE	Tsang and Hufschmied (1988) Tsang et al. (1990)	Leuggern	770 - 1,637	0.14	20	176	50.5	5	9	1.6E-7 to 4.7E-10
	Kelley et al. (1991)	Siblingen	988 - 1,522	0.096	3	21.3	60	6	9	1.3E-6 to 1.7E-8
			988 - 1,522	0.096	1.5	14.4	48	4.5	9	
										1.1E-6 to 2.6E-8
	Guyonnet et al. (1993) Adams and Wyss (1994)	Wellenberg SB2	575 - 1,120	0.159	2.6		>12	2	6	5.4E-7 to 3.9E-8
			1,130 - 1,692	0.159	2.2		>12	2.52	3	3.2E-8 to 6.4E-10
SSDP	Tsang et al. (2016) Doughty et al. (2017)	Åre COSC-1	100 - 1,600	0.102	3.5	70	24	2	7	3.0E-8 to 2.0E-10
			1,600 - 2,496	0.102 - 0.076	2.5	50	8	1	7	
			100 - 2,496	0.102 - 0.076		50		5	7	
			100 - 2,496	0.102 - 0.076		10		6	7	
DDP - GSF	Sharma et al. (2016)	Outokumpu	8 - 2,516	0.22	(a)	(a)	(5 years)	5	15	2.7E-5 to 3.3E-6

(a) Long-term ambient FFEC test conducted under natural borehole and regional hydraulic gradient conditions.
NAGRA – DOE: Cooperative research project between Nationale Genossenschaft für die Lagerung radioaktiver Abfälle and U.S. Department of Energy
SSDP: Swedish Scientific Drilling Program (formerly Swedish Deep Drilling Program)
DDP – GSF: Deep Drilling Project of the Geological Survey of Finland
COSC: Collisional Orogeny in the Scandinavian Caledonides
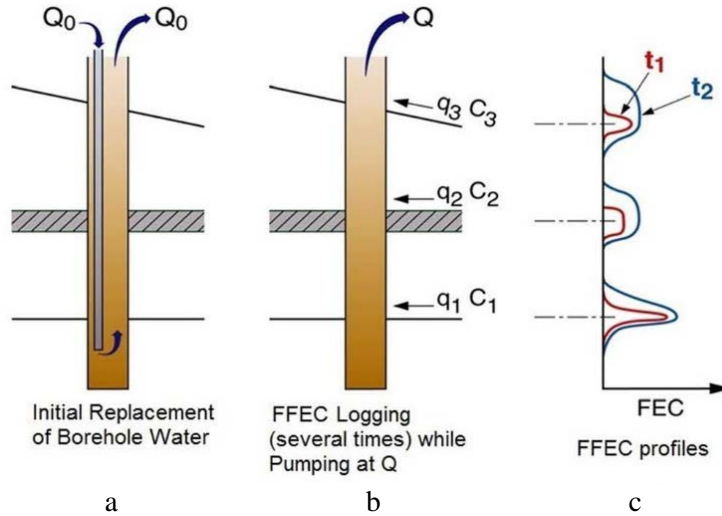
Figure 3.1. Schematic of Various Characteristics of FFEC Logging Surveys (from Doughty et al. 2017)

It should be noted that FEC, as only an indicator of fluid salinity concentration, is influenced not only by the dissolved solid content, but also by the effects of temperature. FFEC measurement profiles collected over an extended borehole length can exhibit significant temperature variation, and therefore, need to be corrected to a standard reference temperature value (e.g., 20 or 25°C). This is accomplished by interpolative use of FEC vs. temperature calibration relationships established in the laboratory for the specific sensor used in the FFEC surveys or through use of empirical, scientifically established FEC vs. temperature relationships. For example, a common FEC temperature-correction equation reported in scientific literature (e.g., Hayashi 2004) for natural waters is expressed as

$$EC_{25°} = EC_t / [1 + \alpha (t - 25)] \tag{3.1}$$

where,

$EC_{25°}$ = water electrical conductivity corrected to 25°C (microSiemens/cm [μS/cm]),
EC_t = water electrical conductivity recorded at measurement temperature, t, and
α = linear temperature-compensation coefficient.

The linear temperature-compensation coefficient, α, is expressed as a decimal fraction, and correction assigned values range between 0 and 0.05 (i.e., 0 to 5% per °C). The α temperature coefficient is also a function of chemical concentration and dissolved chemical species present in the water. Fixed values for α ranging between 0.0191 and 0.025 are most commonly used in electrical conductivity (EC) correction applications for groundwater and geophysical investigations (Hem 1985; Hayashi 2004).

Once the FFEC profile survey results have been corrected to the reference temperature value, salinity concentrations can be calculated based on the temperature-corrected FEC value using the FEC vs. salinity concentration (S_c) relationship listed by Tsang et al. (1990), which is based on a quadratic approximation to FEC vs. S_c measurements for sodium-chloride solution data listed by Shedlovsky and Shedlovsky (1971):

$$FEC = 1,870 \, C_s - 40 \, C_s^2 \tag{3.2}$$

where, FEC and C_s are expressed in microsiemens/cm and kg/m^3, respectively. Figure 3.2 shows the Equation (3.2 relationship for FEC vs. C_s over the indicated range. As noted by Tsang et al. (1990), for test conditions under which fluids exhibit concentrations of ~4 kg/m^3 or less or FEC values of ~6,840 μS/cm or less, the quadratic term in Equation (3.2) can be omitted, and the relationship reduced to

$$FEC \approx 1{,}870 \, C_s \qquad\qquad\qquad (3.3)$$

It should be noted that Equations (3.2) and (3.3) are developed for a reference standard temperature of 25°C, but can be adjusted to a reference fluid temperature of 20°C if the results are multiplied by a value of 0.89, as reported by Hale and Tsang (1988).
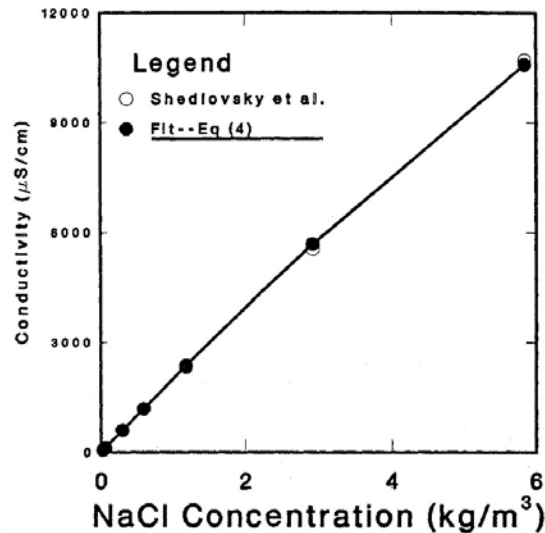
Figure 3.2. Fluid Electrical Conductivity vs. NaCl Concentration Relationship (from Hale and Tsang 1988)

After completion of the ambient, pre-test logging surveys, the dynamic phase of the FFEC test is initiated by removing fluid from the borehole at a low and constant rate (e.g., 2 to 20 L/min). The constant extraction of water from the well causes the composite hydraulic head within the well to decline with time, which induces fluid flow from hydraulically conductive fractures (having higher hydraulic head) to the well (b). Borehole fluid removal during FFEC testing is usually accomplished using an electrical submersible pump (ESP) installed at a well depth commonly ≤250 m below static fluid-level conditions. To minimize analytical and testing uncertainties, multiple constant-rate pumping steps (e.g., 2 to 3) are used during performance of the FFEC test, and the combined pumping test period duration generally ranges between 1 and 7 days. FFEC wireline logging is accomplished using an access tube (e.g., oil-field "Y-tool"; e.g., Schlumberger 2009; PTF® 2015) to bypass the set submersible pump within the well.

As an alternative to fluid extraction using an ESP, air-lift/evacuation pumping can be used. This involves administering compressed air via a conductor pipe (usually through centrally installed injection tubing), and removing/evacuating fluid from the well using the existing well casing, along with a surface wellhead enclosure to divert well flow. FFEC wireline logging in this case is conducted through the central injection tubing using a surface stuffing box or wellhead lubricator mounted on the top of the injection tubing. Multiple pumping rates can be implemented by lowering the injection tubing to greater depths, which will impose greater drawdown in the well and a higher subsequent well discharge rate.

During the pumping or dynamic "flowing" period, multiple FFEC profile surveys are logged (2 to 5 up/down FEC logging passes per each individual constant-rate pumping step) across the selected open borehole characterization section. Repeated logging results obtained progressively during the pumping period establishes changes in the FFEC depth profile within the borehole over time. The inflow of fluid from hydraulically conductive fractures (which, to be observed, must have significantly different salinities than the initially emplaced pre-test borehole fluid) generate discernable FFEC peak patterns that evolve

and expand over time within the borehole depth interval during the FFEC test (Figure 3.1c). Analysis of the FFEC evolution patterns provides a wide spectrum of information for hydraulically conductive fractures intersected by the borehole, including the following:

- precise inflow/outflow location depths
- inflow rates (q_i) and fracture fluid salinity (C_i)
- fracture hydraulic head conditions (h_i).

Fracture inflow depths are delineated by the FFEC peak locations and relative skewness of the profile pattern. Fracture inflow rates and fluid salinities are determined analytically or numerically (e.g., BORE II; Doughty and Tsang 2002) by analysis of repetitive FFEC profile runs. Fracture hydraulic head relationships are discerned by comparing the analysis results for repetitive FFEC profile runs with similar comparisons derived during multiple pumping steps (i.e., comparison of ($q_i C_i$) product estimates obtained from FFEC profiles obtained at different dynamic pumping rates). FFEC-derived analysis results obtained for q_i and H_i are then used with standard transient and steady-state analytical equation relationships to determine discrete fracture transmissivity (T_i) and hydraulic conductivity (K_i).

3.2   FFEC Profile Analysis

The FFEC profile analysis process requires that at least one ambient, baseline FEC profile be determined for the open borehole test interval prior to initiation of the dynamic FFEC phase of the test. The ambient, baseline FEC profile serves as the starting/initial borehole conditions for analysis of the FFEC profile patterns over time, and the evolutionary peak patterns are associated with the inflow rate (q_i) and salinity concentration (C_i) product over time. The FFEC profile at fracture inflow zone locations is distorted or skewed upward due to the composite removal of fluid from the open borehole interval and composite inflow from underlying fluid-transmitting fractures (Figure 3.3a). During early-test times, the evolution of the FFEC pattern for a discrete fracture zone is relatively symmetric, and the area (A_i) of symmetrical FFEC peak pattern that develops over time is a function of the $q_i C_i$ product, reported by Tsang et al. (2016) as follows:

$$A_i = q_i C_i \, \Delta t \tag{3.4}$$

As noted by Doughty et al. (2008, 2017), the fitted regression slope of A_i vs. Δt for isolated, early-time FFEC profile peaks (mass integral analysis) provides an estimate of $q_i C_i$ for each fracture input point within the test interval. During late-test times, the FFEC profile patterns shown in Figure 3.3b may overlap and become skewed vertically in the direction of borehole fluid flow (i.e., up-borehole direction). The degree of skewness exhibited by the FFEC fracture zone profiles is a function of the depth-specific borehole flowrate, which is a function of the collective inflow rates for all underlying fracture inflow zones. Therefore, during late FFEC survey test times it is possible to distinguish q_i and C_i from the early-time $q_i C_i$ determined product, because of the degree of skewness exhibited by each fracture inflow zone during later-test times (Dobson et al. 2016).

Based on the preliminary analysis results using the initial visual FFEC profile assessment to identify fracture zone depths and individual fracture zone $q_i C_i$ input products (i.e., from early-time FFEC peak profiles), a more quantitative evaluation can be performed with the BORE II computer program (Doughty and Tsang 2000) to match the entire FFEC profile pattern over time. BORE II is a one-dimensional numerical model that solves the advection/dispersion equation for vertical borehole flow, using associated fracture inflow (and outflow) sources (Doughty et al. 2017). Matching the FFEC profile patterns using BORE II is an iterative process accomplished by adjusting values for q_i and C_i for each of the FFEC-
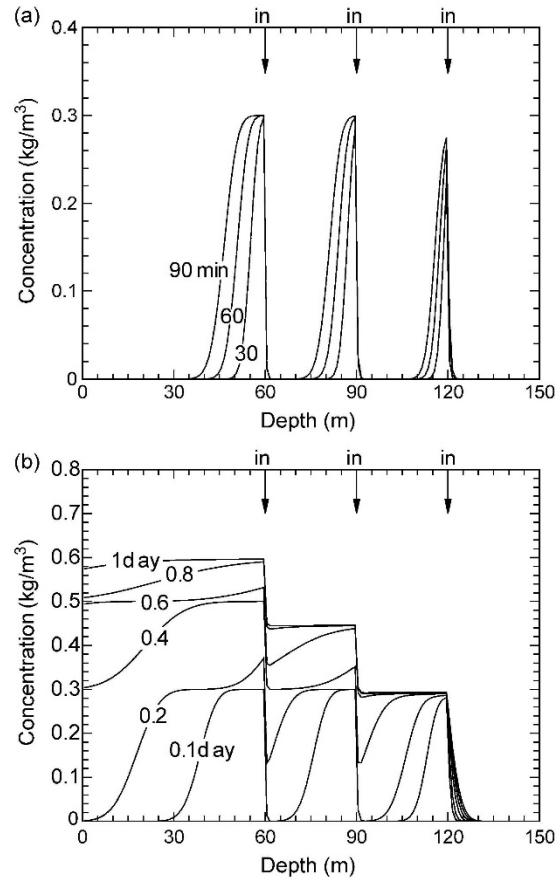
Figure 3.3. Schematic of FFEC Logging Fluid Concentration Profile Characteristics for Three Discrete Fracture Zones during (a) Early-Test Times and (b) Later-Test Times (from Doughty and Tsang 2005).

indicated fracture peak locations for the given well constant pumping rate. In addition, the program parameter identified to describe vertical dispersion within the borehole (D_o) (i.e., the sum of diffusion and mixing due to borehole fluid flow and movement of the logging tool within the borehole during FFEC logging) is adjusted to refine the FFEC profile matches.

Löw et al. (1990, 1994) present an alternative to the BORE II numerical model (or for corroborative applications) based on the analytical moment analysis approach for analyzing evolutionary FFEC. Moment analysis provides a more direct, non-iterative approach for analyzing early-time FFEC profile patterns, which can also be used as initial parameter estimates for use in the BORE analysis process. Kelley et al. (1991) and Guyonnet et al. (1993) report comparable analysis results for q_i and C_i using both BORE II and moment analysis methods for identified fracture zones at a number of deep borehole FFEC test sites. Because of its more widespread use in testing, the rest of the following discussion focuses on BORE II applications for FFEC profile analysis. For a more detailed discussion of moment method applications for FFEC profile analysis, the reader is referred to Löw et al. (1994).

3.2.1   Multi-Rate Testing

Early FFEC profile analyses using the original BORE computer program (Hale and Tsang 1988) assumed that fracture zones within FFEC profile test sections had equal hydraulic head conditions (or relatively

small head differences) in comparison to the drawdown imposed during the dynamic pumping phase of the test. This assumption implies that all hydraulically conductive fractures are contributory as inflow q_iC_i sources during the course of the test, and that the hydraulic head drawdown experienced by each fracture inflow zones is equivalent to the drawdown measured within the well during testing. While this assumption of equal hydraulic head conditions may be valid over small borehole lengths, for extended open borehole sections this is not likely the case. To address heterogeneous head profile conditions and other test complexities not accounted for in the original program, BORE was enhanced (BORE II version; Doughty and Tsang 2000) to allow for both inflow and outflow fracture zone conditions associated with unequal hydraulic head relationships in the FFEC profile simulations. In addition, Tsang and Doughty (2003) developed a multi-rate test method for determining initial hydraulic head fracture zone conditions for the likely situation where fracture inflow zones have unequal initial hydraulic heads. For the multi-rate test, dynamic pumping FFEC profiles are collected at 2 or more, significantly different constant rates (e.g., at ½ and/or 2 times the original pumping rate). FFEC profile developments are analyzed with the BORE II code individually for each pumping phase and then compared to provide information about q_i, C_i, and h_i within the individual fracture zones.

As an example, Figure 3.4 shows a schematic of possible associated fracture zone inflow/outflow relationships during a multi-rate FFEC test, in which three fracture zones have unequal hydraulic heads for the case where the borehole is pumped at a high rate (Figure 3.4a), at a much lower rate (Figure 3.4b), and under non-pumping/ambient conditions (Figure 3.4c). In the schematic, there is a natural downward head gradient between the three fracture zones depicted, where $h_3 > h_2 > h_1$.

For the Figure 3.4a high pumping rate scenario, all individual fracture zones have higher head conditions (h_i) than the composite borehole head drawdown (h_D) imposed by pumping. As a result, evolutionary FFEC patterns associated with all three inflow fracture zones would develop over time (e.g., as shown in Figure 3.3a and Figure 3.3b). For the subsequent low-pumping rate phase (Figure 3.4b), hydraulic head conditions within the two top fracture zones are greater and the bottom fracture zone is lower than the composite borehole head drawdown during pumping. As a consequence, FFEC profile patterns would continue to evolve during the lower pumping rate period for the upper two fracture zones, while the FFEC profile pattern for the lower fracture zone would be expected to stagnate and/or exhibit different FFEC signatures, as discussed by Doughty and Tsang (2005). Figure 3.4c shows the ambient downward hydraulic head conditions (where h3 > h2 > h1) for periods not associated with pumping (i.e., pre-test or
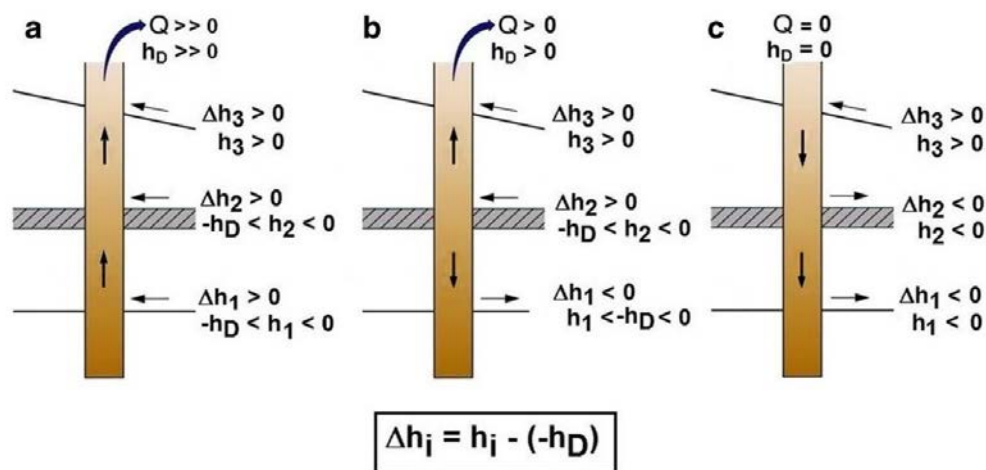

$$\Delta h_i = h_i - (-h_D)$$

Figure 3.4. Schematic of Possible Variations in Fracture Zone Inflow and Outflow Conditions during Multi-Rate Testing for the Unequal Hydraulic Head Case: $h_3 > h_2 > h_1$ (from Doughty et al. 2017).

after full recovery following pumping periods). In this scenario, the uppermost fracture zone possessing the highest hydraulic head condition (i.e., h_i > the composite non-pumping borehole head) would then produce inflow to the borehole that would outflow into the two underlying, lower head fracture zones. The ambient downward and outflow conditions indicated between fracture zones shown in Figure 3.4c would have possible adverse impacts on the analysis of FFEC profile pattern evolution for the bottom two fracture zones that receive a significant incursion of baseline fluid during the pre-test period. The pre-test incursion of non-formational water delays the arrival time of native fracture fluid to the borehole during the FFEC pumping test, and thus, delays the ability to analyze the early-time development of FFEC profile patterns associated with these pre-test outflow fracture zone locations.

In applying the multi-rate FFEC test method, for each fracture zone it is recognized that the inflow rate to the borehole (q_i) during pumping is related to the fracture zone hydraulic head drawdown (h_i) and transmissivity (T_i) using the following variant of the Thiem (1906) equation that describes this steady-state relationship within a confined aquifer, as presented by Dobson et al. (2016) and Doughty et al. (2017):

$$q_i = (2\pi T_i)\,(h_i + h_D)/\ln\,(r_{out}/r_{wb}) \tag{3.5}$$

In this steady-state relationship, h_i is the initial hydraulic head within the fracture zone as referenced to the initial, composite wellbore head, h_D (i.e. to the average of hydraulic heads for fracture zones intersected by the borehole). The r_{wb} parameter in Equation (3.5) is equal to the wellbore radius, while r_{out} is the radius-of-influence for the test or radial distance from the well to where the test drawdown is equal to 0. As has been noted by a number of previous investigators applying the steady-state Thiem equation (e.g., Zeigler 1976; Brainerd and Robbins 2004), calculations of q or T using this relationship are relatively insensitive to uncertainty in the estimated value used for r_{out}. This is largely due to its natural log form in the equation, i.e., $\ln\,(r_{out}/r_{wb})$.

As noted by Doughty et al. (2017), for the homogeneous head profile condition, h_i is equal to zero (i.e., all fracture hydraulic heads are equal), and then q_i values determined from the BORE II numerical model FFEC profile matches (along with observed wellbore drawdown during the test) can be used to calculate individual fracture zone transmissivity (T_i) using the re-organized form of Equation (3.5), as follows:

$$T_i = q_i \ln\,(r_{out}/r_{wb})/2\pi h_D \tag{3.6}$$

For the heterogeneous head fracture zone profile scenario, the multi-rate test results are combined. That is, using the q_i and h_i and h_{Di} results from the BORE II FFEC profile analysis, subtracting Equation (3.5) for the second test result from Equation ((3.5) for the first test, and solving for T_i yields:

$$T_i = (q_1 - q_2) \ln\,(r_{out}/r_{wb})/2\pi\,(h_{D1} - h_{D2}) \tag{3.7}$$

As reported by Doughty et al. (2017), dividing Equation (3.5) for the first test by Equation (3.5) for the second test and solving for h_i produces

$$h_i = (q_2 h_{D1} - q_1 h_{D2})/q_1 - q_2) \tag{3.8}$$

If more than two multi-rate pumping test steps are employed, then Equations (3.7) and (3.8) are applied repeatedly as analysis steps for each sequential FFEC pumping step as it relates to the previous FFEC analysis step (i.e., test 1 – test 2, test 2 – test 3, etc.). Consistent and comparable estimates of T_i and h_i for each multi-rate step analysis indicate that test conditions have been adequately addressed and accounted for in the FFEC profile analysis process. As reported by Doughty et al. (2017), Equations (3.7) and (3.8)

represent a significant improvement for estimating T_i and h_i over the procedure originally identified by Tsang and Doughty (2003) for multi-rate FFEC test analysis.

It should also be noted that the previous test method discussion is specifically for the case in which a uniform, contrasting fluid is emplaced prior to the dynamic pumping phase of the FFEC test. Tsang et al. (2016) describe the potential for conducting FFEC tests without initially replacing the borehole fluid with a uniform, contrasting salinity fluid. For this testing scenario, the existing drilling fluid within the borehole is logged to establish an initial, baseline FFEC profile within the well, and then the multi-rate FFEC test is initiated. The advantage of conducting the FFEC profile test in this manner is that it permits the possible application of the test method during drilling (e.g., during a temporary, non-drilling period). The major detraction of conducting the test in this fashion, however, is the loss of early-time FFEC profile evolution (mass integral approach) to provide initial estimates of $q_i\,C_i$ that serve as input for the subsequent numerical model profile analysis, as discussed by Doughty et al. (2017). Because of the complexity presented by a non-uniform and less contrastive baseline pre-test condition, at least two ambient, pre-pumping profile surveys are also required, as well as additional mixing ratio/mass balance calculations performed for quantitative FFEC profile analysis. These additional analysis calculations and test considerations are presented in more detail by Dobson et al. (2016) and Doughty et al. (2017).

3.2.2   Fracture Hydraulic Property Estimation

Based on the results obtained for q_i and Δh_i determined from the FFEC profile analysis, the individual fracture zone transmissivity (T_i) is calculated using one of the following analytical relationships:

- for radial flow – transient analysis, steady-state method, and normalized flow techniques;

- for linear flow – fracture zone and discrete fracture flow analysis (see conceptual flow regime and analysis equation summary in Figure 3.5).

The selection of the analytical method to use in estimating fracture zone T_i is based on observed test conditions (e.g., pumping test duration, diagnostic drawdown response) and fracture zone attribute characteristics (single discrete vs. shear zone).

T_i estimates based on transient (non-steady) radial flow analysis rely on application of the Cooper and Jacob (1946) approximate solution, through the following relationship:

$$T_i = 2.3\ q_i\,/(4\pi\Delta h_i/\Delta \log t) \tag{3.9}$$

Equation (3.9) is a simplification of the general non-steady equation of radial flow to a fully penetrating, confined aquifer well pumped at a constant rate (i.e., Theis equation) and is valid when the dimensionless well parameter (u) is ≤0.01, and where:

$$u = r_{wb}^2\,S_i\,/4T_i\,t \tag{3.10}$$

where, S_i is equal to the fracture zone storativity. Rearranging Equation (3.10) to assess test times (t) to which the approximate Equation (3.9) solution is applicable, yields:

$$t \geq (100\ r_{wb}^2\,S_i)\,/4T_i \tag{3.11}$$

Radial Flow – Porous Media Equivalent

Transient: Cooper – Jacob (1946):

$$T_i = 2.3\, q_i /(4\pi\Delta h_i /\Delta \log t)$$

Steady-State: Thiem (1906):

$$T_i = 2.3\, q_i /(2\pi\Delta h_i /\Delta \log r)$$

Flow Normalization Method:

$$T_i = T_{tot}\,(q_i /Q_{tot})$$

Fracture Zone – Linear Flow

$$T_i = (q_i^2\, t) /(\pi\, S_i\, L_i^2\, \Delta h_i^2)$$

Discrete Fracture:

$$K_i = (2b_i)^2\, \gamma_w /12\mu_w$$

$$q_i /\Delta h_i = C\,(2\, b_i)^3$$

(Radial Flow)

$$C = [2\,\pi/\ln\,(r_{out}/r_{wb})](\gamma_w /12\,\mu_w)$$

(Linear Flow)

$$C = (W_i /L_i)\,(\gamma_w /12\,\mu_w)$$
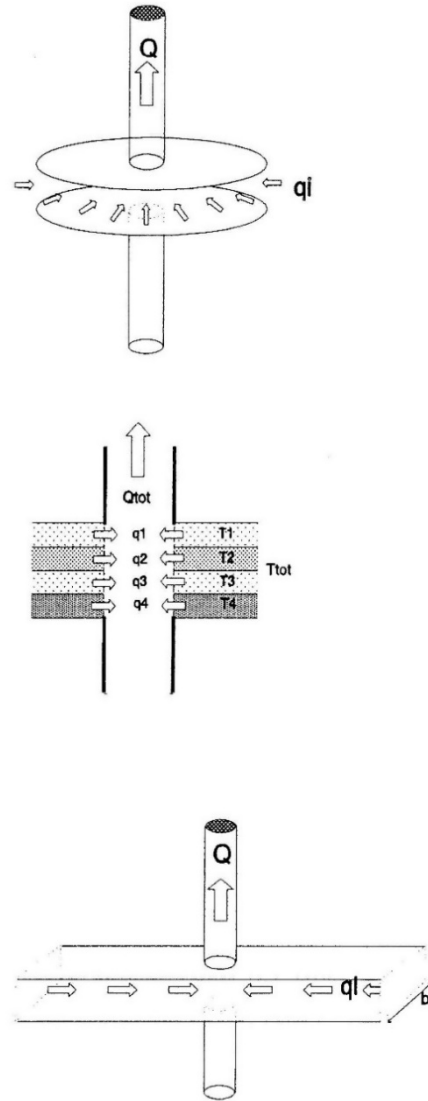
Figure 3.5. Conceptualization of Flow Regimes and Applicable Relationships for the Calculation of Fracture Zone Transmissivity (T_i) (modified from Guyonnet et al. 1993)

Of particular interest to steady-state radial flow analysis comparisons, Lohman (1972) showed that by applying the Cooper-Jacob approach over distance (i.e., $\log \Delta r$), the following expression for T_i was obtained:

$$T_i = 2.3\, q_i /(2\pi\Delta h_i /\Delta \log r) \qquad (3.12)$$

As concluded by Butler (1988), this form of the Cooper and Jacob (1946) expression is a form of the Thiem equation, and demonstrates the equivalence of the two analysis approaches. Equation (3.11) then represents the converted $\log_{10}$ form of the steady-state radial flow Thiem (1906) equation that has been used in most recent FFEC profile analysis reports, e.g., Tsang et al (2016) and Doughty et al. (2017).

T_i estimates based on the flow normalization, radial flow analysis method assume that the fracture flow model, hydraulic head conditions (h_i), and storativities (S_i) are equivalent for all fracture zones intersected by the open borehole test interval. T_i for individual fracture zones can then be calculated if the open borehole composite transmissivity (T_{tot}) is known (i.e., through previous open borehole hydrologic testing), and q_i from the FFEC profile test analysis, using the following relationship, as presented by Tsang and Doughty (2003):

$$T_i = T_{tot} \, (q_i/Q_{tot}) \tag{3.13}$$

Implicit in this relationship is that the flow regime/geometries (i.e., radial, linear) are equivalent for all fracture zones intersected by the borehole. These restrictive conditions, in addition to other inherent analytical weaknesses, limit the application of Equation (3.13) to less quantitative corroborative uses.

T_i estimates based on nonradial fracture flow approaches include fracture zone/linear-flow and discrete fracture cubic law based applications. A general linear-flow analysis relationship relating T_i to fracture zone inflow rate and fracture characteristics was presented by Jenkins and Prentice (1982) as follows:

$$T_i = (q_i^2 \, t) \, / \, (\pi \, S_i \, L_i^2 \, \Delta h_i^2) \tag{3.14}$$

where L_i is the fracture length. With q_i and Δh_i determined from the multi-rate FFEC profile analysis, T_i can be calculated based on estimates for S_i and L_i. S_i can be estimated using the standard hydrologic expression based on formation and water properties, as originally presented by Jacob (1940):

$$S_i = \gamma_w \, m \, (\phi \, c_w + c_r) \tag{3.15}$$

where,

γ_w	=	fracture zone fluid specific weight,
m	=	fracture zone thickness,
ϕ	=	fracture zone porosity, and
c_w and c_r	=	the compressibility of the fracture zone fluid and rock matrix, respectively.

Fracture length, L_i, is normally not known during FFEC testing, but may be estimated by detecting the presence of a no-flow boundary response indicated during independent packer pumping tests conducted on the individual fracture zones (e.g., intersection of the early- and late-time slopes of arithmetic plots of well drawdown (Δh_i) versus the square root of test time (t) as noted by Jenkins and Prentice 1982). Because this information is not normally available during the conduct of a FFEC test, qualitative plots of T_i versus L_i can be developed to put a qualitative bound on fracture zone transmissivity. This approach was used for a possible fracture zone test within a deep borehole, completed in crystalline volcanic rock, as reported by Spane et al. (2012) and shown in Figure 3.6.

For cases in which points of inflow in the FFEC profile development can be described specifically to single, discrete fractures, the "cubic law" for fracture fluid flow can be applied, as discussed by Witherspoon et al. (1980). In this analysis approach, fracture hydraulic conductivity (K_i) for the discrete fracture can be derived from parallel planar plate flow theory and defined as follows:

$$K_i = b_i^2 \, \gamma_w \, / 12 \mu_w \tag{3.16}$$
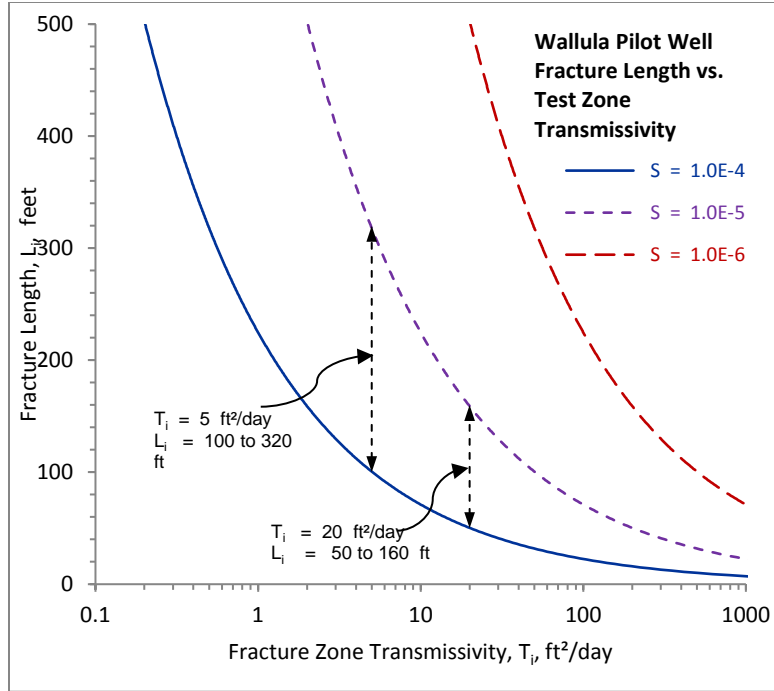
Figure 3.6. Qualitative Assessment of Fracture Length, L_i, versus Fracture Zone Transmissivity, T_i (modified from Spane et al. 2012).

where, γ_{w} and μ_{w} are the specific weight and dynamic viscosity of water within the fracture, respectively, and the fracture aperture (b_i) is described by the "cubic law" (e.g., Witherspoon et al. 1980) and is equivalent to

$$q_i / \Delta h_i = C \, b_i^3 \qquad (3.17)$$

where, the proportional, cubic flow constant, C, is defined for radial flow as follows:

$$C = [2 \, \pi / \ln (r_{out}/r_{wb})] \, (\gamma_w /12 \, \mu_w) \qquad (3.18)$$

and C for linear flow is equivalent to

$$C = (W_i/L_i) \, (\gamma_w /12 \, \mu_w) \qquad (3.19)$$

where, W_i and L_i equal the discrete fracture width and length (extent), respectively.

Based on the q_i and Δh_i estimates obtained from the FFEC profile analysis and the recognized flow regime operative during the test, estimates for the discrete fracture K_i and b_i can be obtained using Equations (3.16) through (3.19). Based on these estimates, discrete fracture zone transmissivity can be calculated using the standard hydraulic conductivity-thickness product relationship:

$$T_i = K_i \, m_i \qquad (3.20)$$

3.3 Test Limitations

A number of technical issues related to conducting FFEC profile tests in deep boreholes have not been adequately addressed by current test performance or analysis considerations. These issues impact the method's ability to calculate q_i and Δh_i, and therefore, its ability to calculate the individual fracture zone hydraulic conductive properties (i.e., T_i). These apparent test method issues include the following:

1. FFEC profile testing assumes that flow from the well is incompressible and fracture inflow responds immediately to pumping imposed during the dynamic (pumping) phase of the test. This assumption ignores the volume of water produced from wellbore storage, which, for lower transmissivity borehole sections, represents a significant water source during the early stages of the FFEC pumping test, specifically for relatively lower transmissivity fracture zones (T_i: 10^{-5} to 10^{-9} m^2/sec).

2. FFEC profile testing assumes the observed surface hydraulic head drawdown within the well is an adequate depiction of pressure-head drawdown occurring at the wellbore/fracture zone boundary, and that the *constant pumping rate* imposed during FFEC testing remains relatively uniform between and during FFEC profile runs. However, the change/increase in the borehole fluid-column density that occurs during the course of the FFEC test (due to inflow of much higher-density fracture fluid) causes pressure drawdown to be variable over the borehole depth. In this scenario, head-measured drawdowns measured at more shallow depth settings would exhibit greater composite borehole head drawdowns, because of the increase in fluid column density below the pump-setting datum. This variable fluid-column density effect is likely to be minor for low transmissivity fracture zone sections of the open borehole (because of less fracture zone high density fluid inflow), but would have some expected significant test impacts for fracture zone sections that have transmissivities of $T_i \geq 10^{-5}$ m^2/sec.

3. Radial flow-based, analytical equations used in calculating fracture transmissivity (T_i) are valid, but their use is restrictive. Transient analysis solutions, e.g., Cooper and Jacob (1946) require infinite-acting radial flow (IRF) conditions to be established (no wellbore storage effects and no outside boundary effects evident), which, for open borehole tests where lower-permeability formation conditions exist, may take considerable time to achieve. Additionally, steady-state–based methods (e.g., Thiem 1906) require even longer time period constraints to be fully applicable, because they assume a steady/stabilized drawdown response within the fracture zone (outside recharge = pumping discharge). Discrete fractures commonly exhibit linear-flow test conditions during early-test times, which eventually transition to radial flow conditions much later in the test. Knowing when wellbore storage effects are diminished and what flow model condition(s) are operative during testing (e.g., linear, bi-linear, or radial) is important for proper selection of the appropriate analytical approach.

4. Well skin caused by drilling-induced alteration of surrounding rock hydraulic properties surrounding the borehole (i.e., either enhancement → negative skin or damage → positive skin) will significantly affect fracture zone q_i and h_i estimates based on FFEC profile analysis. Well-skin conditions, however, can only be quantitatively assessed by using more in-depth, packer hydrologic tests (e.g., pumping, drill-stem).

5. The well drilling process commonly uses an overbalanced or positive pressure borehole fluid condition to support borehole stability and removal of drilling debris produced during borehole advancement. The over-pressure duration, magnitude during drilling, and hydraulic properties of the intersected fracture zone largely control the propagation of higher/elevated pressures into the surrounding fracture zone network. These elevated fracture zone pressure conditions can persist for extended periods of time after cessation of drilling and may adversely affect FFEC tests conducted during the course of borehole drilling (as originally proposed by Tsang et al. 2016).

6. For FFEC tests using replacement of existing borehole fluid with a highly contrasting low-salinity/density fluid as an initial test condition, the circulation emplacement of the low-density fluid

within the borehole causes transient fracture fluid inflow to occur from intersected fluid conveying fractures due to the imposed lowering of the borehole pressure/depth profile.

With regard to Issue 1, wellbore storage provides a significant source of water that is pumped during the early-test time phases of constant-rate pumping tests for relatively lower transmissivity test sections. The contribution of pumped water from wellbore storage can adversely affect the validity of using analytical test methods that assume that water is produced instantaneously and only from fractures zones beginning at test initiation (i.e., proportional to the pumping rate and the ratio of the individual fracture zone transmissivity (T_i) to the total test interval transmissivity (T_{tot}); e.g., Equation (3.13).

Figure 3.7 shows the transition times from pure wellbore storage (i.e., 100% of water pumped purely from wellbore volume drawdown) to initiation of flow from a fracture zone, as a function of the composite fracture zone transmissivity during pumping. As shown in the figure, discernable fracture flow starts to be contributed at ~5 min for a fracture zone for which $T_i = 10^{-5}$ m^2/sec, and ~500 min for a $T_i = 10^{-7}$ m^2/sec fracture zone. Figure 3.8 shows a more detailed simulation of the instantaneous fracture flow inflow contribution as a percentage of the total pumping rate (i.e., q_i /Q_{tot}; where $Q_{tot} = q_i + q_{wb}$). As indicated in the figure, at a test time of ~200 min, 90% of the instantaneous pumped discharge is provided by a fracture zone for which $T_i = 10^{-5}$ m^2/sec, while a fracture zone for which $T_i = 10^{-6}$ m^2/sec takes until ~2,000 min to achieve a similar percentage of fracture flow contribution. Another important feature exhibited in Figure 3.8 is the demonstration that while the surface pumping rate (Q_{tot}) is at a constant rate, *the inflow rate from the fracture zone (q_i) is continually increasing with time during the course of pumping*. A continuously varying q_i condition during the test adversely affects analytical methods that assume constancy in fracture inflow, either as a basis for determining q_i from FFEC profile analysis or as an analytical consideration when calculating fracture zone T_i.

To minimize the potential adverse impact of wellbore storage contributions during FFEC pumping tests, the following practices are recommended:

- Use a smaller test tubing and packer system to reduce the open well diameter.
- Conduct the FFEC test as a constant-drawdown test.

Wellbore storage is a function of the square of the casing radius (r_c) where drawdown in the well (due to pumping) is occurring. If the internal well casing radius were effectively reduced by using an internal packer-tubing string from 0.114 m to 0.045 m, this would decrease the test time when wellbore storage effects are significant during pumping by a factor of ~6. Additionally, conducting the FFEC test as a constant-drawdown test (instead of at a constant rate) by rapidly drawing the fluid column down to a set depth in the borehole and maintaining this level for the duration of the FFEC test would effectively remove the wellbore storage component to Q_{tot} for the remainder of the test.

To examine the impact that varying fluid-column density has on observed pumping test drawdown during an FFEC test (Issue 2), as determined by the fluid-column height above a fracture zone, a semi-log drawdown plot was developed for a fracture zone for which $T_i = 10^{-5}$ m^2/sec (Figure 3.9). The figure shows the predicted drawdown (Δh_D) based on a freshwater, uniform-density fluid-column height (i.e., $\rho_w = 1.000$ g/cm3) as calculated from test pressure measurements made either near the top of the fluid column (e.g., pressure transducer mounted on the submersible pump) or at a fracture zone depth (in this example 2,000 m). The difference in the observed ΔhD values shown is based on the depth of fluid-column measurement (i.e., shallow vs. deep) and the non-uniform fluid-column density conditions during pumping due to the incursion of higher-density fracture fluid (i.e., in this example, $\rho_i = 1.016$ g/cm3) into the borehole during the test. The fracture fluid density (ρ_i) used in the figure comparison is based on calculations for fracture zone water with a total dissolved solids content of 35,000 mg/L at a temperature of 60°C and a pressure of 17.9 MPa (Millero et al. 1980). For homogeneous/uniform fluid-column density
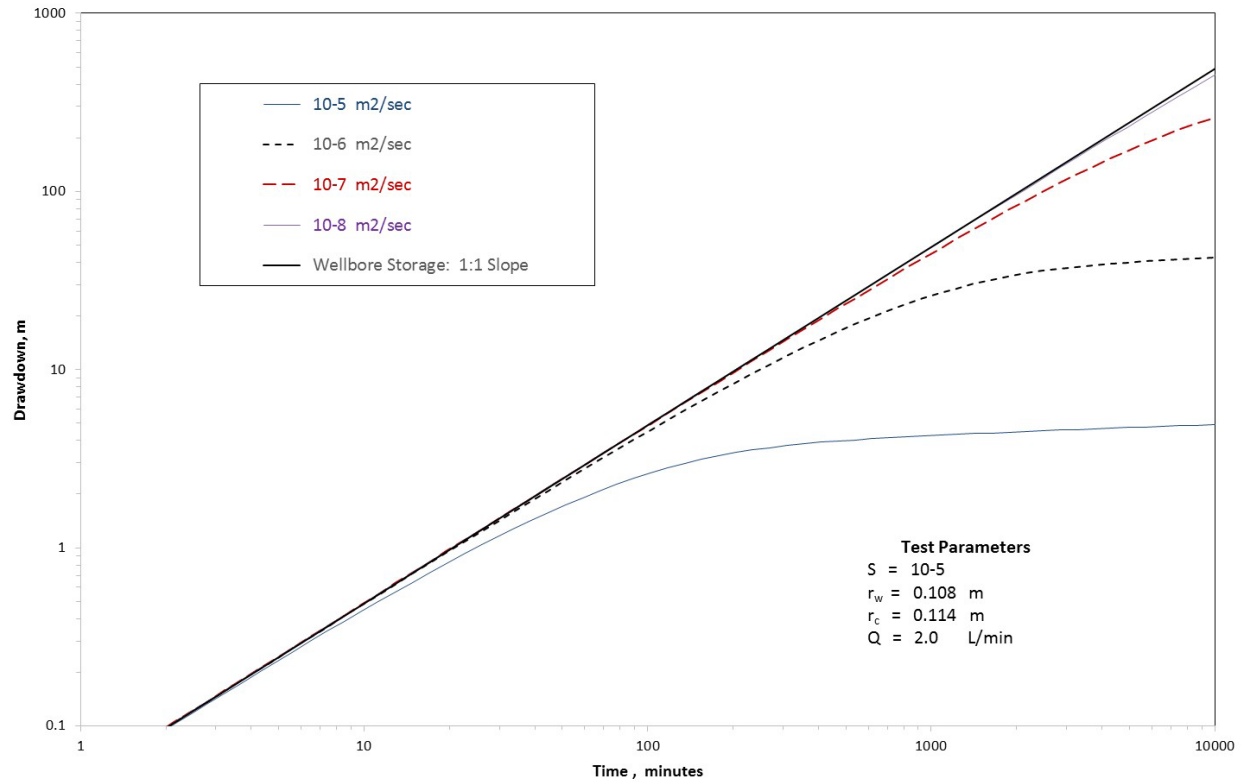
Figure 3.7. Predicted Duration of Wellbore Storage Effects for Selected Fracture Zone Transmissivities (T_i)

(ρ_{fc}) conditions, changes in drawdown pressure (ΔP) and head (Δh_D) would be identical whether the pressure measurements were taken at the top or bottom of the fluid column (i.e., $\Delta P_t = \Delta P_b$; and $\Delta h_{Dt} = \Delta h_{Db}$). Changes in drawdown pressure would not be the same, however, for non-uniform fluid-column density conditions that would arise during FFEC tests, in which much higher-density fracture fluid-density inflow (ρ_i) is expected. This would change the overly ρ_{fc} conditions above the point of pressure measurement, if significant fracture zone inflow were to occur. The higher ρ_{fc}, condition indicates a lower fluid-column height (h_{fc}) that would occur, which, measured at a location near the top of the fluid column (where uniform fluid-column density conditions are maintained), would indicate significantly larger well drawdown conditions (i.e., $\Delta h_{Dt} > \Delta h_{Db}$). The indicated increase in the drawdown (i.e., $\Delta h_{Dt} > \Delta h_{Db}$) relationship, due to incursion of higher-density fracture fluid inflow (ρ_i) is shown in Figure 3.9 for two pumping rates (Q = 2 and 6 L/min) for the listed well test conditions. As shown, significant differences in $\Delta h_{Dt} > \Delta h_{Db}$ occur with different pumping test times, and the greatest differences are exhibited for the higher pumping rates. To minimize the uncertainty of knowing the temporal impact of the non-uniformity of fluid-column density effects, periodic stationary downhole pressure measurements at the base of each fracture zone are required. These measurements are obtained with the wireline probe assembly used in the FFEC profile survey development. These periodic measurements are then used as the basis for calculating Δh_{Db}, and these calculations should not be based on Δh_{Dt} obtained from pressure probe measurements obtained near the top of the well fluid column. Spane and Mercer (1985) present a program that may be useful for quantifying the impacts of fluid-column density variation due to salinity, temperature, pressure, and gravitational acceleration variation on hydraulic head calculations within deep borehole settings.

As noted under Issue 3, radial flow-based transient and steady-state analysis solutions both require that IRF conditions be established (no wellbore storage effects and no outside boundary effects evident) during the test for their applications to be valid. For open borehole tests in which lower-permeability
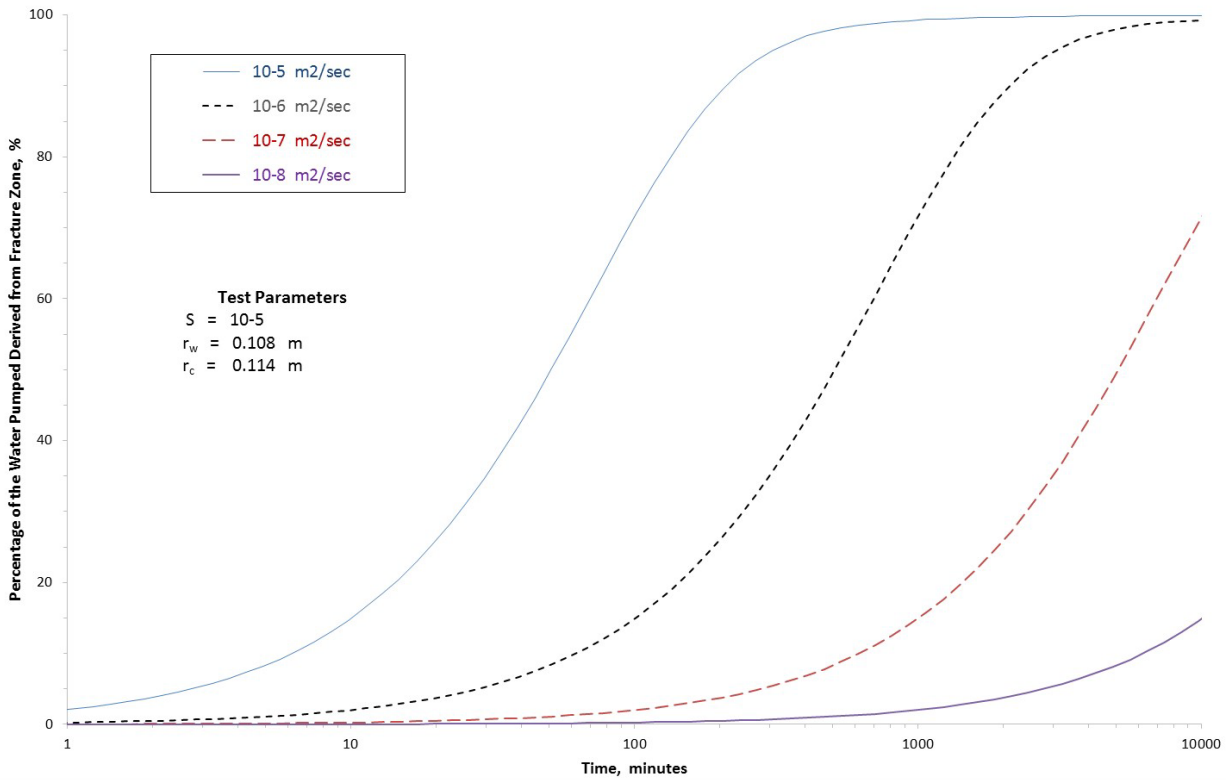
Figure 3.8. Predicted Percentage of Instantaneous Fracture Zone Discharge (q_i) for Selected Fracture
Zone Transmissivities (T_i) versus Pumping Time

formation conditions exist, establishment of IRF conditions may take considerable time to achieve. The
use of derivative plots has been shown to significantly improve the diagnostic and quantitative analysis of
various hydrologic test methods (Bourdet et al. 1989; Spane 1993; Spane and Wurstner 1993). The
improvement in test analysis is attributed to the sensitivity of pressure derivatives to various
test/formation/boundary conditions. As noted by Spane and Wurstner (1993), specific applications for
which derivatives are particularly useful include the following:

- identifying established flow regimes (e.g., radial, linear), presence of wellbore storage, formation-
  response characteristics (non-leaky or leaky; confined or unconfined aquifer), and presence of
  surrounding boundary conditions (impermeable or constant head);

- assisting in the selection of the appropriate type-curve solution through combined type-
  curve/derivative plot matching; and

- determining when wellbore storage effects are over, and whether IRF conditions have been
  established.

To assess when wellbore storage effects are over and when IRF conditions have been fully established,
diagnostic derivative analysis plots can be used for guidance, based on the anticipated range of fracture
zone T_i values to be encountered. For the indicated IRF established test time periods, the Cooper-Jacob
and Thiem equations can be used with q_i and Δh_i obtained from FFEC profile analysis during the IRF-
indicated time period to determine the fracture zone T_i. IRF conditions are established when the change in
pressure drawdown, at the point of observation, increases proportionately to the logarithm of time (i.e.,
change in derivative slope = 0).
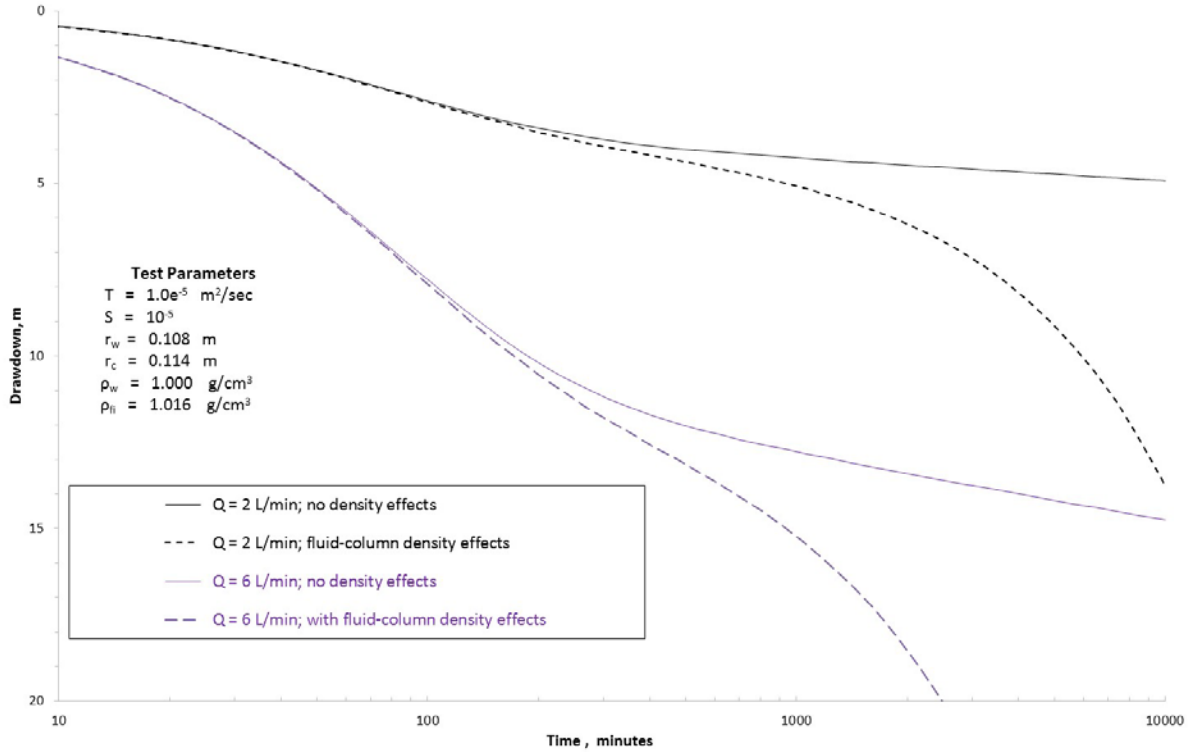
Figure 3.9. Predicted Drawdown as Measured at the Top of the Well Fluid Column under Uniform and Non-Uniform Fluid-Column Density Conditions

As an example, Figure 3.10 shows the diagnostic dimensionless drawdown (s_D) vs. dimensionless time (t_D)/wellbore storage, C_D plot for test conditions shown in Figure 3.7, which can be used for determining the establishment of IRF conditions. These standard dimensionless parameter groupings are those defined by Earlougher (1977) and Moench (1997), as follows:

$$s_D = (4\pi T \Delta h)/Q \tag{3.21}$$

$$t_D = (T t)/(r_{wb}^2 S) \tag{3.22}$$

$$C_D = r_c^2/(2 r_{wb}^2 S) \tag{3.23}$$

Dividing Equation (3.22) by Equation (3.23) yields:

$$t_D/C_D = (2Tt)/r_c^2 \tag{3.24}$$

As indicated in Figure 3.10, the wellbore storage-dominated test response has transitioned to IRF conditions at a dimensionless t_D/C_D value of ~150. For a T_i value of 10^{-5} m^2/sec, this equates to an initiation time for IRF conditions of ~1,620 min, calculated using Equation (3.24). Because IRF time is inversely proportional to T_i, the estimate for IRF time for lower T_i values is equally proportional logarithmically, e.g., $T_i = 10^{-6}$ m^2/sec; IRF time = ~16,200 min. Of particular note is that if the recommendation of using a smaller radius packer test tubing were applied, Equation (3.24) indicates that a significant reduction in IRF time would be realized. For example, if a packer test tubing radius of 0.045 m were installed and set inside the existing 0.114 m well casing, establishment of IRF test conditions would be reduced from 1,620 min (for a $T_i = 10^{-5}$ m^2/sec fracture flow) to 245 min.

3.17
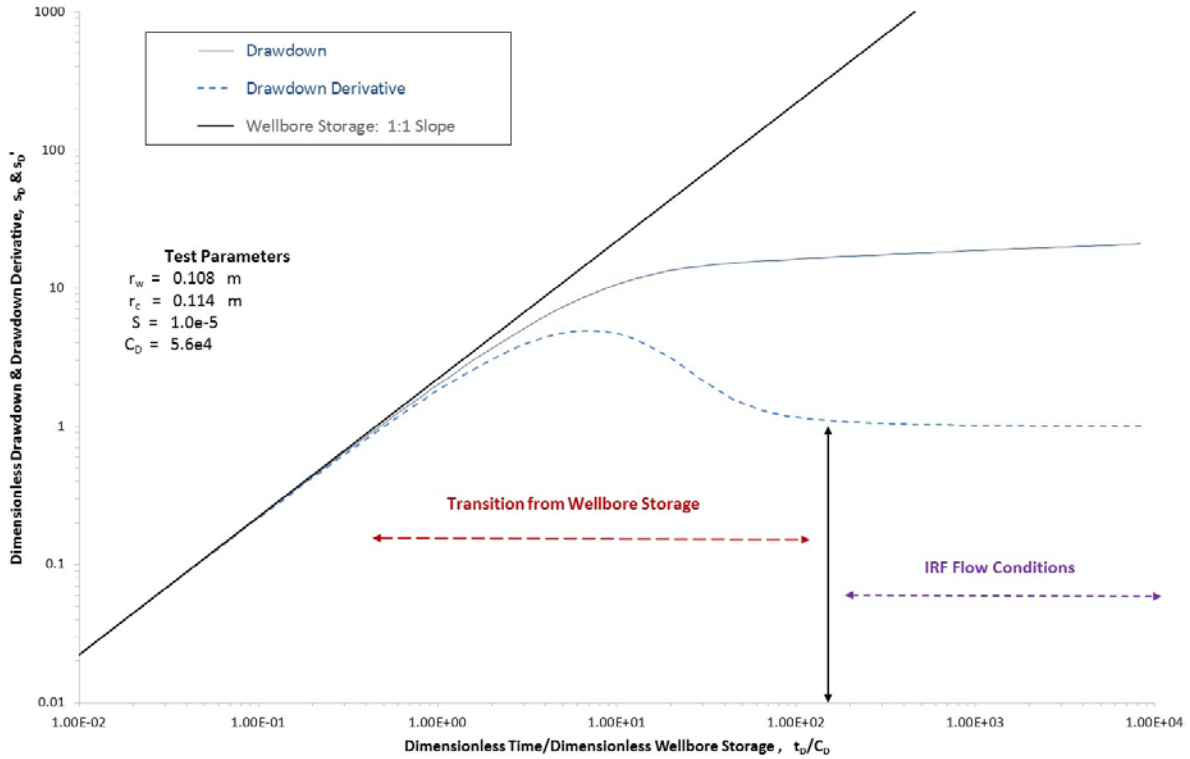
Figure 3.10. Dimensionless Plot for Determining the End of Wellbore Storage and Establishment of IRF Conditions

Similarly, the effects of well skin (s_K) (Issue 4) have a direct bearing on establishing IRF conditions. For a borehole that is damaged by drilling a positive skin is indicated and the start of IRF conditions is delayed, while for negative skin conditions with borehole permeability enhancement, IRF conditions occur earlier n the test time. Figure 3.11 is a semi-logarithmic plot of the drawdown derivative for the same test conditions shown in Figure 3.10. For comparison purposes relative to the "no well-skin" case, well-skin values of +5 and -5 are shown, as well as the IRF plot depicting where no wellbore storage or well-skin conditions exist. As shown in Figure 3.11, negative well-skin derivative response exhibits an earlier (i.e., faster) transition to IRF conditions than does the "no skin" case, while the positive well skin indicates a delay or later transition to the IRF test response.

With respect to Issue 5, the well drilling process commonly uses an overbalanced or positive pressure borehole fluid condition to support borehole stability and removal of drilling debris produced during borehole advancement. The duration and magnitude of over-pressure during drilling, together with the hydraulic properties of the intersected fracture zone, largely control the propagation of higher/elevated pressures into the surrounding fracture zone network. These elevated fracture zone pressure conditions can persist for extended periods of time after cessation of drilling, and they may adversely affect FFEC tests conducted during the course of borehole drilling (as originally proposed by Tsang et al. [2016]). Pre-test drilling-induced conditions have been noted to adversely affect standard hydraulic packer tests (e.g., Pickens et al. 1987), and similar impacts would be expected to influence the test responses related to FFEC pressure/inflow.

To examine the relative magnitude of drilling-imposed pressure effects on subsequent FFEC test conditions, pressure/distance profiles were developed for the composite borehole fracture transmissivity range of 10^{-5} to 10^{-9} m^2/sec and for an assumed drilling-imposed borehole over-pressure head (i.e., above static fracture zone conditions) of 2 MPa (~200 m). The assumed imposed drilling pressure is arbitrary
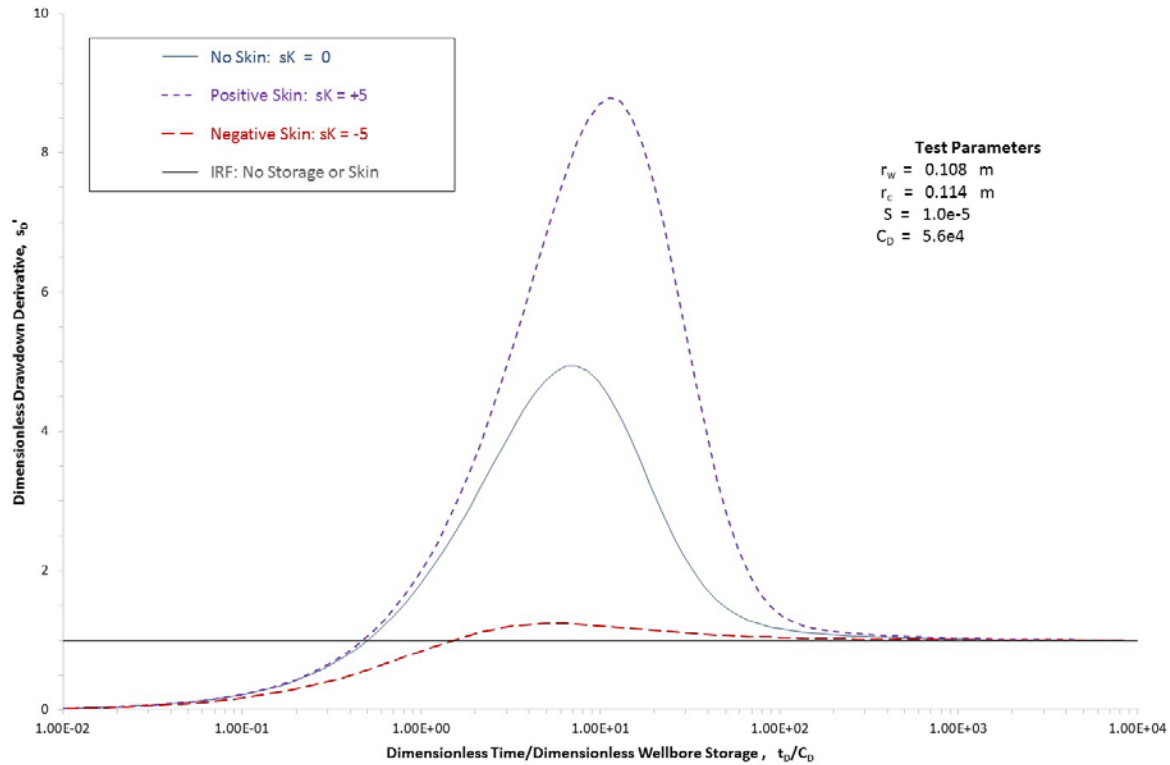
Figure 3.11. Semi-Logarithmic Dimensionless Derivative Plot Comparison for Well-Skin Conditions 0, +5, and -5

and based on overbalanced drilling conditions, which produce a borehole pressure that is greater than in-situ fracture zone pressure conditions. The simulations were developed using the analytical modeling program AQTESOLV (Duffield 2007, 2009). Drilling fluid was assumed to flow freely from the borehole into the fracture zones (due to the over-pressure borehole condition), and without being impeded by mud-cake or well-skin/damage effects. The modeling was also based using the following time-history element conditions:

- 10 days of drilling with a composite borehole over-pressure of 2.0 MPa
- 1-day of recovery following cessation of drilling and preparation for FFEC testing
- 2 days of FFEC testing using a constant pumping/extraction rate of 2 L/min.

Figure 3.12 shows a comparison of the simulated pressure/distance profiles that were developed using AQTESOLV for a composite fracture zone transmissivity of 10^{-6} m^2/sec for three time-history points: at the end of 10 days of drilling, pre-FFEC (1-day of recovery), and at the end of the 2-day FFEC test. This time-history approach of combining sequential testing activities is consistent with the application of the principle of superposition, which is commonly applied in hydrologic studies (e.g., Reilly et al. 1987). As shown, drilling-imposed pressure-head perturbations after 10 days of drilling are significant (i.e., ~200 m at the wellsite) and the area of influence extends out to a distance of ~900 m from the well. For this given composite fracture zone transmissivity, the imposed pressure effects diminish with distance from the well during the 1-day of recovery after cessation of drilling and prior to FFEC test initiation. However, the pressure effects remain significant during the course of the 2-day FFEC extraction/pumping test (also shown in the figure). For comparison purposes, the static fracture zone pressure and simulated pressure distance drawdown relationship that would have developed if drilling over-pressure conditions were not imposed are also indicated.

Figure 3.12. Impact of Borehole Drilling Over-Pressure Effects on Simulated Pressure/Distance Relationships Prior to and at the Completion of a FFEC Pumping Test: $T_i = 1.0e\text{-}6$ m^2/sec

In addition to producing a different pressure distance profile in comparison to non-perturbed in-situ fracture zone conditions, the observed pre-test borehole pressure after termination of drilling will exhibit a significant negative/reducing pressure trend during the performance of FFEC testing. This background trend in most cases would not be recognizable without significant baseline monitoring, and without adequate pre-test delineation it would bias the magnitude of observed drawdown exhibited during FFEC testing. To illustrate this bias, Figure 3.13 compares the apparent distance/drawdown profiles (based on observed pre-test borehole conditions) at the end of a 2-day FFEC test with and without drilling over-pressure effects. As shown in the figure, not adequately accounting for the effects of drilling over-pressure (i.e., the pre-test pressure trend) would bias the observed/apparent drawdown recorded in the borehole. For this example, nearly a factor of two increase in the amount of drawdown over actual fracture zone drawdown conditions is indicated (e.g., in Figure 3.13 @ $r_{wb} = 0.108$ m; without drilling effects, $\Delta hD = 37$ m; with drilling effects trend, apparent $\Delta hD = 73$ m). Not accounting for drilling-imposed pressure effects, therefore, would produce an under-estimation of fracture zone transmissivity (T_i) by a factor of ~2 when calculated using the Thiem relationship commonly used for FFEC test analysis (i.e., Equation (3.5)). Similar T_i under-estimation relationships were exhibited for other fracture zone transmissivities over the range of 10-5 to 10-9 m2/sec and using the identical test/time-history conditions.

In contrast to over-pressuring of the borehole due to drilling practices, for FFEC tests using replacement of existing borehole fluid with a highly contrasting lower-salinity/density fluid as an initial test condition, the circulation emplacement of the low-density fluid within the borehole causes transient fracture fluid inflow to occur from intersected fluid conveying fractures due to the imposed lowering of the borehole pressure/depth profile (Issue 6). Assuming that the replacement low-salinity/density fluid is circulated from the bottom of the borehole and pumped from near the top of the borehole fluid column at identical
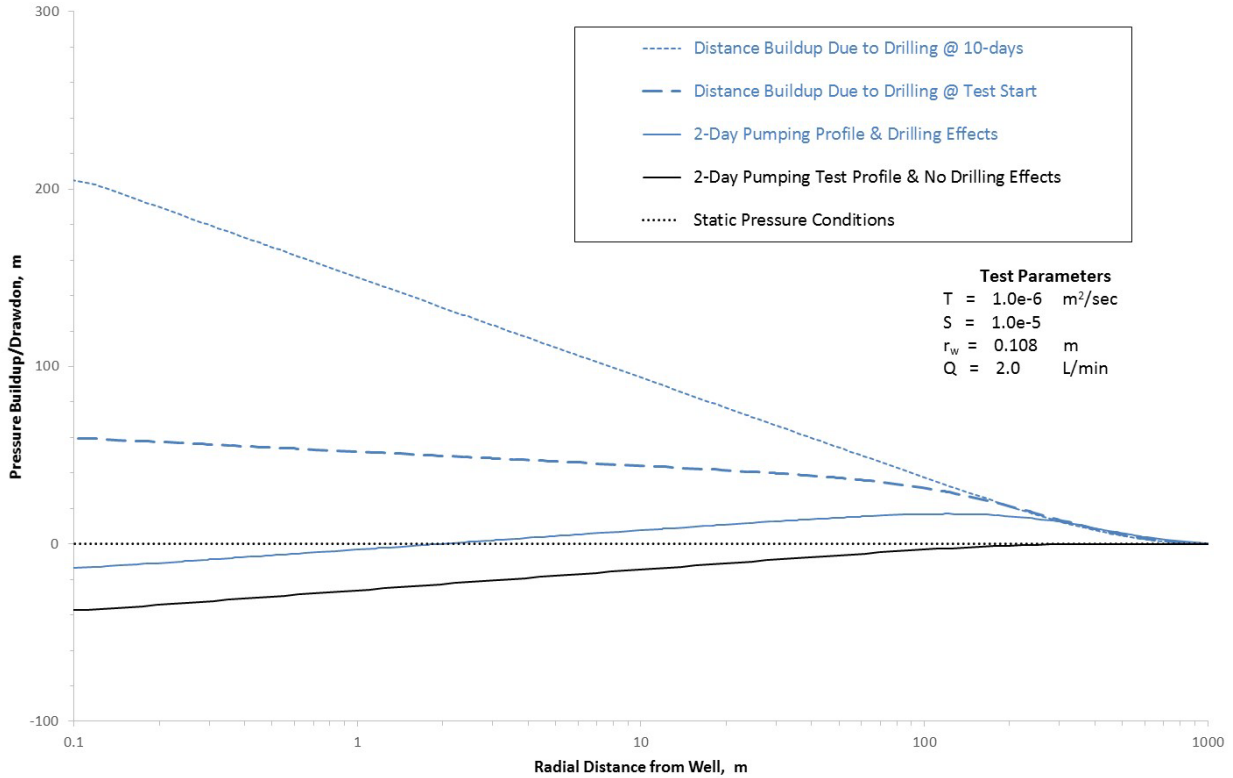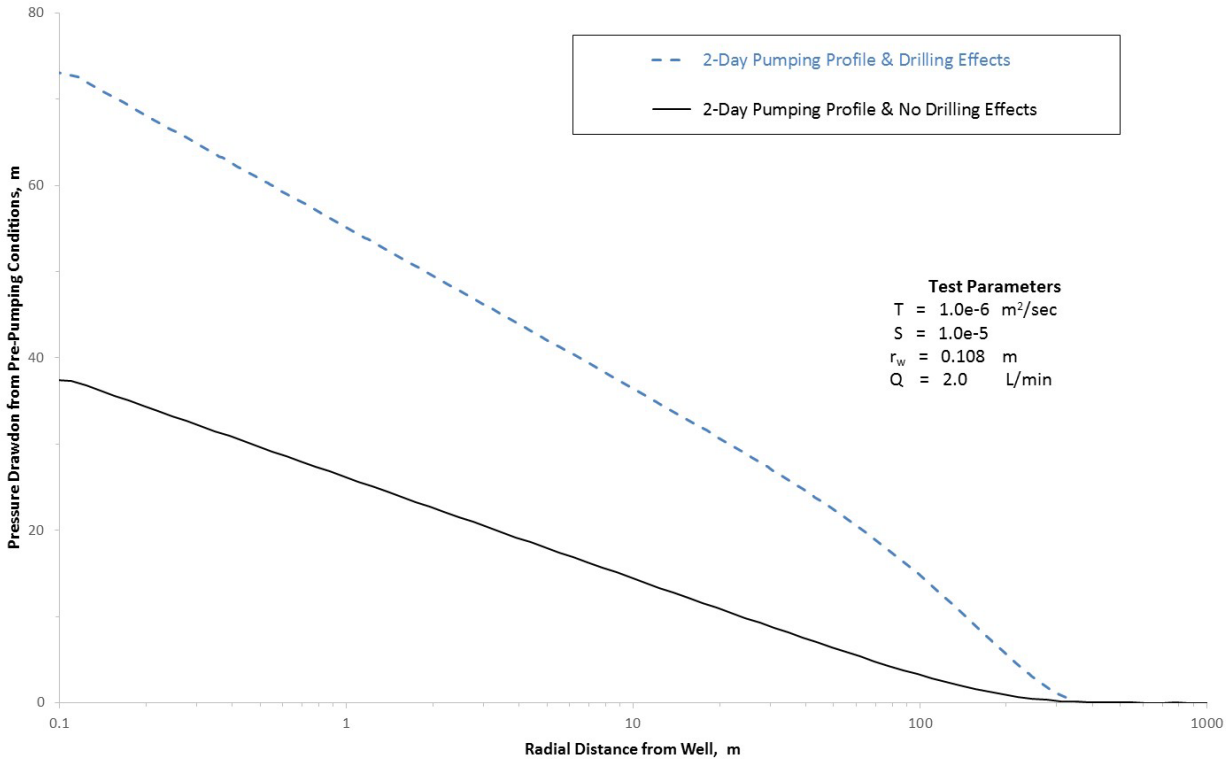
Figure 3.13. Impact of Drilling Borehole Over-Pressure Effects on Simulated Pressure/Distance Drawdown Relationships at the Completion of a FFEC Pumping Test: T_i = 1.0e-6 m^2/sec

injection/extraction rates (to minimize borehole pressure perturbations as recommended by Tsang et al. [1998]), then the pre-FFEC test emplacement of lower density fluid will cause fracture zone inflow to occur during the pre-test period. This fracture zone inflow is transient in behavior (both temporally and with depth location), because the fluid-column density above the fracture zone location continuously changes.

To assess fracture zone inflow characteristics during the pre-test fluid-column replacement process, maximum fluid-column pressure changes along a 5 km deep borehole interval were calculated based on contrasting fluid-density conditions. To maximize fluid-column density contrasts, it was assumed that the initial borehole salinity was equivalent to the fracture zone fluid salinity concentration set at 100 g/L, while the circulated borehole replacement fluid was assumed to be 0.5 g/L. Based on these assumed fluid salinities, associated fluid densities were calculated using an Excel calculator worksheet (Earthward Consulting 2016) that is based on the analytical relationship presented by McCutcheon et al. (1993), which accounts for temperature and salinity effects. As noted by Spane and Mercer (1985), fluid density within deep boreholes is also affected by pressure and changes in gravitational acceleration within the borehole, but their impacts on fluid density are significantly less than either temperature or salinity and will be ignored for this discussion. Subsurface groundwater-flow investigations based on borehole pressure gradients (i.e., pressure/depth) are commonly based on assuming constant fluid-density conditions with depth. For example, the standard freshwater pressure/depth gradient value commonly cited for making field comparisons is equal to 9.797e-3 MPa/m (0.4331 psi/ft; Earlougher 1977).

Based on a standard constant reference temperature of 15.556°C, the fluid density (ρ_w) for the circulated replacement fluid with a salinity of 0.5 g/L is calculated to be 0.99943 g/cm^3. For the assumed fracture zone and initial borehole fluid column that have a salinity of 100 g/L, a fluid density of 1.07699 g/cm^3 is

indicated using the calculator provided by Earthward Consulting (2016). These fluid-column density values yield a borehole pressure gradient of 1.057e-2 MPa/m for the initial borehole fluid-column condition filled with fracture zone fluid (i.e., 100 g/L), and 9.801e-3 MPa/m after replacing the borehole fluid with the lower-salinity (0.5 g/L) contrasting fluid to be used during the FFEC test. For a deep borehole with an open interval between depths of 2 and 5 km, this represents a theoretical reduction of borehole pressure of 1.52 and 3.80 MPa over the indicated respective depths (2 and 5 km). This depth-dependent reduction of borehole pressure produces a transient test condition prior to initiation of the FFEC test, which would induce fracture zone inflow to occur to the borehole during the low-salinity borehole fluid emplacement.

To examine the magnitude of fracture zone inflow during pre-test emplacement of the low-salinity borehole fluid, AQTESOLV was again employed, using the constant pressure analysis method presented originally by Jacob and Lohman (1952) for estimating discharge from artesian flowing wells. Figure 3.14 shows the predicted borehole inflow from a fracture zone with a T_i equal to 10^{-6} m^2/sec at a depth of 5 km for the previously identified borehole pressure reduction of 3.80 MPa during pre-test borehole fluid emplacement. The figure shows the predicted fracture zone inflow for an "instantaneous" emplacement of the low-salinity/density borehole fluid, and for a more gradual fracture zone inflow condition that would occur during circulation emplacement of the low-density fluid. As indicated in Figure 3.14, at a circulation/emplacement rate of 189 L/min, fracture zone inflow builds up gradually until the fluid column is completely replaced (i.e., ~970 min) with the low-salinity/density emplacement fluid; thereupon, it coincides with the predicted inflow for instantaneous replacement.

It should be noted, however, that this fracture zone inflow depiction does not account for the inflow of higher-density fracture zone fluid in the overall circulation model. If it were accounted for, fracture zone inflow would be further reduced, due to the reduction in the overlying fluid-column pressure change, caused by circulation emplacement of the low-salinity/density fluid. These effects were not considered as part of this investigation and are inconsequential (due to low inflow rates) for fracture zones having T_i values of $\leq 10^{-8}$ m^2/sec. After termination of the emplacement of low-density borehole fluid, borehole pressures would exhibit an increasing pressure trend prior to FFEC test initiation due to the induced fracture zone inflow of higher-salinity density fluid. This pre-test trend, if not taken into account, would bias estimates of q_i and Δh_i obtained from FFEC profile analysis, and subsequently provide inaccurate estimates of fracture zone T_i, as discussed previously for Issue 5 and over-pressure borehole conditions.
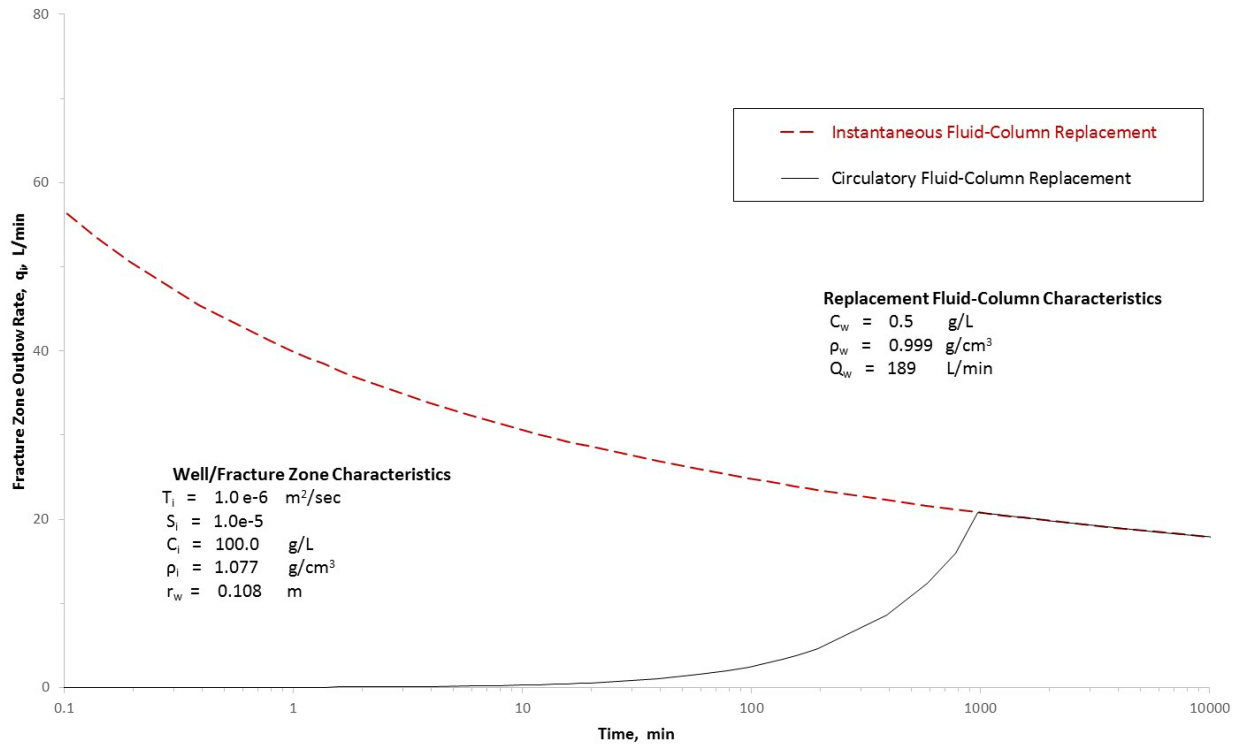
Figure 3.14. Simulated Fracture Zone Inflow Rate during Lower-Salinity/Density Fluid-Column
Replacement

3.4 Test Alternatives

A number of possible alternatives to or variants of the FFEC profile testing method exist for establishing the permeability profile of relatively large open borehole sections. Two techniques that might be considered in-lieu of or as a comparison to FFEC testing include 1) a tracer-injection flow-log (TIFL) method and 2) a tracer-dilution circulation (TDC) testing technique. Neither method has been used as extensively as FFEC profile analysis in deep borehole testing, and both share or have test limitations in addition to those previously identified for FFEC profile analysis. It is worth identifying and briefly describing these techniques, however, in case there is an opportunity to test their performance at deep borehole locations.

3.4.1 Tracer-Injection Flow Log

Gräsle et al. (2003) report results for a TIFL test conducted at a deep borehole site. The test was conducted over a relatively small open borehole test interval (150 m) between the depths of 3,850 and 4,000 m. The method is comparable to FFEC testing in its performance simplicity, does not require use of an in-well submersible pump, and uses similar wireline-based probe sensors to mark the travel front of a salinity-contrast–based tracer that is injected into the well above the test interval. For this test, freshwater was injected, which provided a significant fluid conductivity/resistivity contrast to the resident saline water present within the well. The injection of freshwater was conducted as a "constant-head" or pressure test by simply keeping the well filled to the land surface. Injection flowrates were recorded periodically by terminating water addition to the well casing and monitoring the decline of well water levels vs. time over relatively short well depth distances. This eliminated the need to use in-line flow meters to monitor

injection well rates/volumes, thereby additionally simplifying the process. The injection was performed over a 7-day period and a total of 4.8 m^3 of freshwater were injected during this time ($Q_{avg} \sim 0.5$ L/min).

During the injection, the freshwater/saltwater transition boundary moved downward, and fluid outflow to receptive permeable fracture zone features occurred. The tracer transition front was monitored using a multi-probe sensor, which included measurements for fluid resistivity, temperature, and pressure, as well as a total gamma ray tool used for depth correlation purposes. The tracer front velocity was measured in two ways: 1) logging continuously through the boundary and marking its depth position over time, and 2) then after advancing to a known depth/distance below the tracer front (a "standstill phase"), at which to monitor the arrival of the tracer front boundary. The developed tracer velocity profile can be converted to a borehole flow log (Q_b) versus depth by multiplying it by the caliper-based borehole area/depth profile. The base/depth of major outflow zones is indicated by a significant decrease in the Q_b profile. The results of this test indicated one major fracture zone outflow zone at a depth of ~3,950 m. The fracture zone outflow rate (q_i) can be estimated by subtracting the Q_b values immediately above and below the indicated fracture zone depth. Gräsle et al. (2003) used a non-steady, variable head model to match the resistivity profile indicated by the flow-log results. The model-matching procedure was required because the replacement of the well saline water with freshwater created a variable injection head condition during the 7-day test. This is similar to an earlier technical test limitation identified for FFEC testing.

To qualitatively assess the applicability of the TIFL test for other deep borehole settings, simulated tracer flow-front travel velocities were generated using the gamma-function relationship originally presented by Jacob and Lohman (1952). It can be used to estimate well injection rates under constant injection pressure conditions. Figure 3.15 shows the predicted vertical downward movement of an injected tracer flow-front
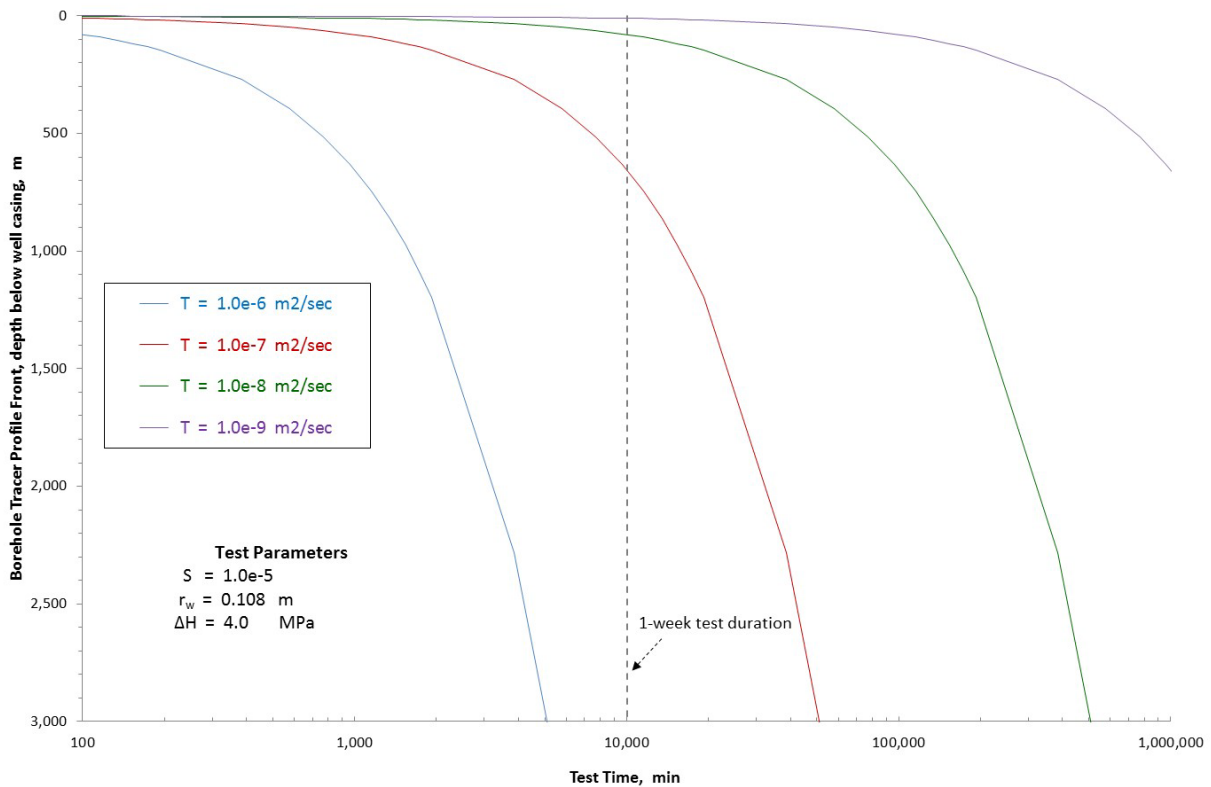

Figure 3.15.   Predicted Vertical Downward Movement of an Injected Tracer Flow-Front Boundary versus Time as a Function of Fracture Zone Transmissivity, T_i: 10^{-6} to 10^{-9} m^2/sec.

boundary by simple-piston flow displacement over time, as a function of fracture zone T_i, ranging between 10^{-6} and 10^{-9} m^2/sec. As shown, even using a relatively large constant injection pressure head of 4 MPa, the vertical displacement of the tracer front boundary over large open borehole distances (e.g., 1000 m) would be limited to underlying fracture zones having T_i values $>10^{-6}$ m^2/sec for injection tests of 1- to 2-day durations. Gräsle et al. (2003) came to a similar conclusion about the practicality of using the TIFL method for characterizing large deep borehole test sections.

3.4.2   Tracer-Dilution Circulation Method

Brainerd and Robbins (2004) describe the successful application of a TDC test using fluorescent dye (uranine) to resolve fracture zones within a relatively shallow crystalline bedrock setting (i.e., <100 m depth). The application is discussed here because earlier, successfully completed TDC tests were conducted at the Leuggern borehole in Switzerland over a much greater depth interval (1,635 to 1,689 m), although these earlier tests were conducted and deployed in significantly different fashion than the tests reported in Brainerd and Robbins (2004).

For the TDC test method described by Brainerd and Robbins (2004), a tracer solution is continuously injected at a constant rate (Q_{in}) via an injection tube at the base of the open borehole test interval, and water is extracted from the well at a constant rate (Q_{out}) using an in-well submersible pump set above the test interval, as shown in Figure 3.16. (Note: this in-well equipment deployment is similar to that described for emplacement of salinity-contrasting borehole fluid prior to initiating FFEC profile testing). The extraction pumping flow rate is designed to be greater than the continuous tracer-injection rate (i.e., $Q_{out} > Q_{in}$; $Q_{dif} = Q_{out} - Q_{in}$) and produces a net wellbore head drawdown (Δh_D). The net well drawdown imposed by the tracer circulation causes intersected fractures by the borehole to produce inflow to the well, assuming that the composite head in the well (h_D) is less than that of the fracture zone (i.e., $h_D < h_i$). The inflow of fracture fluid from fracture zones is deficient of tracer, and thus "dilutes" the tracer solution concentration (C_{in}) that is injected at the base of the test interval and circulated (bottom to top) within the borehole. To facilitate the inflow of all fractures intersected by the borehole during the TDC test, Brainerd and Robbins (2004) recommend that the initial Q_{dif} used be selected to be "…as high as possible, without dewatering the bedrock…." Steady-state flow conditions within the well are suggested after well drawdown (Δh_D) and the tracer concentration within the pumped water from the well (C_{out}) have stabilized. After steady-state flow drawdown and dilution conditions are indicated, discrete fluid depth sampling is performed to establish the tracer depth profile during the TDC test (see Figure 3.15).

Brainerd and Robbins (2004) use the Thiem (1906) steady-state relationship shown in Equation (3.5) to calculate fracture zone transmissivity. As discussed in Section 3.2.1, application of the Thiem equation to calculate fracture zone transmissivity (T_i) requires determination of both the fracture zone inflow rate (q_i) and hydraulic head conditions (h_i). The q_i for individual fracture zones is calculated based on the dilution of the injected tracer solution concentration profile using the following relationship reported by Brainerd and Robbins (2003):

$$q_i = Q_{in} (C_{bf} - C_{af})/C_{af} \qquad (3.25)$$

where, C_{bf} and C_{af} represent the tracer solution concentration within the borehole immediately below and above the fracture zone, respectively.

Equation (3.25) is only valid for the restrictive condition for a fracture zone where there are no contributory fracture inflow zones below it. For conditions under which multiple fracture zones contribute inflow to the circulated tracer solution, Brainerd and Robbins (2004) recommend that Equation (3.25) be
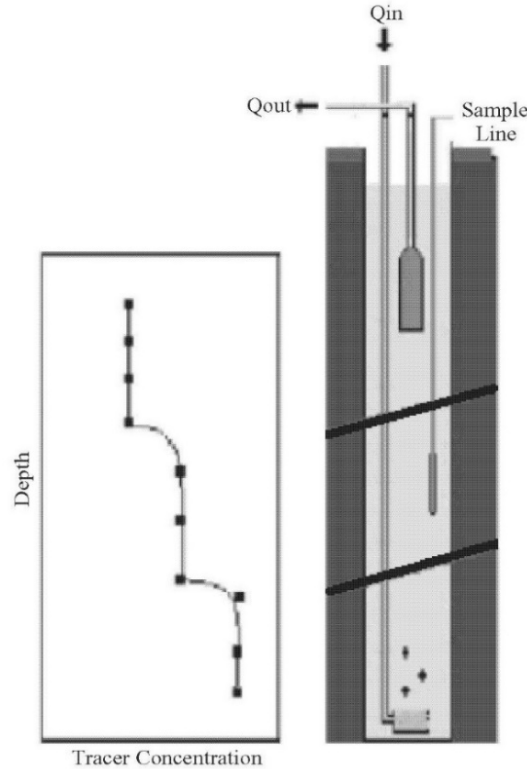
Figure 3.16. Schematic of In-Well Equipment Deployment and Conceptual Concentration vs. Depth Profile during a Tracer-Dilution Circulation Test (adapted from Brainerd and Robbins 2004).

modified to account for these dilutionary inflow sources to

$$q_i = [Q_{in} + \sum q_{fbf}) (C_{bf} - C_{af})]/C_{af} \qquad (3.26)$$

where, $\sum q_{fbf}$ is equal to the sum of inflowing fracture flow rates from fractures occurring below the fracture zone of interest.

Determination of initial fracture zone head conditions (h_i) requires a multi-rate Q_{dif} condition to be established, as was also similarly proposed by Tsang and Doughty (2003) for FFEC profile testing. For TDC testing, however, Brainerd and Robbins (2004) recommend that at least two additional Q_{dif} circulation rates be conducted that are lower than the initial first circulation step. Each Q_{dif} circulation step produces additional values for q_i and h_D, which can then be used for estimating h_i. To determine individual fracture zone h_i, values for h_D are plotted versus q_i, and a linear regression line is fit to the data, as shown in Figure 3.17. At the intercept of the regression line (for $q_i = 0$), the fracture zone head (h_i) is assumed to be equivalent to the head within well (h_D) for the composite test interval. Brainerd and Robbins (2004) then state that this value for h_i is used in the steady-state Thiem equation presented in Equation (3.5), together with the q_i determined for the first circulation step, to calculate the transmissivity (T_i) for individual fracture zones. In addition to estimating fracture zone transmissivity, the individual h_i values calculated for individual fracture zones can be compared to the static h_D within the well to determine the ambient inflow/outflow conditions between fracture zones intersected by the borehole.

The use of discrete depth sampling as a method of establishing the downhole tracer-dilution concentration profile, as reported by Brainerd and Robbins (2004), would limit its application in deep borehole settings.

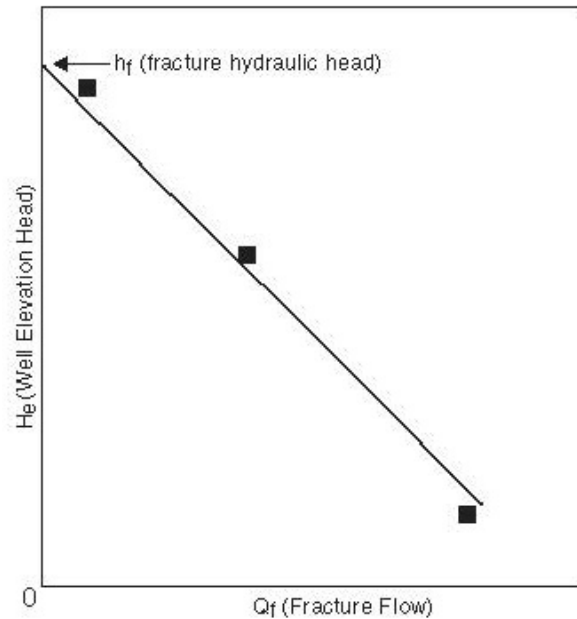**Figure 3.17**. Idealized Well Head vs. Fracture Flow Inflow Rate for Determining Fracture Zone Hydraulic Head Conditions (adapted from Brainerd and Robbins 2004).

However, using downhole wireline geophysical probe sensors and a contrasting salinity fluid as the "tracer" would extend the application of this test method to deep borehole settings. The use of continuous wireline logging surveys to establish the salinity/EC profiles during TDC tests also may mitigate some of the observed tracer profile variability reported by Brainerd and Robbins (2004), who relied on repetitive, discrete depth sampling methods.

As noted previously, similar deep TDC tests were conducted at the Leuggern borehole in Switzerland over a much greater depth interval (1,635 to 1,689 m), as reported by McNiesh et al. (1990a, 1990b) and Spane (1990). However, these deep TDC tests were conducted using packer isolation of specific fracture zones, which eliminated the possibility of downhole wireline tracer monitoring within the isolated test interval. In this situation, the tracer solution was circulated from the test interval to the land surface via small-diameter circulation/injection tubes and the circulation lines at the land surface were periodically sampled to determine tracer concentrations during the course of the test.

One apparent advantage of TDC testing over FFEC testing is that a pre-test baseline profile does not have to be established within the borehole prior to initiating TDC testing. However, based on currently available information, it is not known whether TDC testing would be as effective as FFEC testing in determining fracture q_i, h_i, and T_i conditions. Some insight into the applicability of TDC and how it relates to FFEC testing might be realized by simulating TDC profile responses using the BORE II model (compared to FFEC profiles). In Section 4.0, BORE II model comparison simulations for these two test methods are provided to assess their applicability in deep borehole test settings.

In summary, either the FFEC method or one of the alternative tracer methods may be more appropriate depending on actual site conditions such as formation salinity, permeability contrast, and borehole depth. Of the alternative methods, TDC testing may provide the most practical application for deep borehole characterization settings. BORE II simulations indicate that for similar test conditions, TDC tests can be conducted more rapidly than FFEC tests, but they also exhibit an inherent lack of sensitivity for characterizing discrete fracture zones exhibiting T_i values lower than ~10^{-7} m^2/sec. The limitations

3.27

identified in this assessment for FFEC testing would be applicable for the TDC method as well. Because of these limitations and rapid performance times, TDC testing may also find its best application as an initial reconnaissance tool prior to conducting FFEC profiling and/or hydrologic packer tests.

4.0   BORE II Model Simulations

The previous discussion in Section 3.2 concerning the analysis of FFEC profiles using BORE II is commonly referred to in hydrology as the "inverse analysis problem." In this application, the fracture and wellbore input parameters of q_i, C_i, h_i, and D_o are adjusted for each detected fracture zone to match the overall FFEC depth profile that was observed during testing. Based on the final solution input parameters obtained from FFEC profile matching and observed borehole/fracture zone drawdown during testing, hydraulic properties can then be calculated for each fracture zone using the applicable analytical equations presented in Section 3.2.2 and summarized in Figure 3.5.

When optimizing the design and application of FFEC characterization tests in the field, BORE II can also be used in a *forward solution* predictive mode to simulate FFEC profile development that might be expected given input information concerning fracture zone depth locations (e.g., core, wireline geophysics) and general inferences about fracture zone transmissivity (e.g., fluid loss/production calculations during drilling). This information, together with assigned fracture zone hydraulic head and fluid salinity conditions, can then serve as a basis for predicting FFEC profile evolution within the open borehole for assigned pumping rates, emplaced fluid salinity used, and assumed vertical borehole dispersion conditions. Examples of using BORE II for predictive FFEC applications are presented in Sections 4.1 and 4.2. The FFEC simulations were performed using a pumping/extraction rate of 3 L/min, which is approximately the median value of FFEC pumping rates used for previous deep borehole tests performed within similar open borehole intervals (i.e., ~1,000 m), as summarized previously in Table 3.1 For comparison purposes, BORE II simulations were also performed for TDC tests conducted for the same test conditions, using a bottom-hole circulation rate of 50 L/min and a surface pumping/extraction rate of 53 L/min. The TDC BORE II simulation results are provided in Section 4.3. Table 4.1 lists the assumed fracture zone extraction rates, borehole profile times, and associated report figures for each simulation. Test circulation rates are also shown for the TDC test simulations. General assumptions that are applicable for all the FFEC and TDC simulations are as follows:

- Three discrete fracture zones with a 250 m separation spacing within a 1,000 m open borehole section are assumed (i.e., fracture depths: 250, 500, and 750 m; wellbore radius, r_{wb} = 0.108 m)

- Salinity depth profiles developed are instantaneous "snapshot" type depictions for the borehole for the investigated simulation times. Specified fracture inflow rates are constant during the course of entire simulation period (i.e., no wellbore storage/skin effects, and no multi-rate test conditions).

- Fracture zone baseline test conditions are stable; no significant adverse impacts are associated with prior drilling or pre-test borehole fluid emplacement.

- Inflow fracture zone concentrations (C_i) are uniform and set at 100 g/L, and the borehole emplacement fluid and tracer-dilution circulation concentration used prior to FFEC and TDC testing is assigned a concentration value (C_b) of 0 g/L to maximize the simulated FEC depth profile signatures.

- A fixed, in-well, vertical dispersion/diffusion coefficient (D_o) value of 7.5e-10 m^2/sec is uniformly applied for all simulations.

The FFEC simulation results, in particular, demonstrate the relative impact that q_i, Q_{tot}, C_o, C_i, fracture zone spacing, and T_i might have in the evolution of FFEC profiles within extended open borehole test intervals during the course of FFEC testing. While different simulation results might be developed for various combinations of these input parameters, the examples below demonstrate that the FFEC profile development differences observed during testing can be used to quantify the q_i and C_i characteristics of the evolutionary patterns issuing from inflowing fracture zones to the borehole.

Table 4.1. Summary of Pertinent Information Pertaining to BORE II FFEC and TDC Test Case Simulations

Test Method	Fracture Zone T_i Conditions	Test Pumping Rate[a], Q_{tot}, L/min	Fracture Zone Inflow Rate, q_i, L/min	Test Circulation Rate[b], Q_{in}, L/min	Test Simulation Borehole Profile Times (min)	Report Figures
FFEC	Uniform T_i with Depth	3	$q_3 = q_2 = q_1 = 1.0$	NA	60, 720, 1440, 2880, 4320, 7200, 10080, 12960, 15840, 18720	4.1, 4.2, 4.3
	Increasing T_i with Depth	3	$q_3 = 0.02703$ $q_2 = 0.2703$ $q_1 = 2.703$	NA	120, 720, 2880, 4320, 7200, 10080	4.4
	Decreasing T_i with Depth	3	$q_3 = 2.703$ $q_2 = 0.2703$ $q_1 = 0.02703$	NA	120, 720, 2880, 4320, 7200	4.5
TDC	Uniform T_i with Depth	53	$q_3 = q_2 = q_1 = 1.0$	50	60, 120, 240, 360, 480, 600, 720	4.6, 4.7
	Increasing T_i with Depth	53	$q_3 = 0.02703$ $q_2 = 0.2703$ $q_1 = 2.703$	50	60, 120, 240, 360, 480, 600, 720	4.8, 4.9
	Decreasing T_i with Depth	53	$q_3 = 2.703$ $q_2 = 0.2703$ $q_1 = 0.02703$	50	60, 120, 240, 360, 480, 600, 720	4.10, 4.11

4.1 FFEC Uniform T_i Fracture Zone Profile Conditions

For the first FFEC profile simulation, uniform transmissivity conditions are assumed for the three discrete fracture zones within a 1,000 m long open borehole section. Specific test/fracture zone conditions as summarized in Table 4.1 are listed below:

> Initial borehole C_o: 0.0 g/L
> Total pumping rate (Q_{tot}): 3.0 L/min
> Fracture inflow rate, q_i: 1.0 L/min (for each of the three fracture zones)
> Fracture zone C_i: 100 g/L (for each of the three fracture zones)
> Upward flow rate from borehole bottom: 0.0 L/min

Figure 4.1 shows BORE II FFEC depth profiles for selected early, non-interfering simulation times. For fracture inflow rates (q_i) of 1.0 L/min and a total borehole pumping extraction rate (Q_{tot}) of 3.0 L/min, this equates to an observed steady-state, composite borehole drawdown of 21 m for individual fracture zone transmissivities—T_i = 1.0 e-6 m^2/sec (note: composite borehole T_{tot} = 3.0e-6 m^2/sec)—based on use of Equation (3.5) and an assumed radius-of-investigation for the test of 300 m.

Figure 4.1.   BORE II FFEC Simulation Profiles for Selected Early (Non-Interfering) Test Times: Three Fracture Zones that Have Uniform Transmissivity, T_i = 10^{-6} m^2/sec

As indicated in the figure, neither of the two lower fracture zone FFEC signatures extends up-borehole during pumping to interfere with the overlying fracture zone patterns during early-test times. As discussed in Section 3.2, the evolutionary, early-time (non-interfering) FFEC profiles developed from each fracture during FFEC testing is the preferred time for calculating fracture zone inflow characteristics (i.e., $q_i C_i$), with fracture zone (q_i) largely controlling the degree of skewness of the FFEC pattern peripheral to the fracture zone depth location. After approximately 2 days of FFEC testing (i.e., 2,880 min) a characteristic "stair-step" profile develops, and the middle and top fracture zones (i.e., @ 500 and 250 m, respectively)

exhibit lower concentrations due to the incorporation of increased contributions of underlying initial borehole fluid concentration flux (i.e., middle fracture = 1 L/min of 0 g/L; top fracture = 2 L/min of 0 g/L). As expected, because this simulation is based on a simple mass balance mixing model relationship, the upper two fracture zones exhibit proportionally lower concentration plateaus and extended "stair-step" interval lengths in comparison to the FFEC response immediately above the bottom fracture zone. Similar FFEC concentration "stair-stepping" patterns were also presented for multiple synthetic fracture inflow studies presented by Tsang et al (1990) and Doughty and Tsang (2005), although fracture zone separations and test conditions were different than those considered here.

Figure 4.2 shows a series of simulated FFEC profile responses for early "interfering" responses in which the middle fracture affects the top fracture zone pattern. A FFEC "spike" for the top fracture zone for the 4,320 min FFEC profile, is caused by the initial interference front of elevated borehole salinity concentration flux from the underlying middle fracture zone (i.e., $(q_1 \times q_2)C_2 > (q_1 \times q_2)C_o$), which is averaged with the top fracture zone mass flux (q_3C_3). At the next simulation time shown (7,200 min), the concentration plateau/stair-step has stabilized for the borehole interval above the top fracture zone at a level greater than that for the middle fracture zone. This is due to the fact that concentration flux from the bottom fracture has just reached the depth interval of the overlying middle fracture zone and not established discernable elevated interfering effects for this simulation time.
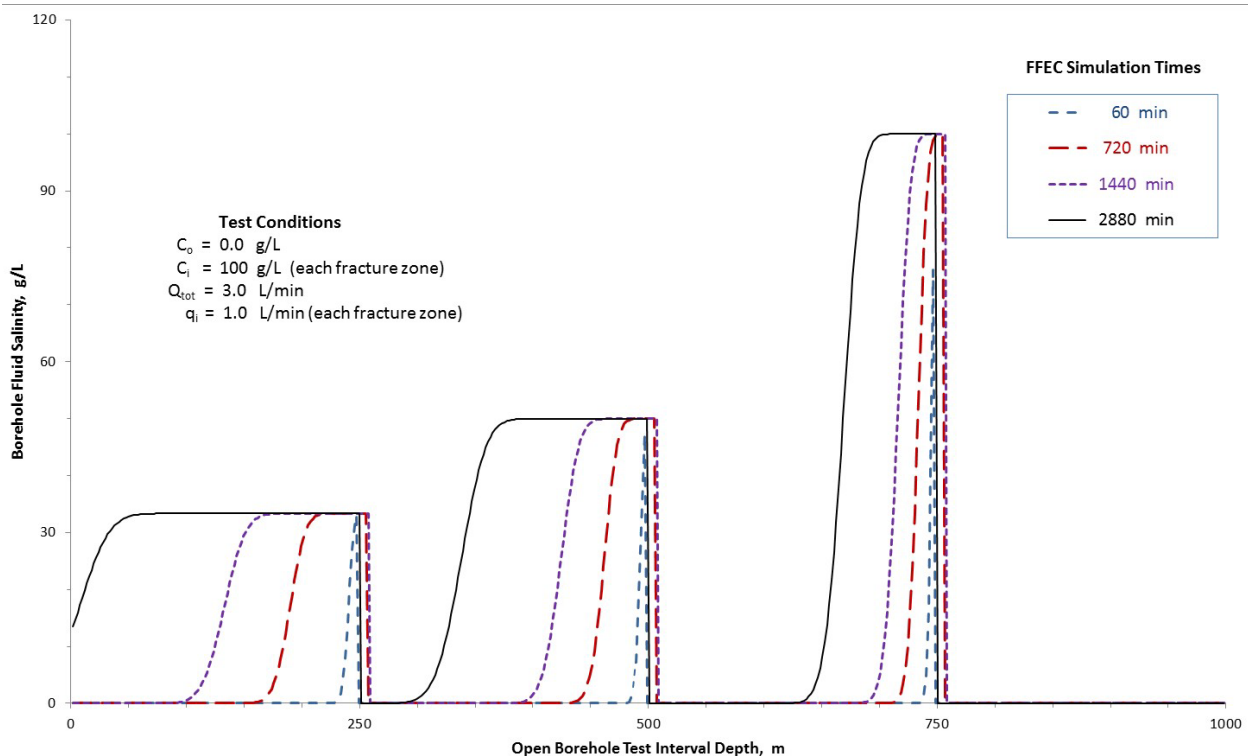

Figure 4.2. BORE II FFEC Simulation Profiles for Selected Early (Middle Zone Interfering) Test Times: Three Fracture Zones that Have Uniform Transmissivity, $T_i = 10^{-6}$ m²/sec

Figure 4.3 shows a series of final FFEC-simulated profile responses that captures the late-time interfering FFEC profile impact of the bottom fracture with the two overlying fracture zones. At a simulation time of 10,080 min (7 days), the bottom fracture zone inflow is interfering with the FFEC profile depth signature for the immediate borehole interval above the middle fracture zone. The small "spike" pattern at the middle fracture zone depth is caused by the increased steepness of the borehole concentration profile front from the underlying bottom fracture. At simulation times of 12,960 and 15,840 min (9 and 11 days), the
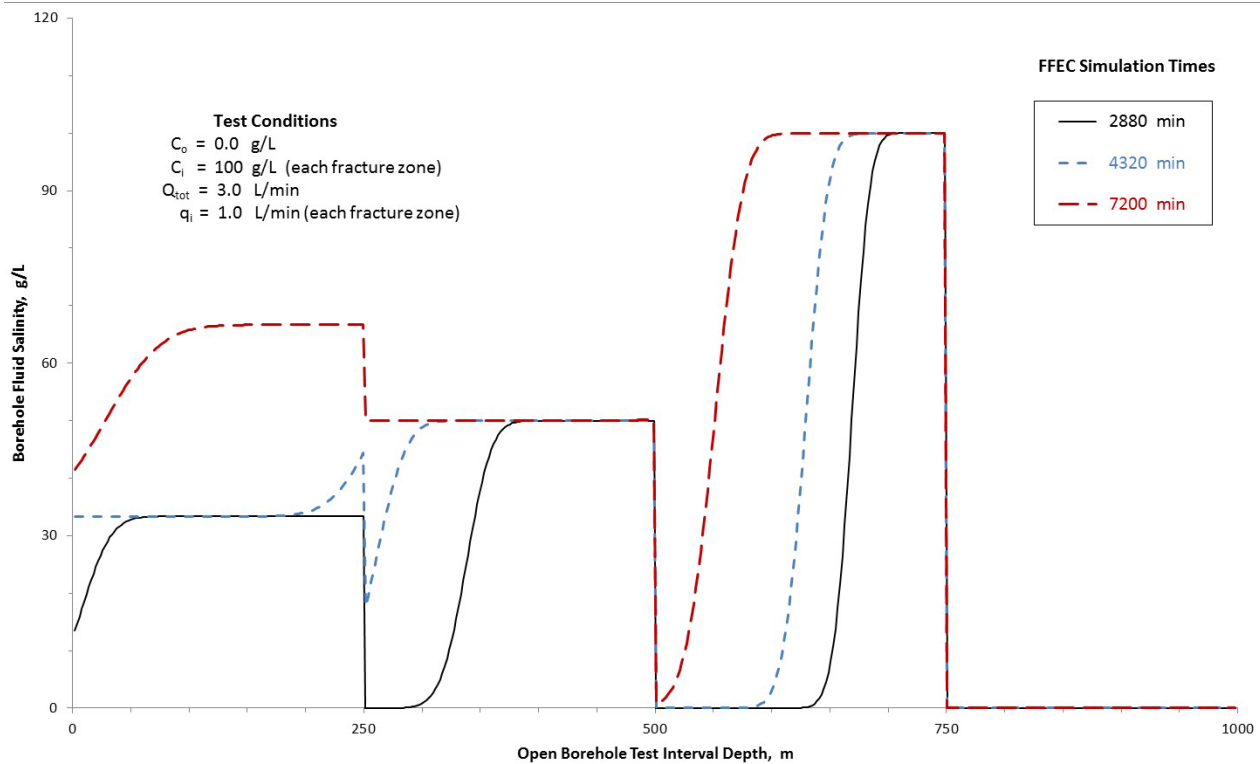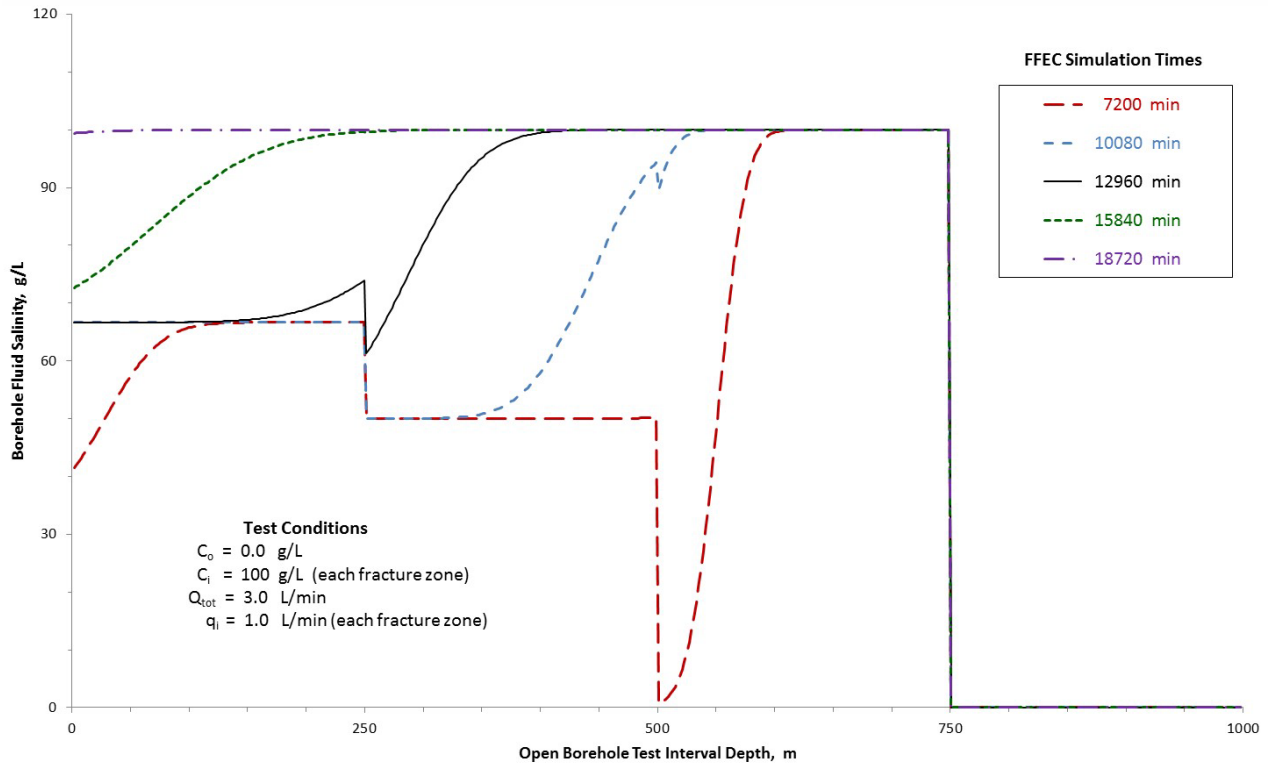
Figure 4.3. BORE II FFEC Simulation Profiles for Selected Late-Test Times (Bottom Zone Interfering): Three Fracture Zones that Have Uniform Transmissivity, $T_i = 10^{-6}$ m²/sec

primary features of the FFEC profile are the interference of the composite underlying middle and bottom fractures zones with the immediate borehole interval above the top fracture zone. By 18,720 min (13 days), the entire open borehole interval has been replaced by fluid produced solely from the bottom fracture zone.

4.2 FFEC Varying T_i Fracture Zone Profile Conditions

For the two variable T_i fracture zone simulation conditions described in the following sections, only one plot is shown for each to capture various evolutionary stages, i.e., early to late-time FFEC profile development.

4.2.1 Transmissivity Increasing with Depth: $T_i = 10^{-8} \rightarrow 10^{-6}$ m²/sec

For this FFEC tracer profile simulation, a general increasing fracture zone transmissivity trend condition is assumed for the three discrete fracture zones within a 1,000 m long open borehole section (i.e., $T_3 = 1.0e\text{-}8$ m²/sec; $T_2 = 1.0e\text{-}7$ m²/sec; and $T_3 = 1.0e\text{-}6$ m²/sec). Specific test/fracture zone conditions are listed below:

Initial borehole C_o: 0.0 g/L
Total pumping rate (Q_{tot}): 3.0 L/min
Fracture inflow rate:
　　Top Fracture (q_3): 0.02703 L/min
　　Middle Fracture (q_2): 0.2703 L/min

> Bottom Fracture (q_1): 2.703 L/min
> Fracture zone C_i: 100 g/L (for each of the three fracture zones)
> Upward flow rate from borehole bottom: 0 L/min

Figure 4.4 shows BORE II FFEC depth profiles for selected simulation times encompassing early non-interfering FFEC signatures and late-time interfering response patterns. For comparison purposes, the same total borehole pumping extraction rate (Q_{tot}) of 3.0 L/min and fracture zone inflow concentrations (C_i) were used, as was the case for the previous example. The proportional fracture inflow rates (q_i) listed above are based on the proportional aspects of the assigned fracture zone transmissivities.

Figure 4.4. BORE II FFEC Simulation Profiles for Selected Test Times for the Case of Three Fracture Zones that Have T_i Increasing with Depth: Top Fracture = 10^{-8} m²/sec → Bottom Fracture = 10^{-6} m²/sec

As indicated in Figure 4.4, early-test times (e.g., 120 min) are non-interfering when the individual fracture zone FFEC profiles are largely a function of the fracture zone inflow rates and salinity concentration. At 720 min, FFEC profiles produced from the bottom and middle fracture zones are interfering with their respective overlying borehole zone profiles. With progressing test time, a characteristic "stair-step" profile develops within the borehole and is dominated by the large borehole input from the bottom fracture zone. This dominance of the bottom or lower higher transmissivity fracture zone in interfering with characterization of the overlying less transmissive fracture zones greatly limits the characterization capabilities of FFEC testing. This has led others to recommend isolation of more highly transmissive fracture zones within the borehole to minimize their associated interfering and masking effects (e.g., Tsang et al. 1990; Tsang and Doughty 2003). As shown in the figure, after ~10,000 min of the test, nearly all of the borehole test interval has been replaced by fluid issuing from the fracture zones—predominately from the bottom fracture.

4.2.2   Transmissivity Decreasing with Depth: $T_i = 10^{-6} \rightarrow 10^{-8}$ m²/sec

For this FFEC tracer profile simulation, a general decreasing fracture zone transmissivity trend condition is assumed for the three discrete fracture zones within a 1,000 m long open borehole section (i.e., $T_3 = 1.0e-6$ m²/sec; $T_2 = 1.0e-7$ m²/sec; and $T_3 = 1.0e-8$ m²/sec). Specific test/fracture zone conditions are listed below:

> Initial borehole C_o: 0.0 g/L
> Total pumping rate (Q_{tot}): 3.0 L/min
> Fracture inflow rate:
>> Top Fracture (q_3): 2.703 L/min
>> Middle Fracture (q_2): 0.2703 L/min
>> Bottom Fracture (q_1): 0.02703 L/min
> Fracture zone C_i: 100 g/L (for each of the three fracture zones)
> Upward flow rate from borehole bottom: 0 L/min

Figure 4.5 shows BORE II FFEC depth profiles for selected simulation times encompassing early non-interfering FFEC signatures and late-time interfering response patterns. For comparison purposes, the same total borehole pumping extraction rate (Q_{tot}) of 3.0 L/min and fracture zone inflow concentrations (C_i) were used, as was the case for the previous example. The proportional fracture inflow rates (q_i) listed above are based on the proportional aspects of the assigned fracture zone transmissivities.
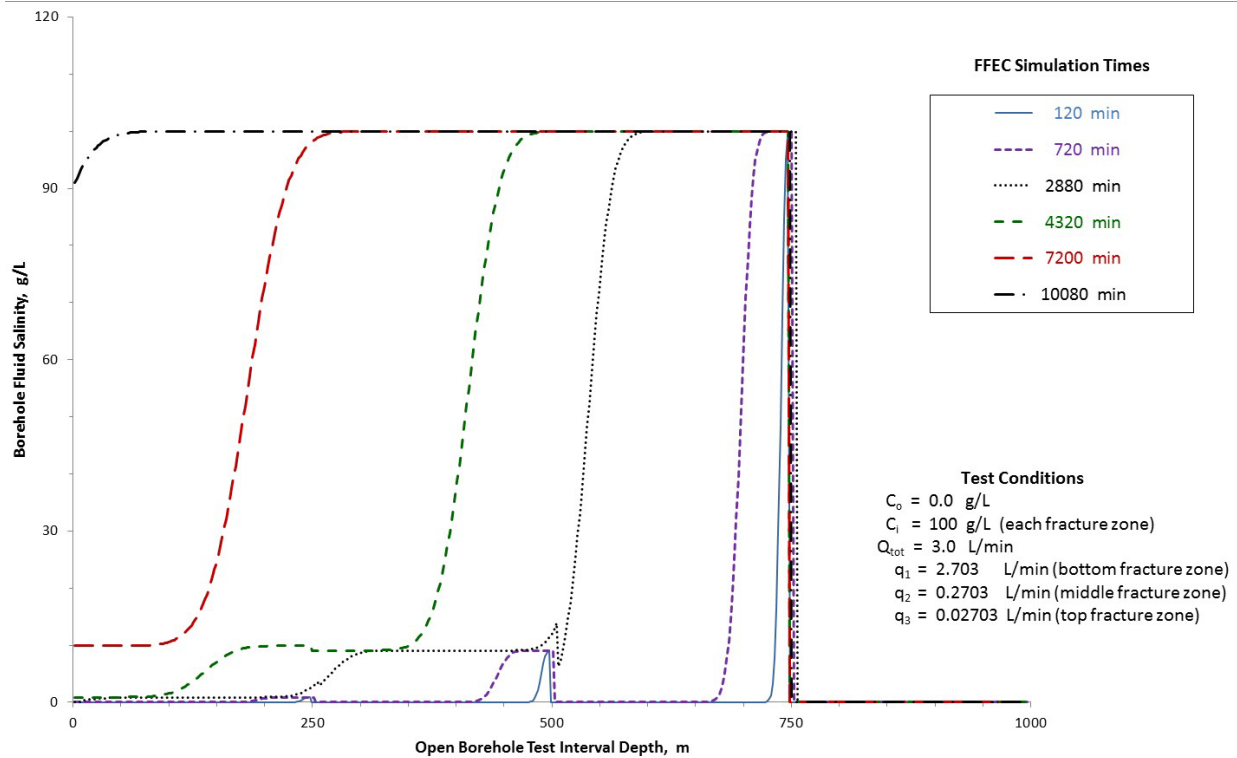

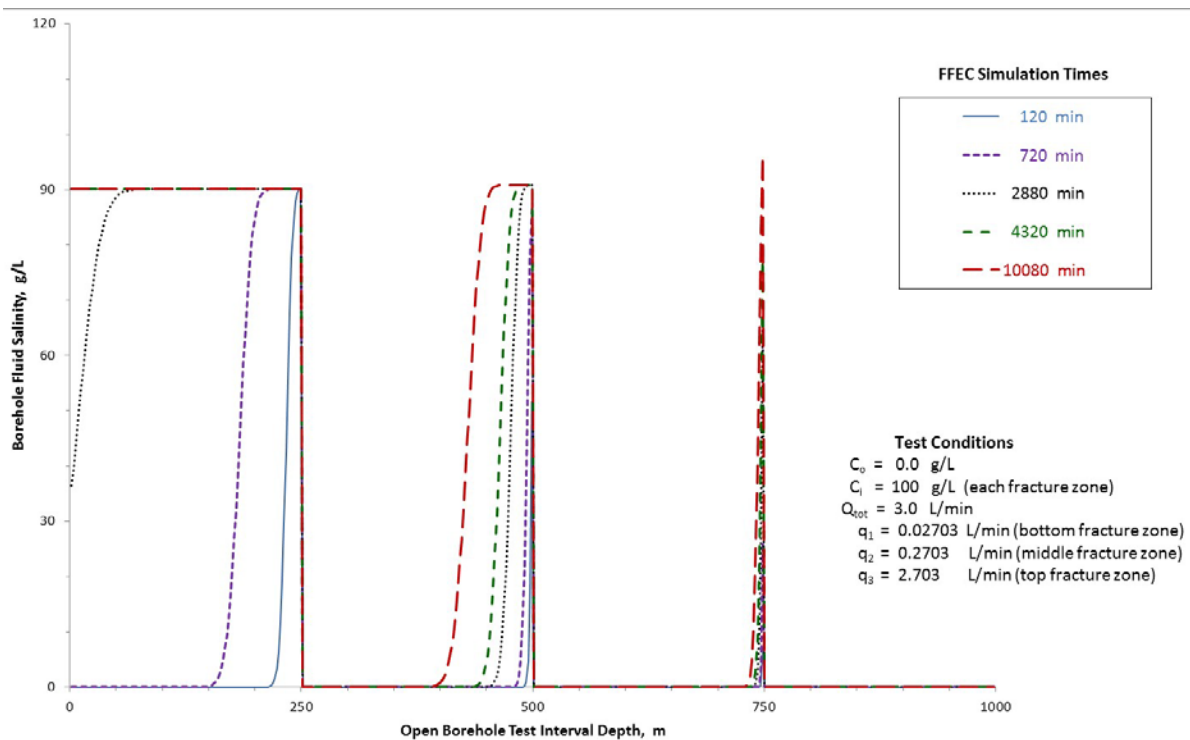**Figure 4.5**. BORE II FFEC Simulation Profiles for Selected Test Times for the Case of Three Fracture Zones that Have T_i Decreasing with Depth: Top Fracture = 10^{-6} m²/sec $\rightarrow$ Bottom Fracture = 10^{-8} m²/sec

In contrast to the previously examined example, no interference between the fracture zones was exhibited during the entire 7-day (10,080 min) simulation period. The response for the 10,080 min profile was

nearly identical to the 7200 min profile shown in Figure 4.5. This lack of interference suggests that there may be inherently greater characterization applications for FFEC testing when decreasing fracture zone transmissivity vs. depth conditions exist. A general decreasing permeability vs. depth trend pattern has been widely observed and reported by others for deep crystalline rock types at various worldwide locations (e.g., Stober and Bucher 2007, 2015).

4.3   TDC Fracture Zone Profile Conditions

For comparison purposes relative to the previously described FFEC profile characteristics, BORE II simulations were also performed for the same existing uniform and varying fracture zone T_i conditions. In addition to the general test conditions identified in Section 4.0 for the BORE II simulations performed, it was assumed that the borehole was initially filled with a salinity concentration of 10 g/L from the drilling/borehole advancement activities, prior to circulating a contrasting borehole fluid with a $C_{in} = 0$ g/L. Specifying this initial borehole fluid condition (C_o) of 10 g/L allows the "snapshot" of TDC profile development due to the inflow of higher-salinity fracture zone fluid (i.e., 100 g/L) and circulation of freshwater from the bottom of the borehole. It should be noted that the evolutionary development of salinity profiles during TDC testing is not only a function of the initial borehole concentration (C_o) and fracture inflow characteristics ($q_i C_i$) but also is influenced by the pumping (Q_{tot}) and the circulation rate (Q_{in}) used during the test.

Results of the BORE II TDC simulations for uniform and varying T_i and the specified test conditions are discussed below.

4.3.1   TDC Profiles: Uniform T_i

For the first TDC profile simulation, uniform transmissivity conditions are assumed for the three discrete fracture zones within a 1,000 m long open borehole section. Specific test/fracture zone conditions are listed below:

> Initial borehole C_o: 10.0 g/L
> Total pumping rate (Q_{tot}): 53.0 L/min
> Fracture inflow rate, q_i: 1.0 L/min (for each of the three fracture zones)
> Fracture zone C_i: 100 g/L (for each of the three fracture zones)
> Upward circulation flow rate from borehole bottom (Q_{in}): 50 L/min
> Upward flow concentration (C_{in}) from borehole bottom: 0.0 g/L

Figure 4.6 shows BORE II TDC depth profiles for selected early, non-interfering and interfering simulation times. For fracture inflow rates (q_i) of 1.0 L/min and a bottom borehole circulation rate (Q_{in}) of 50 L/min, and total borehole pumping extraction rate (Q_{tot}) of 53.0 L/min, this equates to an observed steady-state, composite borehole drawdown of 21 m for the same borehole transmissivity conditions specified for FFEC testing in Section 4.2 (i.e., $T_i = 10^{-6}$ m^2/sec).

As indicated in Figure 4.6 for the earliest, 60 min TDC snapshot profile, the circulated freshwater ($C_{in} = 0.0$ g/L) at the borehole bottom, has not reached the bottom fracture zone (located at a depth of 750 m). Similarly, the mixed initial borehole concentration fluid ($C_o = 10$ g/L) with fluid from the respective fracture zones ($C_i = 100$ g/L) has not reached or interfered with the profiles for the overlying fracture zones. Selected profiles of 120 to 360 min shown in the figure exhibit progressively greater degrees of mixing and interference in the up-borehole direction. At 360 min into the TDC test, the mixture of circulated freshwater at the borehole bottom with fluid from the bottom fracture zone has reached the

middle fracture zone depth, and a stabilized, steady-state TDC profile has been established between the middle fracture zone depth and the borehole bottom (i.e., 500 to 1,000 m).

Figure 4.7 shows later-developing BORE II TDC depth evolutionary profiles after 360 min of testing, within the upper 500 ft of the open test interval. This evolutionary profile is produced by the interference of the mixed middle and fracture zone fluid with the circulated freshwater at the borehole bottom, interfering with inflow from the top fracture zone. As indicated in the figure, at 720 min into the test, the initial borehole fluid-column concentration (C_o = 10 g/L) has been completely replaced by the mixture of circulation of freshwater and fracture zone inflow fluid. The TDC borehole profile has completely stabilized over the entire open borehole test interval, and the characteristic stair-step profile are exhibited directly as a function of the underlying fracture zone q_i C_i conditions (i.e., in comparison to the circulated tracer fluid Q_{in} C_{in}), as discussed in Section 3.4.2. In this case, the transmissivities and inflow rates are identical for each of the three fracture zones; and as a result, essentially identical stabilized stair-step offset magnitudes in the TDC profile above each fracture zone are produced.
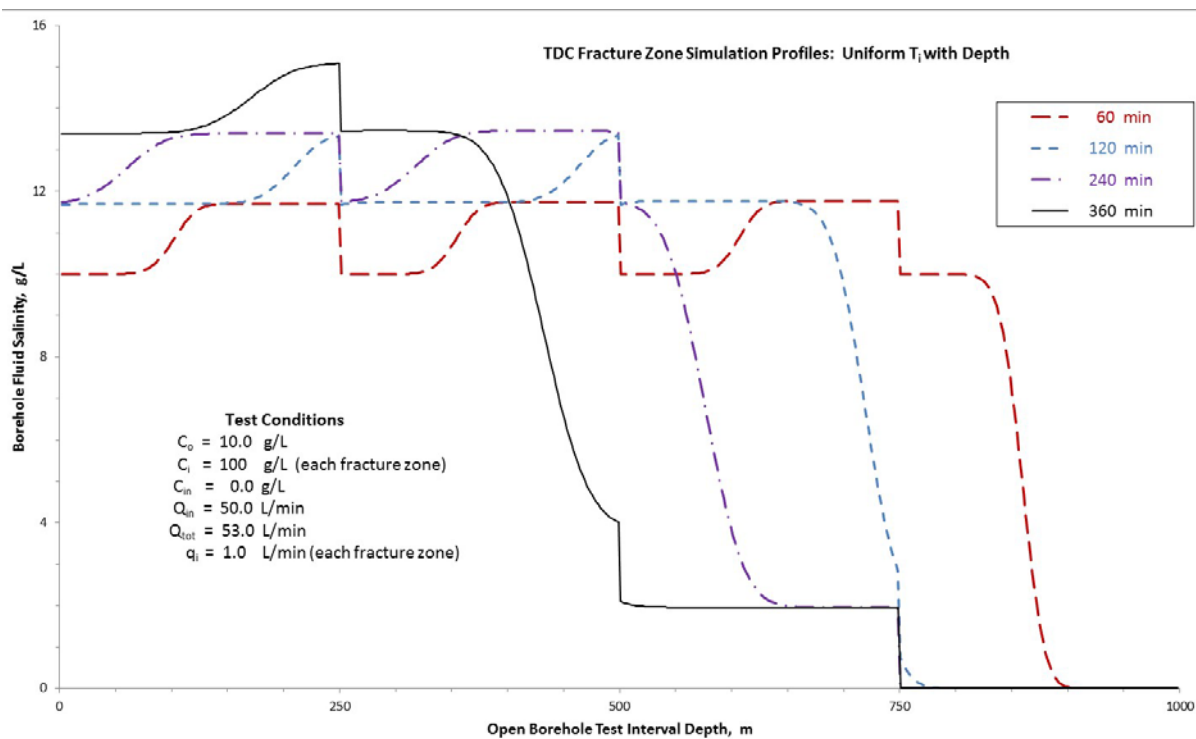

Figure 4.6.   BORE II TDC Simulation Profiles for Selected Early-Test Times for the Case of Three Fracture Zones that Have Uniform Transmissivity, $T_i = 10^{-6}$ m^2/sec
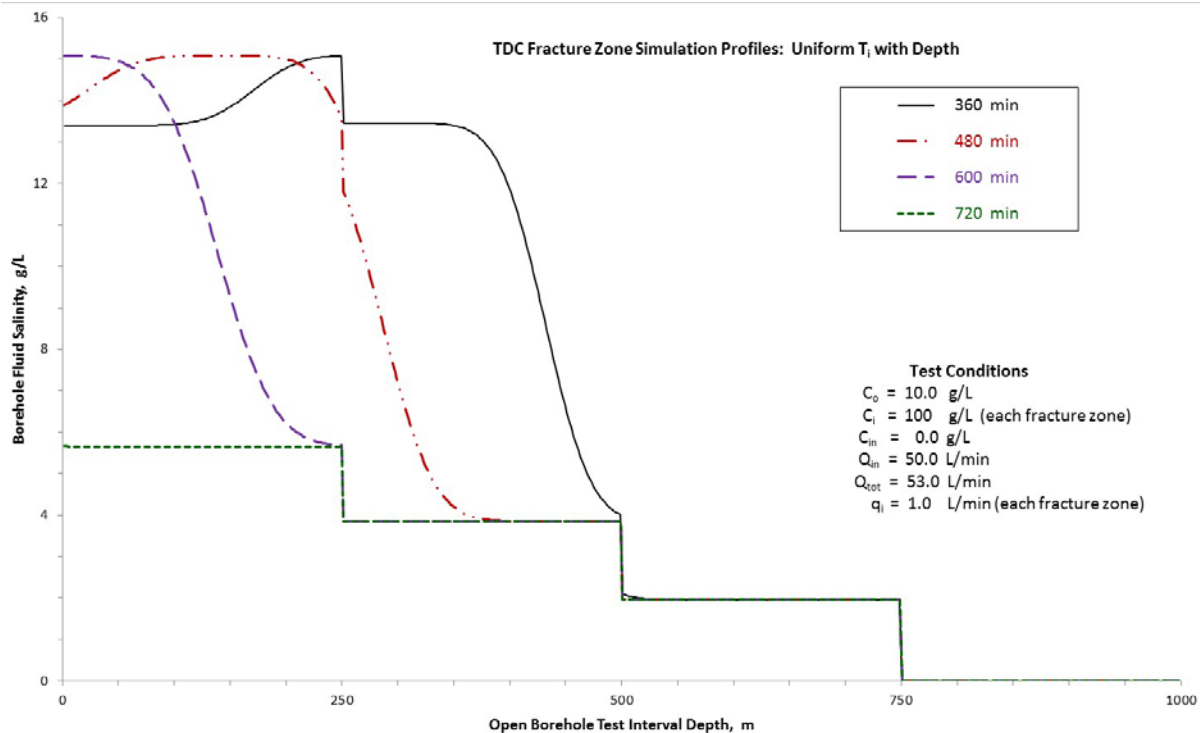
Figure 4.7.   BORE II TDC Simulation Profiles for Selected Later-Test Times for the Case of Three Fracture Zones that have Uniform Transmissivity, $T_i = 10^{-6}$ m^2/sec

4.3.2   TDC Profiles Varying T_i Increasing with Depth: $T_i = 10^{-8} \rightarrow 10^{-6}$ m^2/sec

For this TDC tracer profile simulation, a general increasing fracture zone transmissivity trend condition is assumed for the three discrete fracture zones within a 1,000 m long open borehole section (i.e., $T_3 = 1.0e$-8 m^2/sec; $T_2 = 1.0e$-7 m^2/sec; and $T_3 = 1.0e$-6 m^2/sec). Specific test/fracture zone conditions are listed below:

> Initial borehole C_o: = 0.0 g/L
> Total pumping rate (Q_{tot}): 53.0 L/min
> Fracture inflow rate:
> > Top Fracture: 0.02703 L/min
> > Middle Fracture: 0.2703 L/min
> > Bottom Fracture: 2.703 L/min
>
> Fracture zone C_i: = 100 g/L (for each of the three fracture zones)
> Upward circulation flow rate from borehole bottom (Q_{in}): 50 L/min
> Upward flow concentration (C_{in}) from borehole bottom: 0.0 g/L

Figure 4.8 shows BORE II TDC depth profiles for selected early, non-interfering and interfering simulation times for the given fracture zone inflow conditions identified above, for the same simulation times used for the previous uniform fracture zone T_i case. Because TDC profile development is largely determined based on the arrival time and mixing of the underlying $q_i C_i$ of the circulated freshwater at the borehole bottom, similar evolutionary TDC profiles would be expected for varying fracture zone T_i conditions with test time. The exception would be during early-test times prior to the arrival of the circulated freshwater at respective test interval depths. Prior to the arrival of circulated freshwater, TDC profiles are largely a function of the fracture zone $q_i C_i$ characteristics. As indicated in Figure 4.8, for the
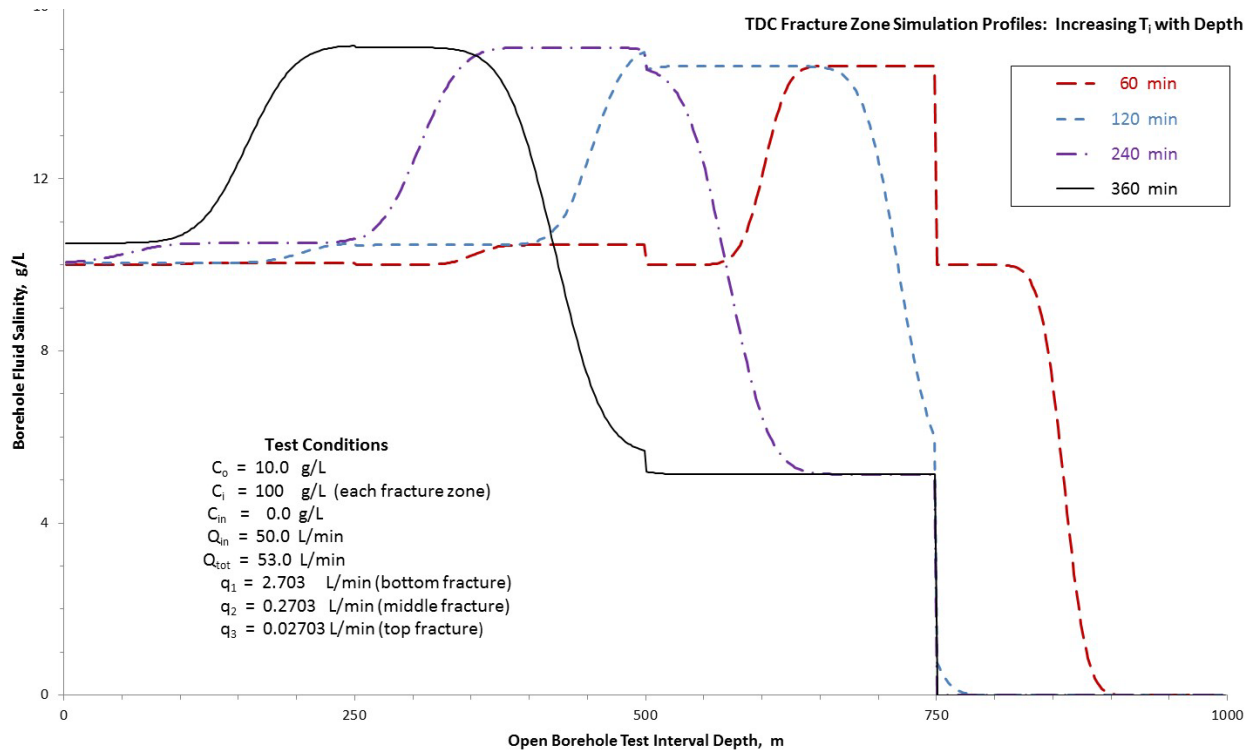
4.10

Figure 4.8. BORE II TDC Simulation Profiles for Selected Early-Test Times for the Case of Three Fracture Zones that Have Increasing T_i with Depth: Top Fracture = 10^{-8} → Bottom Fracture = 10^{-6} m^2/sec

earliest, 60 min TDC snapshot profile, the circulated freshwater ($C_{in} = 0.0$ g/L) at the borehole bottom, has not reached the bottom fracture zone (located at a depth of 750 m). As a result, the 60 min TDC profiles are decidedly different between the increasing T_i with depth and the uniform T_i test cases. Selected profiles from 120 to 360 min shown in Figure 4.8 exhibit progressively greater degrees of mixing and interference in the up-borehole direction, primarily due to the incursion of inflow from the bottom fracture zone with overlying open borehole intervals. The major inflow from the bottom fracture zone greatly diminishes the ability to discern the interference effects for overlying fracture zones having lower inflow magnitudes. At 360 min into the TDC test, the mixed borehole circulation fluid (injected at the borehole bottom) with fluid from the bottom fracture zone has not quite reached the top fracture zone depth, and a stabilized, steady-state TDC profile has been established between the middle fracture zone depth and the borehole bottom (i.e., 500 to 1,000 m), as was exhibited for the uniform fracture zone T_i case.

Figure 4.9 shows later-developing BORE II TDC evolutionary profiles after 360 min of testing, within the upper 500 ft of the open test interval. The profiles developed are produced by the interference of the mixture of middle and lower fracture zone fluid with the circulated freshwater from the borehole bottom interfering with inflow from the top fracture zone. These TDC profile patterns are similar to those developed for the uniform T_i case. As indicated in the figure, at 720 min into the test, the initial borehole fluid-column concentration ($C_o = 10$ g/L) has been completely replaced and a stabilized, steady-state TDC borehole profile has been established over the entire open borehole interval. As previously noted, the steady-state stair-step profile exhibited is directly a function of the underlying fracture zone $q_i C_i$ conditions (i.e., in comparison to the circulated tracer fluid $Q_{in} C_{in}$). Because ~90% of the fracture zone inflow is provided at the bottom fracture zone location, the sum of total stair-step offset magnitude is dominated by the bottom fracture zone, and identification of overlying, lower T_i fracture zone locations in

the stabilized steady-state TDC profile plot is largely masked by the interfering effects of the bottom fracture zone. This steady-state stair-step TDC profile is significantly different than that exhibited by the uniform T_i case, where nearly equal stair-step offset magnitudes in the profile pattern were indicated.

Figure 4.9. BORE II TDC Simulation Profiles for Selected Later-Test Times for Case of Three Fracture Zones that Have Increasing T_i with Depth: Top Fracture $= 10^{-8} \rightarrow$ Bottom Fracture $= 10^{-6}$ m^2/sec

4.3.3   TDC Profiles Varying T_i Decreasing with Depth: $T_i = 10^{-6} \rightarrow 10^{-8}$ m²/sec

For this TDC tracer profile simulation, a general decreasing fracture zone transmissivity trend condition is assumed for the three discrete fracture zones within a 1,000 m long open borehole section (i.e., $T_3 = 1.0e-6$ m²/sec; $T_2 = 1.0e-7$ m²/sec; and $T_3 = 1.0e-8$ m²/sec). Specific test/fracture zone conditions are listed below:

> Initial borehole C_o: = 0.0 g/L
> Total pumping rate (Q_{tot}): 53.0 L/min
> Fracture inflow rate:
> > Top Fracture: 2.703 L/min
> > Middle Fracture: 0.2703 L/min
> > Bottom Fracture: 0.02703 L/min
> Fracture zone C_i: = 100 g/L (for each of the three fracture zones)
> Upward circulation flow rate from borehole bottom (Q_{in}): 50 L/min
> Upward flow concentration (C_{in}) from borehole bottom: 0.0 g/L

Figure 4.10 shows BORE II TDC depth profiles for selected early, non-interfering and interfering simulation times for the given fracture zone inflow conditions identified above, for the same simulation times used for the previous fracture zone T_i cases. Because of the undetectable inflow from the bottom fracture zone (i.e., $q_1 = 0.02703$ L/min), the progressive TDC profile development in the lower 500 m of

the open test interval is largely determined by the arrival time of the circulated freshwater that is introduced at the borehole bottom. The TDC profile for the upper 250 m of the test interval is dominated by the mixing of the inflow from the top fracture zone with the initial borehole fluid concentration (C_o = 10.0 g/L), which reaches the top of the test interval by 360 min into the TDC test. Prior to the arrival of the circulated freshwater, TDC profiles are largely a function of the fracture zone $q_i C_i$ characteristics.

TDC Fracture Zone Simulation Profiles: Decreasing T_i with Depth

- 60 min
- 120 min
- 240 min
- 360 min

Test Conditions
C_o = 10.0 g/L
C_i = 100 g/L (each fracture zone)
C_{in} = 0.0 g/L
Q_{in} = 50.0 L/min
Q_{tot} = 53.0 L/min
q_1 = 0.02703 L/min (bottom fracture)
q_2 = 0.2703 L/min (middle fracture)
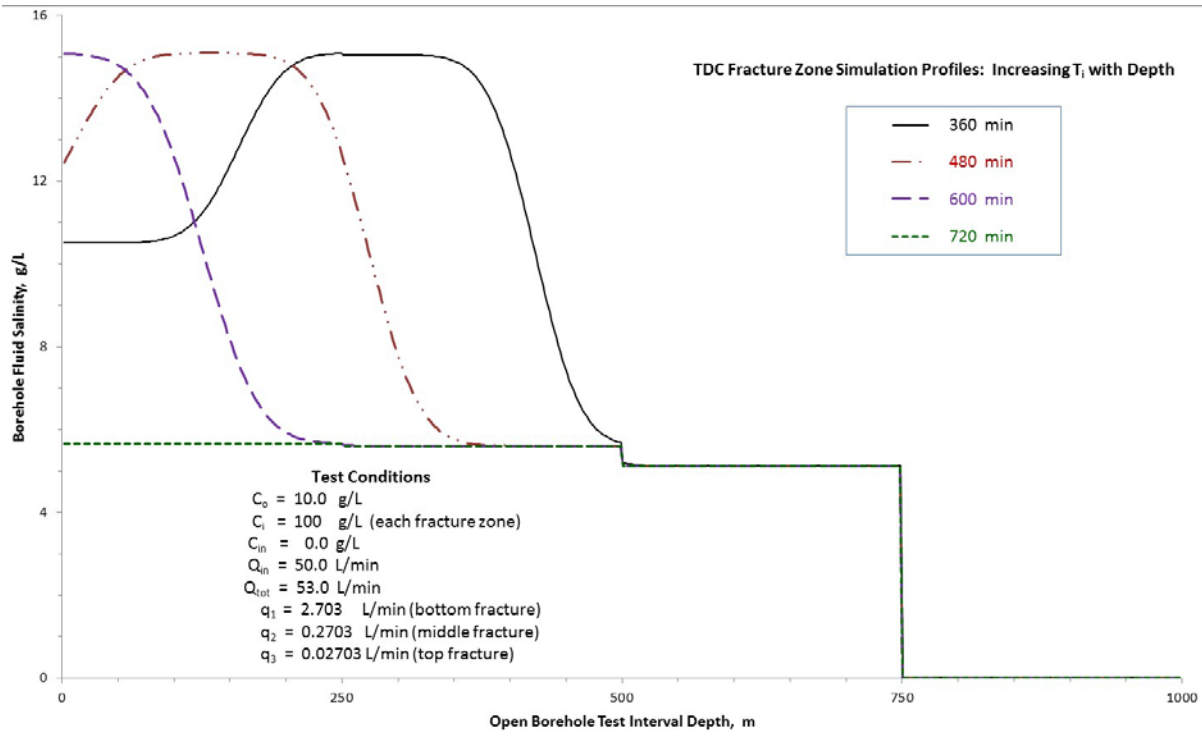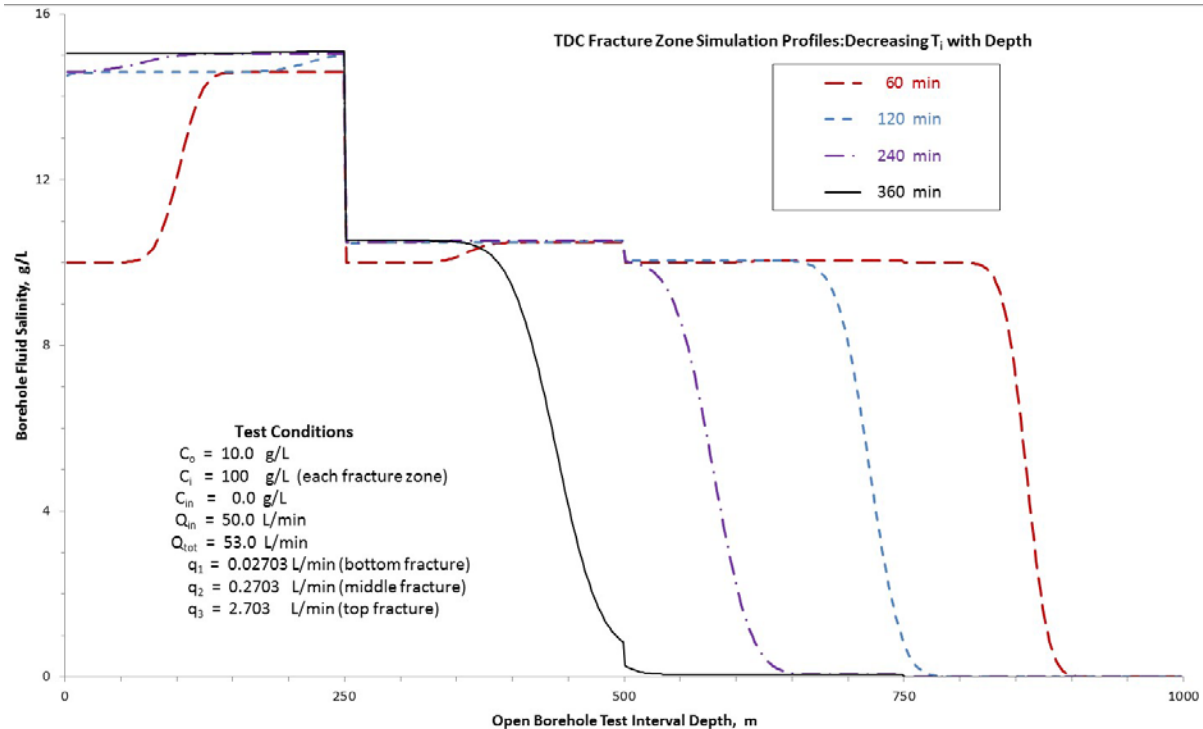q_3 = 2.703 L/min (top fracture)

Figure 4.10. BORE II TDC Simulation Profiles for Selected Early-Test Times for Case of Three Fracture Zones the Have Decreasing T_i with Depth: Top Fracture = $10^{-6} \rightarrow$ Bottom Fracture = 10^{-8} m^2/sec

As indicated in Figure 4.10, for the earliest, 60 min test time, the TDC snapshot profile is significantly different than those of the previously examined T_i cases, because the major fracture inflow component was assigned to the upper fracture zone location. Profiles from 120 to 360 min into the test shown in Figure 4.10 largely exhibit the progressive advancement of circulated freshwater in the up-borehole direction. At 360 min into the TDC test, the mixture of borehole circulation fluid (injected at the borehole bottom) with minor inflow fluid from the bottom and middle fracture zones has not quite reached the top fracture zone depth, and a stabilized, steady-state TDC profile has been established between the middle fracture zone depth and the borehole bottom (i.e., 500 to 1,000 m), as was exhibited for the previous two fracture zone T_i cases.

Figure 4.11 shows later-developing BORE II TDC evolutionary profiles after 360 min of testing within the upper 500 ft of the open test interval. The profiles produced by the interference of the mixture of middle and lower fracture zone fluid with the circulated freshwater from the borehole bottom interfering with inflow from the top fracture zone. These TDC profile patterns are similar to those developed for the previous two T_i cases. As indicated in the figure, at 720 min into the test, the initial borehole fluid column concentration (C_o = 10 g/L) has been completely replaced and a stabilized, steady-state TDC borehole profile has been established over the entire open borehole interval. As previously noted, the steady-state stair-step profile exhibited is directly a function of the underlying fracture zone $q_i C_i$ conditions (i.e., in comparison to the circulated tracer fluid $Q_{in} C_{in}$). Because 90% of the fracture zone inflow is provided at

the top fracture zone location, the sum of total stair-step offset magnitude is dominated by the top fracture zone, and no reliable discernment of inflow from the bottom fracture zone is possible. Figure 4.12 shows a comparison of late-time TDC profiles to demonstrate the impact of different fracture T_i distributions on stabilized, steady-state TDC patterns. As indicated, the steady-state, stair-step TDC profile for the T_i decreasing with depth condition is significantly different than that exhibited by the previous two T_i cases.

Based on the BORE II simulation results completed, the following observations concerning TDC testing were noted:

- The presence of fracture zone inflow locations is most discernable within early-time TDC profiles (i.e., prior to the arrival of the circulated contrasting borehole fluid) or after stabilized, steady-state profiles are established.

- Although the magnitude of fracture zone inflow (and magnitude of TDC profile offsets) can be manipulated to a degree by modifications in borehole circulation rate (Q_{in}) and surface borehole pumping rate (Q_{tot}), TDC profile simulations appear to be limited to fracture zones with transmissivities of $T_i \geq 10^{-7}$ m^2/sec.

- As with FFEC testing, masking of TDC up-hole profile development will occur because of the presence of underlying fracture zones that exhibit elevated $q_i C_i$ characteristics.
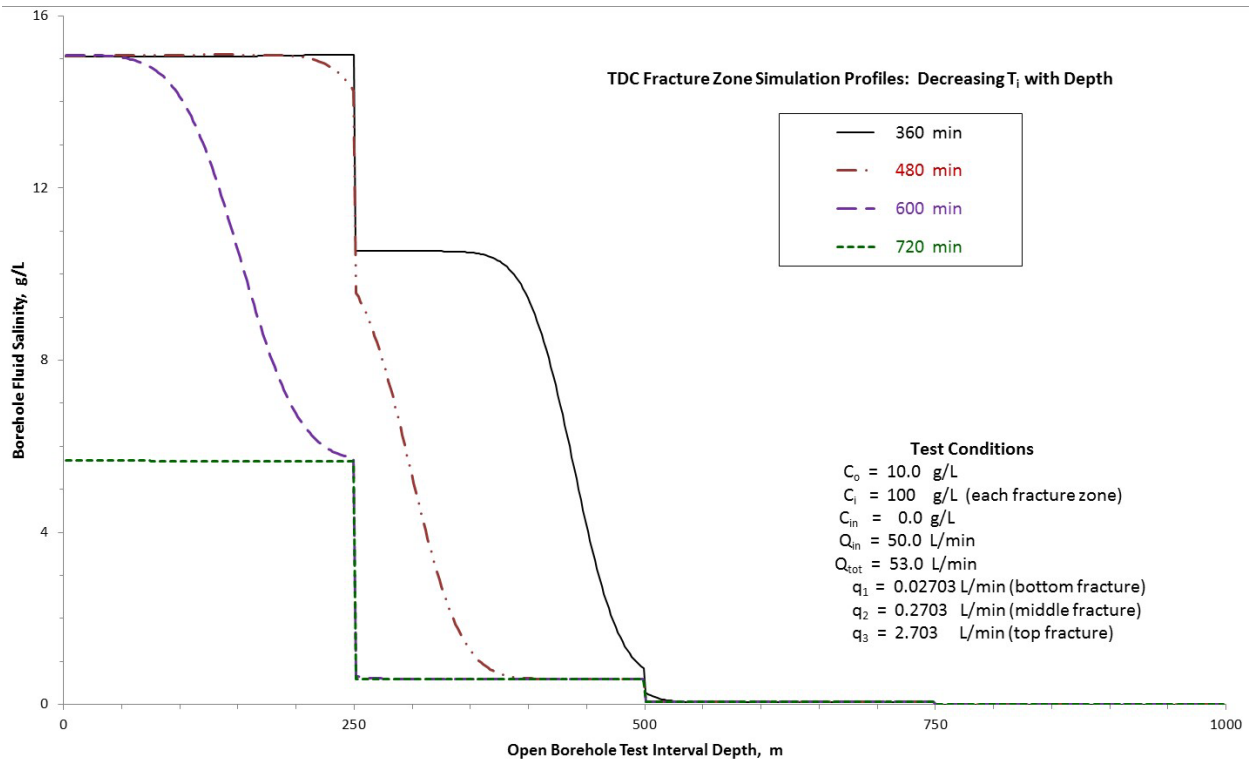

Figure 4.11. BORE II TDC Simulation Profiles for Selected Later-Test Times for the Case of Three Fracture Zones that Have Decreasing T_i with Depth: Top Fracture = 10^{-6} → Bottom Fracture = 10^{-8} m^2/sec
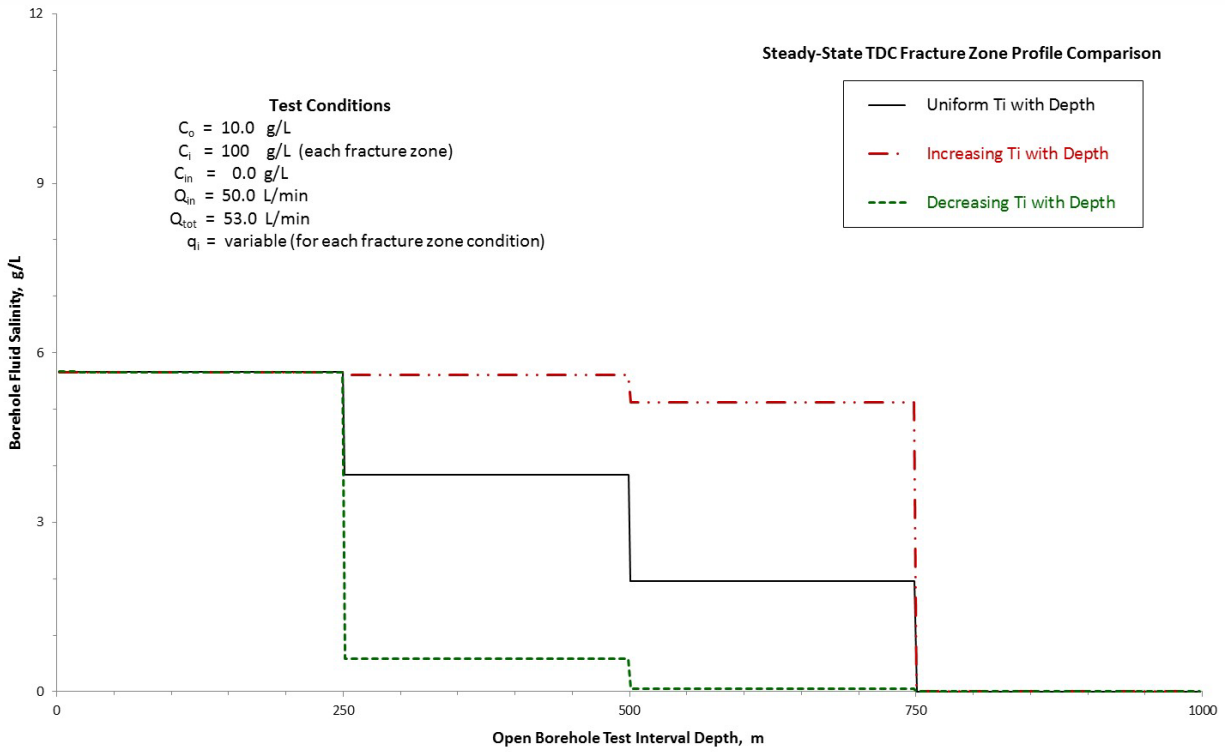
Figure 4.12. BORE II TDC Steady-State Fracture Zone Profile Comparison

5.0   Applicability of FFEC Testing in Deep Borehole Settings

The simulation results support the application of FFEC testing within deep crystalline boreholes that exhibit fracture zone transmissivity values of $\leq 10^{-5}$ m^2/sec, and they are consistent with previous reports of successful characterization applications at a number of deep borehole locations (see Table 3.1). As discussed previously, the rapidity and sensitivity of the method within low-permeability test sections, as well as the availability of standard, commercially obtainable standard test equipment to perform the tests, makes FFEC testing particularly attractive for deep borehole characterizations. However, the use of FFEC testing as a primary characterization tool for fracture zone hydraulic property determination within deep boreholes may be limited because of the issues identified and discussed in Section 3.3. These issues may limit the quantitative characterization applications of FFEC testing within boreholes that exhibit minimal well-skin damage, and for fracture zones that have well-established, equilibrated pressure conditions. For more restrictive borehole conditions, FFEC testing can still be used effectively as a reconnaissance-level characterization tool to identify the location of higher permeability/fluid-conducting fracture zones within large open borehole intervals. In this capacity, FFEC survey results would *complement* and focus test characterizations performed by more exacting (and more costly) packer tests that can accommodate more complex borehole test conditions. And, if a hydraulic property correspondence between limited fracture zone packer testing and FFEC analysis can be established, hydraulic property characterization of the entire borehole can be extended through use of FFEC survey profile analysis. This particular complementary characterization aspect for FFEC testing was also originally recognized by Tsang et al. (1990), and more descriptively articulated by Doughty et al. (2005) when discussing the role of FFEC testing and other hydrologic test characterization methods:

> "In general, using a variety of techniques for hydrogeological characterization is preferable to using just one. The strengths and weaknesses of different methods complement each other, providing a much more reliable picture of the subsurface, particularly for heterogeneous or fractured media…."

Similar combined characterization approaches for extending and calibrating open borehole wireline logging surveys (e.g., combined magnetic resonance, dynamic flowmeter logging, etc.) with more precise (but more limited) straddle-packer hydrologic field tests and core laboratory analysis results have been reported by Spane et al. (2006, 2013). However, these successful applications of extending wireline survey results for continuous permeability borehole profile determinations were conducted at shallower borehole depths (e.g., 1.2 to 2.8 km) and in sedimentary rock formation environments.

Of the two alternative tracer test methods considered, the TDC test appears to provide the most practical application for deep borehole characterization settings. BORE II simulations indicate that for similar test conditions, TDC tests can be conducted more rapidly than for FFEC tests, but they also exhibit an inherent lack of sensitivity for characterizing discrete fracture zones exhibiting T_i values lower than ~10^{-7} m^2/sec. Additionally, the limitations identified in this assessment of FFEC testing would also be applicable for the TDC method. Because of these limitations and rapid performance times, TDC testing may also find its best application as an initial reconnaissance tool prior to conducting FFEC and hydrologic packer tests.

6.0 References

[This list also contains references cited in Appendix A.]

Adams J and E Wyss. 1994. "Hydraulic packer testing in the Wellenberg boreholes SB1, and SB2." Nationale Genossenschaft für die Lagerung radioaktiver Abfälle, Nagra Technical Report NTB-93-38, Wettingen, Switzerland.

Barton CA, MD Zoback, and D Moos. 1995. "Fluid flow along potentially active faults in crystalline rock." *Geology* 23(8):683-686.

Barton CA, S Hickman, RH Morin, MD Zoback, T Finkbeiner, J Sass, and D Benoit. 1997. "Fracture permeability and its relationship to in-situ stress in the Dixie Valley, Nevada, geothermal reservoir." Proceedings of the Twenty-Second Workshop on Geothermal Reservoir Engineering, Stanford University, Stanford, California, January 27-29, 1997, pp. 147-152.

Beauheim, RL and WH Pedler. 2007. "Fluid electrical conductivity logging in borehole DGR-1 at the Bruce site." SAND2007-3473 C, Sandia National Laboratories, Albuquerque, New Mexico.

Bourdet DJ, A Ayoub, and YM Pirard. 1989. "Use of pressure derivative in well-test interpretation." *SPE Formation Evaluation* June: 293–302.

Brainerd RJ and GA Robbins. 2004. "A tracer-dilution method for fracture characterization in bedrock wells." *Ground Water* 42(5):774-780.

Butler JJ Jr. 1988. "Pumping tests in nonuniform aquifers – the radially symmetric case." *Journal of Hydrology* 101:15-30.

Cooper HH, Jr., and CE Jacob. 1946. "A generalized graphical method for evaluating formation constants and summarizing well-field history." *American Geophysical Union, Transactions* 27(4):526–534.

Dobson P, C-F Tsang, T Kneafsey, S Borglin, Y Piceno, G Andersen, S Nakagawa, K Nihei, J Rutqvist, C Doughty, and M Reagan. 2016. "Deep borehole field test research activities at LBNL." LBNL-1006044, Lawrence Berkeley Laboratory, Berkeley, California.

DOE (U.S. Department of Energy). 1988. Consultant draft, site characterization plan, reference repository location, Hanford Site, Washington. DOE/RW-0164, Vols. 1 and 2, Washington, D.C.

DOE (U.S. Department of Energy). 2017. "Studying the feasibility of deep boreholes." Office of the Under Secretary for Science and Energy: https://www.energy.gov/under-secretary-science-and-energy/articles/studying-feasibility-deep-boreholes; update May 23, 2017.

Doughty C and C-F Tsang. 2000. "BORE II ─A code to compute dynamic wellbore electrical conductivity logs with multiple inflow/outflow feed points including the effects of horizontal flow across the well." LBL-46833 (revised February 2004, September 2012, and July 2014), Lawrence Berkeley Laboratory, Berkeley, California.

Doughty C and C-F Tsang. 2002. "Inflow and outflow signatures in flowing wellbore electrical-conductivity logs." LBL-51468, Lawrence Berkeley Laboratory, Berkeley, California.

Doughty C and C-F Tsang. 2005. "Signatures in flowing fluid electric conductivity logs." *Journal of Hydrology* 310:157-180.

Doughty C, C-F Tsang, S Yabuuchi, and T Kunimaru. 2013. "Flowing fluid electric conductivity logging for a deep artesian well in fractured rock with regional flow." *Journal of Hydrology* 482:13.

Doughty C, S Takeuchi, K Amano, M Shimo and C-F Tsang. 2005. "Application of multi-rate flowing fluid electric conductivity logging method to well DH-2, Tono site, Japan." *Water Resources Research* 41:16, DOI 10.1029//2004WR003708,2005.

Doughty C, C-F Tsang, J-E Rosberg, C Juhlin, PF Dobson and JT Birkholzer. 2017. "Flowing fluid electrical conductivity logging of a deep borehole during and following drilling: estimation of transmissivity, water salinity, and hydraulic head of conductive zones." *Hydrogeology Journal* 25:501-517, DOI 10.1007/s10040-016-1497-5.

Duffield GM. 2007. *AQTESOLV for Windows Version 4.5 User's Guide*. HydroSOLVE, Inc., Reston, Virginia (http://www.aqtesolv.com).

Duffield GM. 2009. "Upgrading aquifer test analysis, by William C. Walton." *Ground Water - Comment Discussion Paper* 47(6):756-757.

Earlougher RC, Jr. 1977. *Advances in well test analysis*. Monograph Vol. 5, Society of Petroleum Engineers, Richardson, Texas.

Earthward Consulting, Inc. 2016. "Fluid density calculator (accounting for temperature and salinity); http://www.earthwardconsulting.com/density_calculator.htm

Gräsle W, W. Kessels, and H. Rifai. 2003. "A tracer based flow-log technique to assess hydraulic properties in deep fractured-porous aquifers of low permeability applied in the 4000 m pilot borehole of the KTB/Germany." International Conference on Groundwater in Fractured Rocks, September 15-19, 2003, Prague.

Guyonnet D, A Rivera, S Löw, and N Correa. 1993. "Analysis and synthesis of fluid logging data from Wellenberg Boreholes SB1, SB2, SB3, SB4, and SB6." Nationale Genossenschaft für die Lagerung radioaktiver Abfälle, Nagra Technical Report NTB-92-01, Wettingen, Switzerland.

Hale FV and C-F Tsang. 1988. "A code to compute borehole fluid conductivity profiles with multiple feed points." Nationale Genossenschaft für die Lagerung radioaktiver Abfälle, Nagra Technical Report NTB-88-21, Baden, Switzerland; also Lawrence Berkeley Laboratory report LBL-24928, Berkeley, California.

Hayashi M. 2004. "Temperature-electrical conductivity relation of water for environmental monitoring and geophysical data inversion." *Environmental Monitoring and Assessment* 96:119-128.

Hem JD. 1985. "Study and interpretation of the chemical characteristics of natural water." U.S Geological Survey, *Water-Supply Paper 2254,* 3rd Edition. Washington, D.C.

Ito T and MD Zoback. 2000. "Fracture permeability and in-situ stress to 7 km depth in the KTB scientific drillhole." *Geophysical Research Letters* 27(7):1045-1048.

Jacob CE. 1940. "On the flow of water in an elastic artesian aquifer." *Transactions of the American Geophysical Union* Part 2:574-586.

Jacob CE and SW Lohman. 1952. "Non-steady flow to a well of constant drawdown in an extensive aquifer," *Transactions of the American Geophysical Union* 33(4):559-569.

Jenkins DN and JK Prentice. 1982. "Theory of aquifer test analysis in fractured rocks under linear (nonradial) flow conditions." *Ground Water* 20(1):12-21.

Kelley VA, JM Lavanchy, and S Löw. 1991. "Transmissivities and heads derived from detailed analysis of Siblingen 1989 fluid logging data." Nationale Genossenschaft für die Lagerung radioaktiver Abfälle, Nagra Technical Report NTB-90-09, Wettingen, Switzerland.

Kuhlman, KL, BW Arnold, PV Brady, DC Sassani, GA Freeze, and EL Hardin. 2015. "Site characterization for a deep borehole field test." International High-Level Radioactive Waste Management Conference, Proceedings of the American Nuclear Society, Charleston, South Carolina, April 12-16, 2015, pp. 624-631.

Lohman SW. 1972. "Ground-Water Hydraulics." U.S. Geological Survey, *Professional Paper 708*, Washington, D.C.

Long CS, K Karasaki, A Davey, J Peterson, M Landsfeld, J Kemeny, and S Martel. 1991. "An inverse approach to the construction of fracture hydrology models conditioned by geophysical data – an example from the validation exercises at the Stripa mine." *International Journal of Rock Mechanics and Mining Science, & Geomechanics Abstracts* 28(2-3)121-142; also Lawrence Berkeley Laboratory report LBL-29381, Berkeley, California.

Long CS, EL Majer, SJ Martel, K Karasaki, JE Peterson, Jr., A Davey, and K Hestir. 1990. "Hydrologic characterization of fractured rocks ─ an interdisciplinary methodology." NAGRA-DOE Cooperative Project Report, NDC-12; also Lawrence Berkeley Laboratory report LBL-27863, Berkeley, California.

Löw S, C-F Tsang, FV Hale, and P Hufschmied. 1990. "The application of moment methods in the analysis of fluid electrical conductivity logs in boreholes." LBL-28809, Lawrence Berkeley Laboratory, Berkeley, California.

Löw S, V Kelley, and S Vomvoris. 1994. "Hydraulic borehole characterization through the application of moment methods to fluid conductivity logs." *Journal of Applied Geophysics* 31:117-131.

McCutcheon SC, JL Martin, TO Barnwell, Jr. 1993. "Water density as a function of temperature and concentration." Water Quality in Maidment, Handbook of Hydrology, McGraw-Hill, New York.

McNeish JA, RW Andrews, and S Vomvoris. 1990a. "Interpretation of the tracer testing conducted in the Leuggern borehole." NTB 89-27, Nagra, Baden, Switzerland.

McNeish JA, RW Andrews, S Vomvoris, and F A Spane. 1990b. "Tracer testing within a deep borehole in northern Switzerland." Paper presented at the American Geophysical Union Fall Meeting, December 3-7, 1990, San Francisco, California.

Millero F, C Chen, A Bradshaw, and K Schleicher. 1980. "A new high-pressure equation of state for sea water." Deep Sea Research, Part A, (27):255-264 (calculator used based on this method: http://www.csgnetwork.com/water_density_calculator.html)

Moench AF. 1997. "Flow to a well of finite diameter in a homogeneous, anisotropic water-table aquifer." *Water Resources Research* 33(6):1397-1407.

Paillet FL and WH Pedler. 1996. Integrated borehole logging methods for wellhead protection applications." *Engineering Geology* 42:155-165.

Pedler WH, MJ Barenvik, C-F Tsang, and FV Hale. 1990. "Determination of bedrock hydraulic conductivity and hydrochemistry using a wellbore fluid logging system." Proceedings of the 4th National Water Well Association Outdoor Action Conference; pp. 39-51.

Power Feed-Thru Systems & Connectors, LLC (PFT®). 2015. "Black Gator® Logging Bypass System (Y-Tool)"; Product Sheet, http://pftsys.com/PDF/1_ESP_LoggingBypass_PDS.pdf

Pickens JF, GE Grisak, JD Avis, DW Belanger, and M Thury. 1987. "Analysis and interpretation of borehole hydraulic tests in deep boreholes: principles, model development and applications." *Water Resources Research* 23(7):1341-1375.

Reilly TE, OL Franke, and GD Bennett. 1987. "The principle of superposition and its application in ground-water hydraulics." In *Techniques of Water-Resources Investigations, Book 3*. Applications of Hydraulics, Chapter B6, Reston, Virginia: U.S. Geological Survey, 28p.

Rogers SF. 2003. "Critical stress-related permeability in fractured rocks." Geological Society, London, Ameen, M (ed.) *Fracture and In-Situ Stress Characterization in Hydrocarbon Reservoirs*, Special Publications (209):7-16.

Schlumberger, LTD. 2009. "Product sheet: Y-Tool and pump bypass system.", http://www.slb.com/~/media/Files/artificial_lift/product_sheets/dual_esp_ps.pdf

Sharma, P, C-F Tsang, C-F, IT Kukkonen, and A Niemi. 2016. "Analysis of 6-year fluid electric conductivity logs to evaluate the hydraulic structure of the deep drill hole at Outokumpu, Finland." *International Journal of Earth Science* 105:1549-1562, DOI 10.1007/s00531-015-1268-x.

Shedlovsky T and L Shedlovsky. 1971. "Conductometry, techniques of chemistry." In *Physical Methods of Chemistry, IIa, Electrochemical Methods*. A Weissberger and BW Rossiter (eds.); pp 164-171, John Wiley, New York.

SNL (Sandia National Laboratories). 2016a. "Deep borehole field test conceptual design report." FCRD-UFD-2016-000070 Rev. 1. U.S. Department of Energy, Office of Used Nuclear Fuel Disposition.

SNL (Sandia National Laboratories). 2016b. "Deep borehole field test laboratory and borehole testing strategy." SAND2016-9235 R, Albuquerque, New Mexico.

Spane FA, Jr. 1990. "Description and results of tracer tests conducted for a deep fracture zone within granitic rock at the Leuggern borehole." Nagra Technical Report NTB 90-05, Nagra, Baden, Switzerland.

Spane FA, Jr. 1993. *Selected hydraulic test analysis techniques for constant-rate discharge tests*. PNL-8539, Pacific Northwest Laboratory, Richland, Washington.

Spane FA and RB Mercer. 1985. *HEADCO: A Program for Converting Observed Water Levels and Pressure Measurements to Formation Pressure and Standard Hydraulic Head*. RHO-BW-ST-71P, Rockwell Hanford Operations, Richland, Washington.

Spane FA, Jr. and SK Wurstner. 1993. "DERIV: A program for calculating pressure derivatives for use in hydraulic test analysis." *Ground Water* 31(5):814-822.

Spane FA, A Bonneville, BP McGrail, and PD Thorne. 2012. "Hydrologic characterization results and recommendations for the Wallula basalt pilot well." PNWD-4368, Pacific Northwest National Laboratories, Richland, Washington.

Spane, FA, EC Sullivan, PD Thorne, and M Kelley. 2013. "Integration of Selected Wireline Logs, Core Analysis, and Borehole Testing Results for Detailed Reservoir Permeability Characterization: Results from the FutureGen Characterization Borehole." Presented by FA Spane at the 12th Annual CCUS Conference 2013, Pittsburgh, Pennsylvania, May 13-16, 2013. PNNL-SA-92986, Pacific Northwest National Laboratory, Richland, Wasington.

Spane, FA, PD Thorne, N. Gupta, P. Jagucki, TS. Ramakrishnan, and N. Mueller. 2006. "Results Obtained from Reconnaissance-Level and Detailed Reservoir Characterization Methods Utilized for Determining Hydraulic Property Distribution Characteristics at Mountaineer AEP #1". PNNL-SA-48622, in Proceedings, International Symposium on Site Characterization for CO_2 Geological Storage, CO2SC 2006, Lawrence Berkeley National Laboratory, Berkeley, California, March 20-22, 2006.

Stober J and K Bucher. 2007. "Hydraulic properties of the crystalline basement." *Hydrogeology Journal* 15:213-224.

Stober J and K Bucher. 2015. "Hydraulic conductivity of fractured upper crust: insights from hydraulic tests in boreholes and fluid-rock interaction in crystalline basement rocks." *Geofluid*, 15:11-178.

Thiem G. 1906. "Hydrologische methoden." Gebhardt, Leipzig, Germany, 56 pp.

Tsang C-F and P Hufschmied. 1988. "A borehole fluid conductivity logging method for the determination of fracture inflow parameters." Nationale Genossenschaft für die Lagerung radioaktiver Abfälle, Nagra Technical Report NTB-88-13, Baden, Switzerland.

Tsang C-F, P Hufschmied, and FV Hale. 1990. "Determination of fracture inflow parameters with a borehole fluid conductivity logging method." *Water Resources Research* 26(4):561-578.

Tsang C-F, J-E Rosberg, P Sharma, T Berthet, C Jublin, and A Niemi. 2016. "Hydrologic testing during drilling: application of the flowing fluid electrical conductivity (FFEC) logging method to drilling of a deep borehole." *Hydrogeology Journal* 24:1333-1341, DOI 10.007/s10040-016-1405-z.

Witherspoon PA, JSY Wang, K Iwai, and JE Gale. 1980. "Validity of cubic law for fluid flow in a deformable rock fracture." *Water Resources Research* 16(6):1016-1024.

Zeigler TW. 1976. "Determination of rock mass permeability." U.S. Army Engineer Waterways Experiment Station, Technical Report 5-76-2, Vicksburg, Mississippi.

Appendix

DBFT Recommendations

Appendix

DBFT Recommendations

The following discussion was developed specifically for the performance of FFEC testing within the proposed DBFT CB. Many of the elements described, however, would be relevant for consideration of FFEC testing in other deep crystalline rock boreholes.

Although, as noted in Section 3.2.1, FFEC testing can be performed in the course of drilling during temporary periods of non-advancement, the following test recommendations are specifically identified for FFEC testing after the proposed DBFT CB has been drilled to final depth. It is also assumed that FFEC testing will be performed using a workover rig (i.e., drilling rig de-mobbed from site) to reduce program costs. The primary objective of open-borehole hydrologic testing within the basement rock at the proposed DBFT CB is to demonstrate various test method capabilities for identifying/characterizing fluid-transmitting fractures/structural features within the crystalline basement section. In the context of the entire characterization program for the CB, the following sequence of test/characterization activities are envisioned to take place shortly after reaching total CB depth.

1. Detailed wireline geophysical logging program (Section 6.7 in SNL 2016b)

2. Pre-test CB conditioning/development (optional)

3. Production profile (spinner flowmeter/fluid temperature) pumping test

4. *Multi-Rate FFEC testing (Section 6.8 in SNL 2016b)*

5. Hydrologic packer test program for detailed hydraulic property and fluid hydrochemical/isotopic sample characterization (hydraulic tests in Sections 6.5.2, 6.9.1 through 6.9.6; hydrochemical/isotopic discussion in Sections 6.1.2.6, 6.5..3, 7.1.1, 7.1.2 in SNL 2016b)

6. Hydromechanical/in-situ stress-field characterization (Sections 6.6, 6.9.7, and 6.9.8 in SNL 2016b).

The detailed wireline geophysical logging program will provide information concerning fracture attribute characteristics within the crystalline basement and information that can support subsequent characterization activities e.g., hydrologic and geomechanical tests. This will be followed either by pre-test CB conditioning/development (if indicated by drilling/borehole conditions) and/or production profile flowmeter and FFEC testing. As noted by Tsang and Doughty (2003), multi-rate FFEC testing should be preceded by a standard open borehole constant-rate pumping test (over the entire open borehole test interval). The purpose of the composite borehole pumping test is to select optimum pumping rates for the subsequent multi-rate FFEC test, and to determine the total transmissivity (T_{tot}) for the open composite borehole section. Determining the T_{tot} for the composite borehole section supports FFEC profile evolution analysis and, when combined with standard flowmeter and fluid temperature logging, is extremely useful in identifying highly transmissive fracture zones that may adversely affect the successful performance of FFEC testing within the CB (i.e., a highly transmissive fracture zone in the lower section of a test interval would adversely affect FFEC profile development of overlying, less transmissive fractures). Given the scenario of a highly transmissive fracture/fault feature that might interfere with the development of associated FFEC profile signatures during testing, the highly transmissive fracture zone can be isolated from the surveyed interval using standard isolation packer(s), as has been done at other sites where FFEC testing was conducted in deep basement crystalline rock settings (e.g., Tsang and Hufschmied 1988).

The following general test/activity steps are recommended for the performance of multi-rate FFEC characterization surveys within the proposed DBFT CB or similar deep characterization boreholes.

1. After drilling the CB to a prescribed or designed completion depth (i.e., to 5 km) and completing wireline and pre-FFEC testing activities, replace the existing borehole fluid with water the salinity of which contrasts significantly with in-situ fracture formation fluid.

    a. Because deep crystalline basement sections are expected to have elevated salinities (i.e., $C_s > 6$ kg/m^3), use a low C_s replacement fluid (i.e., $C_s = 0.03$ to 0.2 kg/m^3; FEC = 60 to 300 µS/cm) to provide an adequate contrasting fluid for developing dynamic FFEC test profiles for hydraulic property analysis.

    b. To minimize the incursion of non-formational emplacement water into surrounding intersecting fracture systems, emplace the fluid near the base of the test interval at a prescribed low injection rate, while simultaneously removing fluid from the well at the same rate near the top of the fluid-column.

    c. Use simultaneous injection of emplacement fluid (at the base of the test interval) and removal of well water from near the top of the fluid column using the same rates to minimize borehole pressure buildup and incursion of non-formation well fluid into permeable fractures intersected by the borehole.

    d. Equip the submersible pump with an attached real-time, recording pressure transducer for monitoring well drawdown/buildup pressures during the course of borehole fluid emplacement.

    e. Consider the use of an internal packer-tubing string assembly (that would reduce internal well casing test diameter/volume) to reduce the volume of baseline replacement fluid in the borehole and to effectively reduce wellbore storage effects during the performance of the subsequent FFEC profile test.

2. When the surface-monitored pumping fluid indicates a uniform FEC or salinity concentration level (that is similar to the injection water), terminate fluid emplacement activities and remove the submersible pump and injection tube from the borehole.

3. After injection tube removal, re-install the packer-tubing string and submersible pump (along with the attached downhole, real-time pressure probe) with an appropriate bypass installation (e.g., "Y-tool") to accommodate wireline logging during the course of the dynamic phase of FFEC testing.

    a. Install the submersible pump at a well depth that will ensure that pumping drawdown will not reach the submersible setting depth during the course of pumping; e.g., ≤ 250 m below static well fluid-level conditions.

4. After re-installing the submersible pump, use commercially available FEC, temperature, and pressure probe wireline probe/recording system to determine the ambient, pre-test FEC, fluid temperature, and fluid pressure vs. depth profile characteristics within the borehole.

    a. Log the FFEC profile surveys using a stacked, multi-probe assembly system that includes sensors for not only measuring FEC, fluid temperature, and fluid pressure, but also a formational depth indicator (e.g., gamma ray).

5. After completing the ambient, pre-test logging surveys, initiate the dynamic phase of the FFEC test by removing fluid from the borehole at a low and constant rate (e.g., 2 to 20 L/min).

    • Flow rates within this range should be within the laminar (non-turbulent) flow range (i.e., Reynolds number < 2000) and minimize impacts on FFEC profile development

6. To minimize analytical and minimize testing uncertainties, use multiple constant-rate pumping steps (e.g., 2 to 3) during performance of the FFEC test and a combined pumping test period duration that ranges from 1 to 7 days.

7. During the pumping or dynamic "flowing" period, log multiple FFEC profile surveys (2 to 5 up/down FEC logging passes per each individual constant-rate pumping step) across the selected open borehole characterization section.

8. Compare the repeated logging results obtained progressively during the pumping period to establish changes in the FFEC depth profile within the borehole over time.

9. Note how the inflow of fluid from hydraulically conductive fractures generates discernable FFEC peak patterns that evolve and expand over time within the borehole depth interval during the FFEC test period.

    In particular, analysis of the FFEC evolution patterns provides a wide spectrum of information for hydraulically conductive fractures intersected by the borehole, including:

    - precise inflow/outflow location depths
    - inflow rates (q_i) and fracture fluid salinity (C_i)
    - fracture hydraulic head conditions (h_i).

10. Determine whether the presence of underlying, higher permeability fracture zones dictates the need to isolate higher permeability fracture zones from FFEC testing and to divide the FFEC profile characterization of the entire 2 to 5 km open borehole section into individual FFEC survey test segments. (note: previous deep borehole FFEC profile test characterizations have demonstrated this method's capabilities to rapidly characterize permeability profile of intersected fracture zones over open borehole test sections of ~ 1,000 m.)

11. As an alternative to fluid extraction using an ESP, use air-lift/evacuation pumping.

    a. Administer compressed air via a conductor pipe (usually through a centrally installed injection tubing).

    b. Remove/evacuate fluid from the well using the existing well casing, along with a surface wellhead enclosure to divert well flow.

    c. Conduct FFEC wireline logging conducted through the central injection tubing using a surface stuffing box or wellhead lubricator mounted on the top of the injection tubing.

    d. Implement multiple pumping rates by lowering the injection tubing to greater depths, which will impose greater drawdown in the well and a higher subsequent well discharge rate.

[References cited in this appendix are listed in Section 6.0.]

Distribution

**No. of
Copies**

   1   ME Kelley
      Battelle Columbus Operations
      505 King Ave.
      Columbus, Ohio 43201

   1   KL Kuhlman
      Applied Systems Analysis and
      Research/6224
      Sandia National Laboratories
      P.O. Box 5800, MS 0747
      Albuquerque NM 87185-0747

   1   RJ MacKinnon
      Applied Systems Analysis and
      Research/6224
      Sandia National Laboratories
      P.O. Box 5800, MS 0747
      Albuquerque NM 87185-0747

**No. of
Copies**

   #   **Local Distribution**
      Pacific Northwest National Laboratory (pdf)

D Appriou	K7-73
A Bonneville	K4-18
CF Brown	P7-54
BD Hanson	P7-27
TL Liikala	P7-54
P McGrail	K4-18
DR Newcomer	K7-73
FA Spane	K7-73
PD Thorne	K7-73
SD Unwin	K9-69
VR Vermeul	K4-18